Norwegian University of Life Sciences
Faculty of Environmental Sciences and Technology
Department of Mathematical Sciences and Technology

Master Thesis 2015
30 credits

Developing an In-Vitro Dynamic Model of the Stomach and Small Intestine for Milk Products - Second Prototype

Stian Stenberg

Preface

This Master thesis is written by Stian Stenberg at the Norwegian University of Life Sciences. The duration of this thesis has been approximately 5 months and is credited 30 points. It is the final project in the Mechanics and Process Technology program. During these 5 months, knowledge about process technology and especially product development has been put at assessment.

This thesis is a further development of last year's prototype made by master student May Helen Tysse, who carried out the first step in developing an in-vitro dynamic model of the stomach and small intestine for milk product with rheological monitoring.

I would like to thank my supervisor, Professor Carlos Salas-Bringas for good advice, practical help and flexibility throughout this semester.

Thanks to my co-supervisor professor Reidar Barfod Schüller for guiding me in the laboratory.

Thanks to Irene Comi and Ellen Kathrine Ulleberg for helping me start my testing and giving advice throughout the semester. I would also like to thank Tove Devold and Gerd Vegarud for helping me with theoretical and practical knowledge.

Thanks to Johan Andersen for assisting me in the microscope lab and thanks to Spectrum Labs who has answered all my emails.

Ås, 15.05.2015

_____

Stian Stenberg

Abstract

This thesis is written as part of a project lead by researchers at NMBU who wishes to replicate the physical processes of the digestion system in a human body (in-vivo). To replicate such a system is beneficial for understanding the biochemical-and biomechanical processes in the digestive system.

The aim of this study has been to further develop the first prototype of a dynamic in-vitro (laboratory work) model of the digestive system, considering the stomach and the small intestine.

There are several challenges related to making a dynamic model of the digestive system. For example the imitation of the peristaltic movement in the intestines. The properties of the fluids in the dynamic system need to be the same as for blood and the intestinal fluids. The temperature of the system needs to be the same as for the human body. To keep unwanted organisms out of the system. Choosing and applying a membrane for replicating the intestine and also the practical challenges related to the use of the system.

This thesis has focused on designing parts for solving some of these problems. A "water bath" filled with water keeps a steady temperature of the system and works as foundation for other parts. The "stomach" is replicated by a small glass cup and a "buffer tank" holds the liquid that imitates blood. "Hoses" are used as intestine and leads the fluids in and out of their containers ("stomach" and "buffer tank"). A membrane unit consists of parts for simulating the digestion in the small intestine. Parts for monitoring and stabilizing has also been made or added to the system and ensure a good repetitive system. Finally a user manual for the system is made.

The new prototype can be placed onto a rheometer for viscosity readings, but can also be used without the rheometer which makes it a mobile system. Many parts have been made transparent which ensures good visibility of the physical processes. Problems with membrane attachment, membrane collapse and membrane permeation have been solved or improved. The wish of creating a mathematical model for the diffusion of the membrane has been the reason for doing a lot of permeation tests and two models have been suggested.

For future work the main motivation will be to simulate the digestion of milk mixed with HGJ and HDJ by using the prototype presented in this thesis.

The new prototype is an improvement of the first and ensures a repetitive system as well as estimates to flux can be made.

Sammendrag

Denne oppgaven er skrevet som en del av et prosjekt ledet av forskere på NMBU som ønsker å simulere de fysiske prosessene i kroppens fordøyelsessystem. Å simulerer et slikt system er hensiktsmessig for å forstå de biokjemiske- og biomekaniske prosessene i fordøyelsessystemet.

Målet med denne oppgaven har vært å videreutvikle den første prototypen av en dynamisk in-vitro (labarbeid) modell av fordøyelsessystemet, med tanke på magen og tynntarmen.

Det er flere utfordringer relatert til å lage en dynamisk modell av fordøyelsessystemet. For eksempel den peristaltiske bevegelsen i tarmene. Egenskapene til fluidene i det dynamiske systemet må være likt som for blod og fluidene i tarmene. Temperaturen i systemet må være den samme som i menneskekroppen. Det er nødvendig å hindre uønskede partikler i å komme inn i systemet. En membran må velges og settes sammen med systemet på en måte som etterlikner tynntarmen best mulig.

Denne oppgaven har fokusert på å designe deler for å løse noen av disse problemene. Et "vannbad" fylt med vann holder temperaturen i systemet konstant og fungerer som et stativ for andre deler. "Magen" etterliknes av et lite glass og "buffer tanken" holder væsken som imiterer blod. "Gummislanger" brukes som tarmer og fører væskene inn og ut av deres beholdere ("magen" and "buffer tanken"). En membranenhet består av deler for å simulere fordøyelsen i tynntarmen. Deler for overvåking og stabilisering av systemet har også blitt laget eller lagt til og de sikrer et repeterende system. En bruker manual for systemet har også blitt laget.

Den nye prototype kan plasseres på et reometer for å måle viskositet, men kan også brukes uten reometeret som gjør at systemet er allsidig. Mange deler er blitt laget i glass for å sikre at de fysiske prosessene er synlige. Problemene med å feste membranen, kollaps av membranen og diffusjon i membranen har blitt løst eller forbedret. Ønske om å lage en matematisk modell for diffusjon i membranen har vært grunnen til å gjennomføre alle diffusjonstester og flere modeller for diffusjonskoeffisienten har blitt foreslått.

Videre arbeid bør omhandle simulering av fordøying av melk mikset med menneskelig magesaft og tolvfingertarmsaft ved bruk av modellen som er presentert i denne oppgaven.

Den nye prototype er en forbedring av den første og sikrer et repeterende system som også gjør det mulig å estimere resultater før testing.

Contents

List of figures

List of tables

List of equations

List of symbols

Table 1: Table with names, symbol and units.

Name	Symbol	Unit
Molar flux	j_A	$mol/m^2 * s$
Diffusion coefficient	D_v	m^2/s
Effective diffusion coefficient	D_e	m^2/s
Concentration	c_A	mol/m^3
Distance/thickness	b	m, cm, mm
Porosity	ε	-
Number of pores	n_p	-
Average pore radius	r	m, cm, mm
Membrane area	A_m	m^2
Diameter	D	m, cm, mm
Average velocity	$\bar{V}$	m/s
Density	ρ	kg/m^3
Dynamic viscosity	μ	$kg/m * s$
Kinematic viscosity	ν	m^2/s
Molar flux per volume	N_1	$mol/m^3 * s$
Area per volume	a	m^2/m^3
Overall mass transfer coefficient	K	m/s
Concentration difference	$(c - c_1^*)$	mol/m^3
Mass transfer coefficient	k	m/s
Diffusion coefficient in water	D_w	m^2/s
Boltzmann constant	K_b	J/K
Temperature	T	$^0C \text{ or } K$
Molecular radius	r_0	cm
Absorbance	A	-
Molar absorptivity	ϵ	$L/mol * cm$
Molar volume of solute	V_A	$cm^3/g\ mol$
Molecular weight of solvent	M_B	g/mol
Association parameter for solvent	ψ_B	-
Partition coefficient	H	-
Length of curve	L_C	m, cm, mm
Arc length	C	m, cm, mm
Friction factor	f	-
Reynold's number	R_e	-
Volume	V	m^3, cm^3, mm^3
Concave Volume	V_c	m^3, cm^3, mm^3
Basal	G	m^2, cm^2, mm^2
Molar	M	mol/L
Constriction factor	σ_c	-
Tortuosity	τ	-
Ratio	β	-

Abbreviations

Table 2: Abbreviations with explanation to the expressions.

Expression	Explanation
PDMS	Pressure-driven membrane separation
MF	Microfiltration
UF	Ultrafiltration
NF	Nanofiltration
RO	Reverse Osmosis
MWCO	Molecular weight cut-off
DMSO	Dimethyl sulfoxide
HGJ	Human gastric juices
HDJ	Human duodenal juices
MW	Molecular weight
SPM	Spectrophotometer
ABS	Absorption
UiO GBD	University of Oslo glass blowing department

1 Introduction

1.1 Motivation

This thesis is written in collaboration with the institute of Mathematical Sciences and Technology (IMT) and the Institute of Chemistry, Biotechnology and Food Science (IKBM) at the University of Life Sciences (NMBU). It is part of a project that aims on developing an in-vitro dynamic model of the stomach and small intestine for milk products with rheological monitoring (Tysse 2014).

1.1.1 Prototype 1

As mentioned, the first prototype was built last year as a master thesis (Tysse 2014) and a report was written. The structure of this thesis is similar to the first report. The reason for this is that it will make it easier to compare these thesis as to which changes has been made.

1.2 Objective

The main objectives of this thesis are to make improvements and further development of the first prototype that May Helen Tysse built during her work on this project in 2014.

1.2.1 Sub Objectives

- Troubleshooting the problems encountered with the diffusion through the membrane.
- Find the diffusion coefficient of the membrane.
- Make the membrane stick to the glass to prevent leakages.
- Solve the problem with membrane collapse.
- Make it easier to get a visual perspective on the process.

1.2.2 Limitations

Factors such as volume flow, velocity, temperature, feed type, and pH is more or less set by the previous work done or cannot be changed due to the apparatus or for the sake of equality between the in-vitro and in-vivo conditions.

1.3 Procedure

1.3.1 CAD Simulation and 3D drawing

Solid works has been used extensively throughout writing this report. 3D drawings have been the main key to making the parts and to fit them together. Simulations of the 3D drawings has helped to further design the equipment.

1.3.2 Experimental work

Experimental work has been done to get an understanding of prototype 1 (Tysse 2014), to test new designs and to make a mathematical model of the diffusion of the membrane.

1.4 Structure of the thesis

- **Chapter 1: Introduction**
- **Chapter 2: Theory**
- **Chapter 3: Prototype development**
- **Chapter 4: User manual**
- **Chapter 5: CAD simulation**
- **Chapter 6: Experimental work**
- **Chapter 7: Problems encountered**
- **Chapter 8: Discussion and future work**
- **Chapter 9: Conclusion**

2 Theory

2.1 Membranes

A membrane is a thin pliable sheet with many pores so that certain molecules (must be smaller in diameter than the pores) can flow through and other molecules are rejected from passing due to the pore size of the membrane. The way of separation can be caused by several factors known as the selectivity of the membrane. These factors are; impurity size, shape, electrostatic charge, diffusivity, physicochemical interactions, volatility and polarity/solubility. However, this is not enough for molecular passage. The driving force that allows molecules to pass the membrane is either a pressure difference across the membrane or a concentration difference across the membrane. (Lekang 2013). When choosing a membrane it is especially important to consider the selectivity.

2.1.1 Biological membranes

Biological membranes are found on or inside living organisms. They serve to protect whatever they surround from the outside environment. For example one might say that the human skin is a biological membrane that protects the inside of our body from the surroundings. Another example is the inside wall of the small intestine which will be relevant for this thesis. Here we can find a membrane through which nutrients pass and are taken up in the body (Tysse 2014). These conditions are what we call an in-vivo model (in living).

2.1.2 Artificial membranes

Artificial membranes are often made from polymers. They come with different pore sizes and or materials. They are called artificial membranes because their function is to mimic the conditions in biological membranes.

2.2 Membrane classification

As mentioned above the factors of separation varies, and these are part of the way we classify membranes. However, the conventional classification method is based on the size of the impurities that are rejected and the size of the pores in the membrane. The size is given in Dalton or atomic mass unit (amu) and is defined as one twelfth of the weight of a carbon-12

atom. Furthermore, it is always a pressure- or concentration difference that promotes separation.

PDMS membranes uses pressure difference as promoter. It is typical to separate PDMS (pressure driven membrane separation) filters into four categories; microfiltration, ultrafiltration, nanofiltration and reverse osmosis (Lekang 2013). Their differences lie in the size of the pores, where MF has the biggest pores and RO has the smallest. MF filtration is usually used for rejecting particles bigger than 0,1 µm. UF rejects particles particles bigger than 0,01 µm, NF rejects particles bigger than 0,001 µm and RO rejects particles bigger than 0,0001 µm. These values tend to overlap and therefore the pore size in the membrane is slightly smaller than these values. (Lekang 2013). The particles size refers to the diameter of the particles, assuming spherical particles.

Membranes are also classified by the flow configuration of the liquid relative to the membrane. The flow configuration may be either "dead end" or "cross flow" (Lekang 2013).

2.2.1 Relating molecular weight to diameter

To be able to relate the molecular weight to its diameter, we have to assume a shape of the molecule. The most common shape would be a spherical shape which is also the shape of the whey proteins (Ulleberg 2011). By knowing the density and weight of the substance it should be possible to calculate the diameter by using equation below.

$$V = \frac{4}{3}\pi r_0^3 = \frac{m}{\rho} \qquad \textit{Eq. 1}$$

Eq. 1 shows that the volume is the product of mass divided by density

2.3 Membrane configuration

2.3.1 Dead end

"Dead end" configuration implies that the feed flows normal to the membrane surface. It is analogous to a liquid flowing in a tunnel, except that there is a membrane blocking the exit. Those particles that are small enough are pushed through, but the bigger particles (impurities) get stuck on the membrane surface with no way to go. As more feed enters the tunnel, the layer of impurities will rise, causing the pressure difference across the membrane to rise and this will

harm the membrane if not cleaned. A cleaning of the membrane is necessary before separation can go on (Lekang 2013).

2.3.2 Cross flow

"Cross flow" is a more widely used configuration and it is the one that is used in this thesis. Here the feed flows parallel to the membrane surface. An advantage in this type of configuration is the hindrance of premature clogging because of the increased shear conditions caused by the flow. The permeate will flow perpendicular to the membrane surface such as in "dead end" configuration. Because of the pressure most of the feed will flow parallel to the membrane and not being able to permeate. It is therefore typical to arrange a closed loop, so that some of the reject flow back into the membrane housing (Lekang 2013).

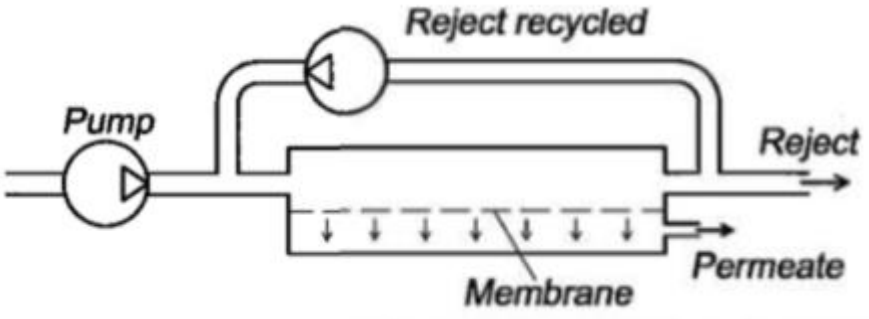

Figure 1: Cross flow in closed loop. Obtained from "Aquaculture engineering", by Odd-Ivar Lekang, 2013. The figure shows that some of the reject, containing valuable substance, is recycled thus securing more permeate production.

2.4 Membrane morphology

The morphology of membranes can be divided into porous and non-porous membranes. For porous membranes the porosity varies with the type of membrane. A MF membrane will have a porosity of 5-70 %, while a UF membrane have a porosity of 0,1-1 % (Lekang 2013). The porosity is given by equation 2.

$$\varepsilon = \frac{n_p \pi r^2}{A_m} \qquad \textit{Eq. 2}$$

Where $n_p = number\ of\ pores$

$r = pore\ radius$

$A_m = membrane\ area$

Eq. 2 expresses the surface porosity. Obtained from "Aquaculture engineering", by Odd-Ivar Lekang, 2013.

Non-porous membranes do not have pores and are judged from how good is the diffusivity and solubility of the membrane. Since there are no pores, the pressure needs to be greater in order to push the permeate through the membrane (Lekang 2013). RO is a process for cleaning salt from water and uses these principles for separation. The water molecules diffuse through the membrane and because of the salt rejecting chemical composition of the membrane, salt is not diffused. Diffusion is explained in chapter 2.8.

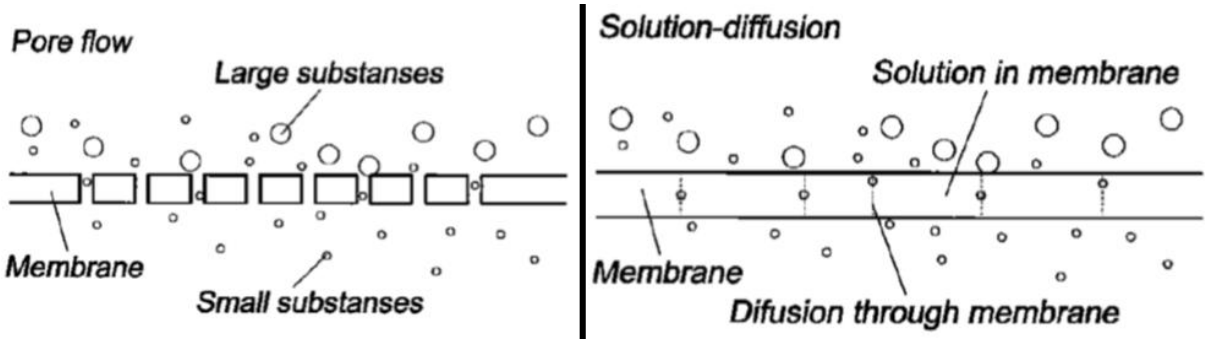

Figure 2: Left: Separation through pore flow. Right: Separation through diffusion. Obtained from "Aquaculture engineering", by Odd-Ivar Lekang, 2013.

2.5 Membrane fouling

After running the membrane for some time, it is always the case that the substances in the flow affect the membrane in a negative way. The effect is either lower flux of permeate through the membrane or higher pressure across the membrane which can damage it. Lower flux is a result of larger substances that block the pores and build up a particle cake on the membrane surface, which causes a thicker membrane. The flux through a membrane is as described in equation 11 inversely proportional to membrane thickness. Higher pressure drop across the membrane is usually caused by biofouling. This is the establishment of a biofilm on the pore surfaces, and also has a negative effect on flux. Another phenomenon that effects the flux negatively is concentration polarization. This is a second resistance to flux which is caused by a concentration gradient close to the membrane surface (Lekang 2013).

Fouling happens only after a few minutes or after several months and when it is too severe it needs to be removed. Methods for removal is hydraulically, chemically, physically or a combination (Lekang 2013).

2.6 Membrane area per volume

One of the requirements to ensure a good separation of substances is a high area per volume relationship. This applies not only to membranes, but to all kinds of separation. Taking the example of blood dialyzers that seek a large mass transfer flux in a small volume, the flux per volume is given by equation 3 (Cussler 2009):

$$N_1 a = Ka(c_1 - c_1^*) \qquad \textit{Eq. 3}$$

Where $N_1 = The\ volume\ flux$ [mol/m^3 $*$ s]

$a = Area\ per\ volume$ [m^2/m^3]

$K = Overall\ mass\ transfer\ coefficient$ [m/s]

$(c_1 - c_1^*) = Concentration\ difference$ [mol/m^3]

From the equation above we can see that large values for K, a, and the concentration difference will give us a large flux. A large a-value comes from choosing the right membrane or designing the membrane so that we get a lot of surface inside a specific volume. Typical membranes used for blood dialyzers are hollow fiber membranes (Cussler 2009). They consist of many small permeable pipes situated inside a housing (shell) which secures a big "area per volume" relationship.

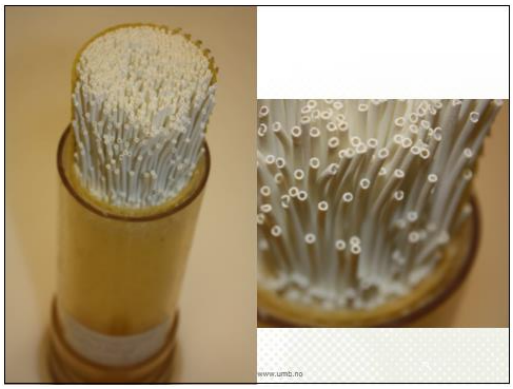

Figure 3: Shows a hollow fiber membrane. Diffusion occurs along the tube side of the many white pipes. Obtained from lecture notes in TMPP 100.

The value of the overall mass transfer coefficient, K, is estimated by using analogies between diffusion and heat transfer which gives us equation 4.

$$\frac{1}{K} = \frac{1}{k(liquid)} + \frac{1}{k(membrane)} + \frac{1}{k(liquid)} \qquad \textit{Eq. 4}$$

Eq. 4: In this thesis, K is the overall mass transfer coefficient and k is the mass transfer coefficient for the liquids on both sides of the membrane and the membrane itself. This equation as it stands, shows the overall resistance for a substance to be transferred from one liquid into the other liquid (Cussler 2009).

$$k(liquid) = \frac{D_w(liquid)}{l(liquid)} \qquad \textit{Eq. 5}$$

Eq. 5 shows individual mass transfer coefficient (Cussler 2009).

Where $k = \ Individual\ mass\ transfer\ coefficient\ [m/s]$

$D_w = diffusion\ coefficient\ for\ liquid\ [m^2/s]$

$l = boundary\ layer\ thickness\ [m]$

2.7 Dimensionless numbers

This section deals with the most important dimensionless numbers in mass transfer, for describing a certain system. To describe a certain system accurately with these numbers is almost impossible and that is also the reason why there are so many different relations of only one equation. For example, 27 different Sherwood relations are given for turbulent flow of Newtonian fluids (BERG et al. 1989). This thesis deals with those relations best suited for this specific system.

2.7.1 Sherwood number

The Sherwood number is a dimensionless group used for analysing mass transfer by convection. It expresses the ratio between the convective mass flux in the boundary layer and a pure diffusional flux. It is useful for estimating the film mass transfer coefficient, k (Heldman 2003). There are several ways to express this number and one of them is using Graetz number.

$$Sh = \frac{mass\ transfer\ velocity}{diffusion\ velocity} = 1{,}76Gz^{0{,}33} \qquad Eq.\ 6$$

Where $Gz = \frac{\pi}{4} Re\ Sc\ \frac{D}{L_t}$

Eq. 6 gives the Sherwood number for laminar flow inside a pipe as a function of Graetz number. This equation has been used to predict the internal mass transfer resistance for separation processes using hollow fiber membranes. (McCabe et al. 2005).

$$Sh = \frac{k * l}{D_w} = 0{,}023 * Re^{0{,}8} * Sc^{0{,}33} \qquad Eq.\ 7$$

Where $Sc = \frac{\nu}{D_v} = \frac{\mu}{\rho D_v}$

Eq. (7) shows the Sherwood number for turbulent flow for a wide range of Reynolds and Schmidt number (McCabe et al. 2005).

2.7.2 Graetz number

Graetz number gives the ratio between a liquids ability to transfer momentum to that liquids ability to transfer mass by molecular means.

$$Gz = \frac{momentum\ diffusivity}{molecular\ diffusivity} = \frac{\pi}{4} Re\ Sc\ \frac{D}{L_t} \qquad Eq.\ 8$$

Where $D = diameter\ of\ tube$

$L_t = length\ of\ tube$

Eq. 8: Gz is expressed by Re and Pr when dealing with heat transfer problems, but in the case of mass transfer Pr is replaced with Sc which deals with mass transfer problems (McCabe et al. 2005).

2.7.3 Schmidt number

Schmidt number is the ratio of the kinematic viscosity to the molecular diffusivity. It usually ranges from 10^2 to 10^5 for liquids (McCabe et al. 2005), and is expressed by:

$$Sc = \frac{kinematic\ viscosity}{molecular\ diffusivity} = \frac{\nu}{D_v} = \frac{\mu}{\rho D_v} \qquad Eq.\ 9$$

Eq. 9 shows Schmidt number for liquids and gases (McCabe et al. 2005).

2.8 Diffusion

2.8.1 Diffusion through membrane

This thesis focuses on the use of an artificial membrane for separation of material through the membrane. Separation in some membranes depends on the diffusivity of the membrane and the influence of the surroundings. *Diffusion is the movement, under the influence of a physical stimulus, of an individual component through a mixture* (McCabe et al. 2005).

As mentioned earlier, diffusion in membranes is caused by concentration gradients or pressure gradients. This means that if the concentration of a substance is greater on one side of the membrane, then the concentration gradient tends to move the substance so that the concentration difference equalizes. The same counts for the pressure gradient. The general form of describing chemical flux related to the concentration gradient is according to (Logan 2012).

$$J_A = -D_v \nabla c_A \qquad \textit{Eq. 10}$$

Where $j_A = molar\ flux\ of\ component\ A, [\text{mg}/cm^2\ \text{h}]$

$D_v = volumetric\ diffusivity, [cm^2/\text{h}]$

$\nabla c_A = concentration\ gradient\ of\ component\ A$

We can also calculate the flux through a membrane by using Fick's first law of diffusion for one dimensional problems.

$$j_A = -D_v \frac{dc_A}{db} \qquad \textit{Eq. 11}$$

Where $c_A = concentration, [\text{mg}/cm^3]$

$b = distance\ in\ direction\ of\ diffusion/thickness, [cm]$

Eq. 11 shows Fick's first law of diffusion for one dimension (McCabe et al. 2005).

The flux through a membrane may in many practical problems be affected by the convection if convection does not occur perpendicular to diffusion. In systems with fast mass transfer, the diffusion itself will be responsible for this convection. (Cussler 2009). In this thesis the phenomenon of convection is neglected as it is expected that the mass transfer will be creeping to slow.

2.8.2 Diffusion in liquids

Diffusivities for large spherical molecules in dilute solution can be predicted from the Stokes-Einstein equation, which was derived by considering the drag on a sphere moving in a continuous fluid (McCabe et al. 2005). This equation holds true by assuming creeping flow (very laminar), big spherical particles and no slip at surface (Logan 2012).

$$D_v = \frac{K_b T}{6\pi r_0 \mu} \qquad \textit{Eq. 12}$$

Eq. 12 is the Stokes-Einstein equation (Logan 2012).

Where $K_b = Boltzmann\ constant, [1{,}38 * 10^{-23}\ J/K]$

$T = Temperature, [K]$

$r_0 = Molecular\ radius, [cm]$

$\mu = Dynamic\ viscosity\ of\ fluid, [cP]$

Equation 12 is valid for large spherical particles in liquid. For smaller solutes (M < 400), the diffusivity is greater because the drag is less and another equation called the *Wilke-Chang equation* is used for determining the coefficient of diffusion (McCabe et al. 2005).

$$D_v = 7{,}4 * 10^{-8} \frac{(\psi_B M_B)^{0,5} T}{\mu V_A^{0,6}} \qquad \textit{Eq. 13}$$

Eq. 13 is the Wilke-Chang equation (McCabe et al. 2005) and is the most relevant to this thesis because the solute used in experimental work have a MW<400.

Where $D_v = diffusivity, [cm^2/s]$

$T = absolute\ temperature, [K]$

$\mu = Dynamic\ viscosity\ of\ fluid, [cP]$

$V_A = molar\ volume\ of\ solute\ as\ liquid\ at\ its\ normal\ boiling\ point,$

$[cm^3/g\ mol]$

$M_B = molecular\ weight\ of\ solvent\ [g/mol]$

$\psi_B = association\ parameter\ for\ solvent$

Recommended values of ψ_B is 2,6 for water (McCabe et al. 2005).

2.8.3 Effective diffusivity

The effective diffusivity is the net diffusivity when dealing with flow across a porous media. It is a product of the fluid diffusion coefficient (discussed in previous chapter) and membrane properties such as porosity (ε), tortuosity (τ) and constrictivity (δ). These are considered to be the most important parameters of microstructural effects of flow in porous media (Holzer et al. 2012). The porous media acts as a barrier to liquid diffusion. The resulting effective diffusivity accounts for the fact that (Fogler 2006):

1: Not all of the area normal to the direction of the flux is available (i.e., the area occupied by solids) for the molecules to diffuse.

2: The paths are tortuous

3: The pores are of varying cross-sectional areas.

The effective diffusivity can be expressed as follows:

$$D_e = \frac{D_v \varepsilon \sigma_c}{\tau} \qquad \textit{Eq. 14}$$

Eq. (14) shows the effective diffusivity (Fogler 2006).

2.8.3.1 Constriction factor

The constriction factor, σ_c, accounts for the variations in in the cross-sectional area normal to diffusion. It is a function of the ratio of the maximum to minimum pore cross sectional areas. When the maximum and minimum area are equal, the constriction factor equals 1. When the ratio, β, is equal to 10, then the constriction factor is approximately 0,5.

$$\beta = \frac{A_{max}}{A_{min}} \qquad \textit{Eq. 15}$$

Eq. (15) is the ratio of maximum to minimum cross section area in pore (Fogler 2006).

$$\sigma_c = f(\beta) \qquad \textit{Eq. 16}$$

Eq. (16) shows that the constriction factor is a function of the ratio of maximum to minimum cross section pore area (Fogler 2006).

2.8.3.2 Tortuosity

Tortuosity relates the arc length of a pore to the shortest distance between the openings of the pore. A straight line gives a tortuosity of 1, whereas a circle gives a tortuosity of infinity. By definition, tortuosity takes the simplest form in 2-D where it is defined as (Fogler 2006).

$$\tau = \frac{Actual\ distance\ molecule\ travels\ from\ A\ to\ B}{Shortest\ distance\ between\ A\ and\ B} = \frac{L_C}{C} \qquad \textit{Eq. 17}$$

Eq. (17) gives the tortuosity of a line in x-y plane,

Where $L_C = length\ of\ curve\ [m]$

$C = arc\ length\ [m]$

A report written by (Holzer et al. 2012), states that for membranes of electrolysis cells with porosities between 0,27 and 0,8, the tortuosity remains nearly constant at 1,6.

2.8.3.3 Constrictivity

The constrictivity, δ, should not be confused with the constriction factor. The constrictivity is also a parameter which influences the transport properties, but lies always between 0 (for trapped pores) and 1 (for cylindrical pores with constant radius). A geometrical definition of the constrictivity is still lacking and therefore not considered in this thesis. It is still important to know as much about those factors that may change our expectations.

According to Fogler (Fogler 2006), typical values for the constriction factor, the toruosity, and the pellet porosity are respectively, $\sigma_c = 0.8$, $\tau = 3.0$ and $\varepsilon = 0.4$. It is important to realize that these values are typical for a catalyst pellet and not necessarily the RC membrane used in this thesis.

2.8.4 Finding the diffusion coefficient

According to Cussler (Cussler 2009), the diaphragm cell method is a good method for determining the diffusion coefficients. The method consists of two cells, one with low concentration and one with high concentration, separated by a porous diaphragm. A big concentration difference between the two cells is required.

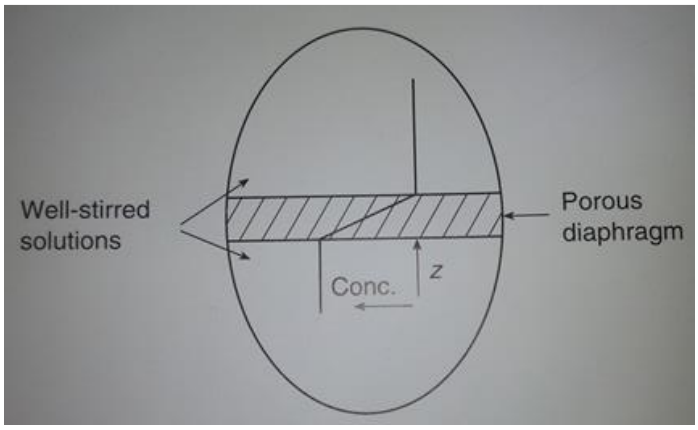

Figure 4: A diaphragm cell for measuring diffusion coefficients. (Cussler 2009).

The concentration profiles from the wall of the diaphragm /membrane and into the liquid indicates a well-stirred solution. The concentration profile within the membrane indicates a steady-state value and is because of the much smaller volume of the membrane than that of the cells. The flux across a membrane is given by equation 11 and is the same for this diaphragm cell.

$$j_A = \frac{D_v H}{l} * (c_1 - c_1^*) \qquad \textit{Eq. 18}$$

Eq. (18) gives the flux across a thin membrane. This equation is equal to Fick's first law of diffusion, only that the partition coefficient is involved. The partition coefficient is the concentration in the membrane divided by that in the adjacent solution (Cussler 2009).

Where $H = partion\ coefficient$

2.8.5 Osmosis vs dialysis

In osmosis, the solvent is moved from an area with low solute concentration, across a permeable membrane and into a region of higher solute concentration. The reason for this movement is the osmotic pressure across the membrane and that the nature seeks to obtain equilibrium. At equilibrium, the concentration difference across the membrane is zero.

Dialysis works almost the same way, but instead of the movement of liquid, we see movement of solute from a high concentration area to a low concentration area. This is also called reverse osmosis (RO). The separation of solutes is most often dependent on the pore size in the membrane.

2.8.6 Surface tension

Surface tension may offer some problems with diffusion. For example if a sponge is soaked in oil (till it's saturated) and then later put in water, the sponge will suck up very little or perhaps no water because of the surface tension of oil. There are membrane materials that is not suitable for separating different solutes because of their surface tension. See 5.3.6 and *(M. Cassidy, [personal communication, 28 jan. 2015]).*

2.9 Molecular size versus molecular weight

If one assumes spherical molecules it is possible to find the size of that molecule by knowing the MW and density. The following equation for estimating size of amino acids is actually meant for estimating protein size, as they tend to fold into globular domains (Harold 2009).

$$V\ (nm^3) = \frac{\frac{1}{\rho}\left(\frac{cm^3}{g}\right) * \left(\frac{10^{21} nm^3}{cm^3}\right)}{N_A} * MW(Da) \qquad \textit{Eq. 19}$$

Eq. (19) shows how the volume of a spherical molecule with density ρ and molecular weight MW can be calculated (Harold 2009).

The volume of a sphere is directly dependent on the radii of that sphere. Rearranging the equation for the volume of a sphere gives:

$$r_0 = \sqrt[3]{\frac{3V}{4\pi}} \qquad \textit{Eq. 20}$$

Eq. (20) gives the radius of a sphere.

2.10 Cross flow filtration

The membrane configuration of this thesis will be a mass flow as shown in figure 5. The ideal membrane for this kind of filtration should have a high porosity and a narrow pore size distribution, with the largest pores slightly smaller than the molecules to be retained (McCabe et al. 2005). As mentioned earlier, one way to classify membranes is to look at the molecular size of those molecules to be rejected. On the outside of the membrane, it should be a support with larger pores to minimize the hydraulic resistance. The yellow arrows indicates that more substance will permeate closer to the entrance of the membrane because of higher concentration of the permeating substance. Knowledge about the concentration profile in counterflow separation can come to use when estimating the dimensionless numbers. These numbers says something about the behaviour of the system, and is explained in chapter 2.7.

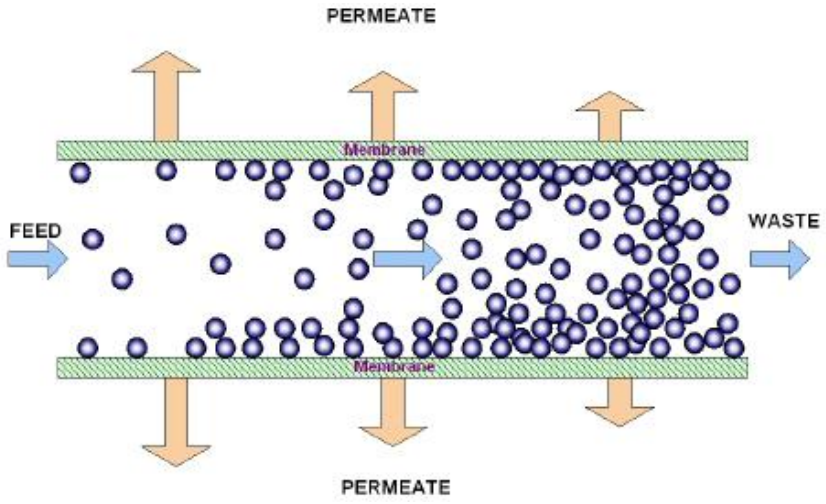

Figure 5: Cross flow filtration in membrane. (McCabe et al. 2005)

2.11 Content of undigested milk

The fluid flow, as well as diffusion will be dependent on the size and shape of the substances in the fluid. Therefore it was set up a table showing the most common nutrients of milk which is the fluid to be tested. Data of the most common nutrients are obtained from the report of *rheological Characterization of milk during digestion with human gastric and duodenal enzymes (Devle et al. 2012)* and by *(T. Devold, [personal communication, 11 mar. 2015]).*

Table 3: Shows the most common nutrients in undigested skimmed milk and the size and shape of these. Obtained from (Ulleberg 2011), (T. Devold, [personal communication, 11 mar. 2015]) and (Harold 2009).

Nutrients	Composition [g/L]	Amount [%]	Diameter [µm]	MW [kDa]	Shape
Lipids			1-4		
Casein protein	26-34	2,5-3	0,170-0,180	20	globular
Whey protein	10,9	1	0,130-0,510	15-60	globular
fat	32,7-43,6	3-4	3-4	346-461	globular
salts					

2.11.1 Lipids

In cow milk, lipid spheres range in diameter from 0,5 µm to 15µm. Spheres < 1µm are by far most numerous, but spheres in the range of 1-4 µm account for 90 % of the volume of milk lipid (H et al. 1988).

2.11.2 Casein protein

There are 4 different caseins (alfa S1-, alfa S2-, beta- and kappa casein). Their molecular weight is approximately 20 kDa. These are not present as a soluble solution but as colloidal aggregate. Thousands of casein molecules form this aggregate with a mean diameter of 170 – 180 nm. In milk with neutral pH level, they are stabile because of the negative excess charge. Furthermore the casein protein make up about 80 % of the total protein content in bovine milk (Ulleberg 2011).

2.11.3 Whey protein

There are several different types of whey protein with molecular weight of 15-60 kDa. These exist as a true soluble solution.

2.11.4 Fat

In unhomogenized milk, most of the fat is available as "solid" lumps more like an emulsion of oil in water. Their mean diameter range from 3 – 4 µm. The milk consist of about 3-4 % fat.

2.11.5 Salts

Salts exists as true soluble solutions, both as dissociated (Ca++, K+, Mg+, Cl-, SO4--) and undissociated (CaPO4). About 60 % of Calcium and phosphorus is bound to the colloidal aggregates of casein.

2.12 Fluid mechanics

Fluid mechanics is an important part in this thesis because diffusion may be dependent on the flow of the liquid. It will also play an important part in how the substances in the fluid are distributed. For example, the transition from the tube "small intestine" into the membrane "house" may cause vortexes, which can be a collection point for these substances. Another important factor is the velocity of the substance relative to that of the fluid.

2.12.1 Pressure drop in tubular pipe

The pressure drop in a circular pipe with fully developed flow is expressed by Eq. (21). It is expressed in terms of dynamic pressure and friction factor (Çengel 2003).

$$\Delta P = f * \frac{L_t}{D} * \frac{\rho \bar{V}^2}{2} \qquad \textit{Eq. 21}$$

Where $f = friction\ factor$

The friction factor is dependent on whether the flow is laminar or turbulent. For a fully developed laminar flow, the friction factor is independent on the roughness of the tube and is given by Eq. (22) (Çengel 2003).

$$f = \frac{64}{R_e} \qquad \textit{Eq. 22}$$

For fully developed turbulent flow in pipes the friction factor can be decided by using the Colebrook equation, Eq. (23). It is dependent on surface roughness and Reynolds number (Çengel 2003).

$$\frac{1}{\sqrt{f}} = -2.0\log\left(\frac{\varepsilon/D}{3.7} + \frac{2.51}{R_e\sqrt{f}}\right) \qquad \textit{Eq. 23}$$

2.12.2 Reynolds number

There are tens of different dimensionless numbers in fluid mechanics for describing relationships between physical properties and/or states. Some of them already mentioned. One of the first of these numbers that was introduced is the Reynolds number and is used in most fluid mechanics issues (Bar-Meir, Genick). "*The Reynolds number can be viewed as the ratio of the inertia forces to viscous forces acting on a fluid volume element"* (Çengel 2003). It is a dimensionless number that tells us whether a fluid moves with a laminar or turbulent flow. For liquid in a tube, the flow is always laminar as long as the Reynold's number is below 2100, but may be laminar even for numbers greater than 2100 (McCabe et al. 2005).

$$R_e = \frac{inertia\ forces}{viscous} = \frac{D\bar{V}\rho}{\mu} = \frac{D\bar{V}}{\nu} \qquad \textit{Eq. 24}$$

Eq. 24 is the Reynolds number for a Newtonian fluid (McCabe et al. 2005).

Where $D = Diameter\ of\ tube\ [m]$

$\bar{V} = Average\ velocity\ of\ liquid$ [m/s]

$\rho = Density\ of\ liquid\ [kg/m^3]$

$\mu = Dynamic\ viscosity\ of\ liquid\ [kg/m * s]$

$\nu = kinemtic\ viscosity\ of\ liquid\ [m^2/s]$

2.13 Rheology

"Rheology is the science of the deformation and flow of matters. There are three ways to deform a substance; shear, extension, and bulk compression" (Tysse 2014). The reason for considering the rheology is that it may have an effect on separation through the membrane. The diagram below comes in handy when doing tests with rheological monitoring as this will give an indication to what kind of fluid behaviour the system deals with.

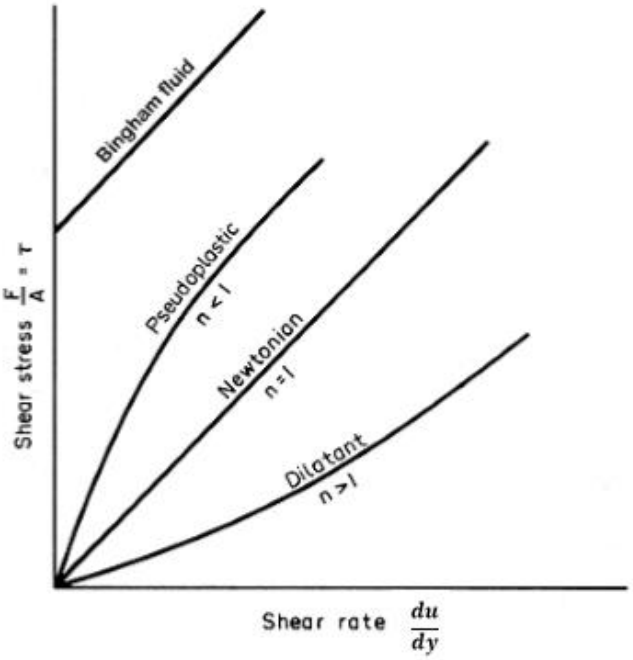

Figure 6: Relationships between shear stress and shear rate in different kind of fluids at constant pressure and temperature. Obtained from (Tysse 2014). The n-value represents the fluid flow behaviour.

2.13.1 Viscosity

Viscosity is a fluids resistance to flow, which is supplied by the internal stickiness of the layers that move parallel to each other. This means that a viscous fluid is more difficult to make flow than a less viscous fluid. This will of course have an effect on the separation in a membrane. It is the cohesive forces between the molecules that determines the degree of viscosity and if these forces are great, then the molecules will have problems detaching from one another and the opportunity for separation decreases (Çengel 2003).

2.13.2 Rheological properties of water

The tests executed in this project are with water added with Evan's blue, L-tryptophan or P-nitrophenol. Evan's blue is a colorant, L-tryptophan is an amino acid and P-nitrophenol is a phenolic compound. Water is a Newtonian fluid which means that the relationship between shear stress and shear rate is constant and that the shear stress is a result of shear rate. See figure 6. The dynamic viscosity of water at 35˚C is $0{,}720*10^{-3}$ kg/m*s (Çengel 2003).

2.13.3 Rheological properties of milk

Milk or milk products is the intended fluid for this project, and the differences in properties of these varies depending on the type of milk product. The first tests with milk products will most likely be whole milk or skimmed milk. These have a water content of 88% and 91% respectively. The viscosity of whole milk at 20˚C is $2{,}12*10^{-3}$ kg/m*s. The viscosity of skimmed milk at 25˚C is $1{,}4*10^{-3}$ kg/m*s (Tysse 2014). These are expected to fall as temperature rises.

2.14 Spectrophotometry

Spectrophotometry is a way to measure the amount of substance in a solution by sending a beam of light through that solution. The idea is that the intensity of the light that is sent through (incident light beam) the solution changes because the molecules in the solution absorbs some of the beams at certain wavelengths. Which wavelengths that are absorbed and how many beams of light that are absorbed is dependent on the molecules and the amount of molecules respectively. The light that is not absorbed is called "transmitted light beam". The spectrophotometer measures the absorbance (ABS) which is only a number without units. Trough Beer Lamberts Law (discussed later) or from a standard curve, it is possible to relate ABS to the concentration of the solute (Eijsink et al. 2014).

2.15 Standard curve

The SPM is used to detect solutes in a solvent. This is done by sending a light beam through a cuvette containing the sample as explained above. A standard curve expresses the relationship with the measured ABS value in the SPM and a concentration in the solvent. By making a solution of known concentration and measuring the ABS value, it is possible to make

a standard curve for that solute at a specific wavelength. In order to get a curve, one needs to measure the ABS after every dilution. Three dilutions is a minimum.

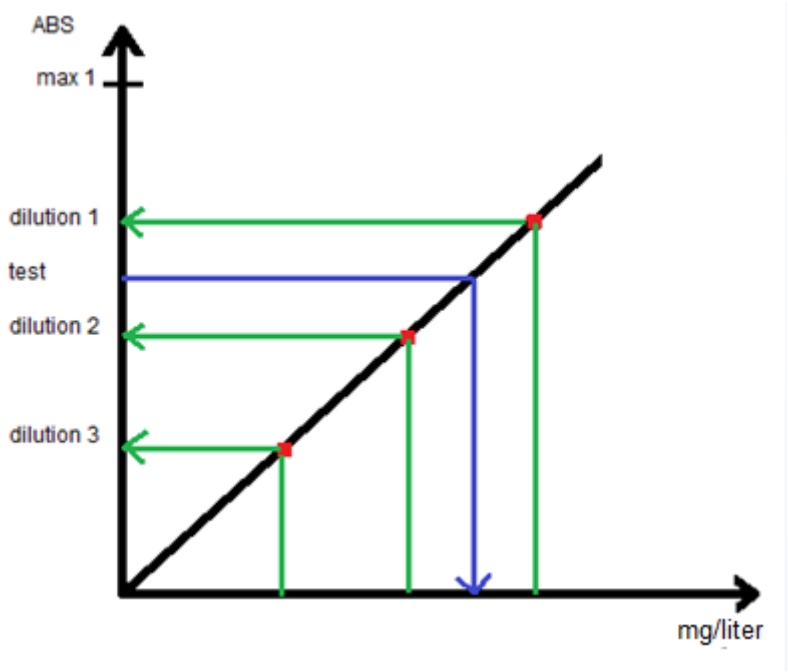

Figure 7: To make a standard curve for a solute, a known concentration is diluted x number of times and between every dilution run through a SPM to measure absorbance of light (ABS). This yields a more or less straight line. For a given ABS value of that solute, one can read the concentration.

If the use of the SPM proves that there is a linear relationship between absorbed light and the concentration of a sample, then it is possible to use Beer-Lambert law to calculate the concentration.

$$ABS = \epsilon b c_A \qquad \textit{Eq. 25}$$

Eq. (25) is the Beer Lambert law

Where $ABS = absorbance$

$\epsilon = absorptivity\ [L/mol * cm]$

$b = path\ length\ of\ sample\ [cm]$

$c_A = concentration\ [mol/L]$

2.16 Absorption of wavelength

In this thesis, the use of one amino acid called L-tryptophan and another phenolic compound called P-nitrophenol will be used as feed in the membrane. They absorb light at wavelength 280 nm (Scmid 2001) and 400 nm respectively. 400 nm represents the color yellow which is the color of P-nitrophenol.

L-tryptophan is an aromatic amino acid because of its aromatic side chain. This side chain absorb light in the far-UV range (180-230 nm) (Scmid 2001).

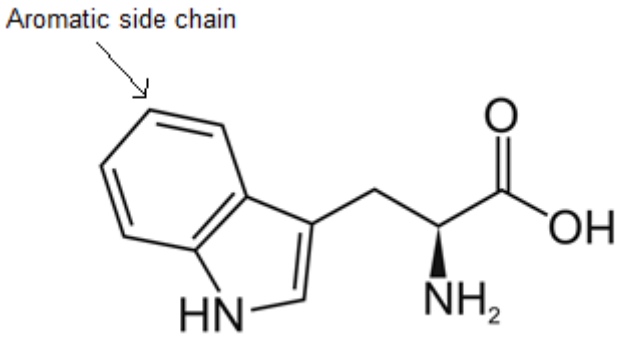

Figure 8: This picture illustrates the structure of L-tryptophan with its aromatic side chain. Picture taken from (en.wikipedia.org/wiki/Tryptophan, 04.05.15).

3 Prototype development

3.1 The model of the system

The setup of the system is shown in figure 9 below. There are three pumps that pump fluids in their respective circuits. Pump 1 is for the buffer circuit. Pump 2 is for the intestine circuit and pump 3 is for the stomach circuit. Pump 3 works alone and is turned off when pump 1 and 2 is turned on because of volume limitations. The dosing mechanism for HGJ is not presented in this thesis, but will in practice be a syringe of some kind. The working method of the titrator is also not considered but attachment mechanism for the titrator has been made.

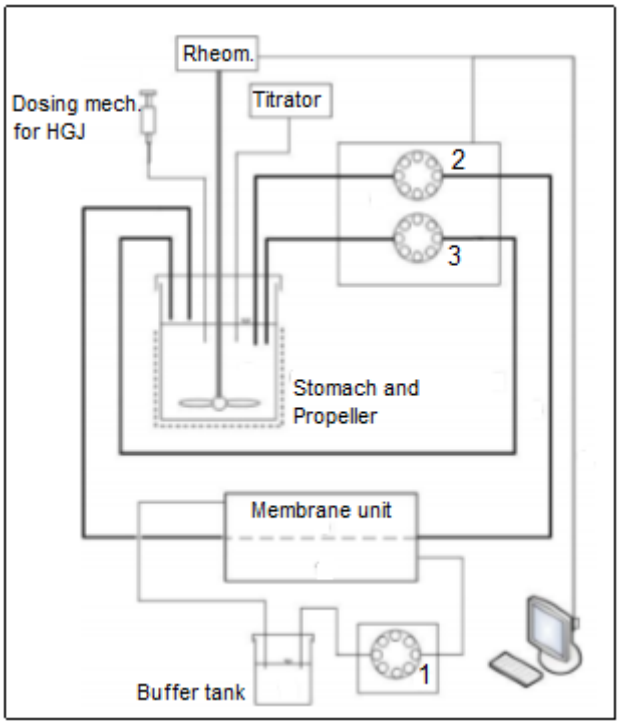

Figure 9: This picture shows the simulation of both stomach and membrane (Salas-Bringas et al. 2014).

3.1.1 Method

The testing of the system can be divided in three steps. First the mixing of the milk and saliva for half hour. This can be accomplished without any hoses. After thirty minutes HGJ is added and the hoses are attached, but only through a peristaltic pump. The volume of these hoses cannot be bigger than the volume of these three fluids (14,5 ml) that are added. The volumes are given in table 4. Lastly the HDJ is added and the membrane is connected to the system. This significantly increases the volume of the intestine system and it cannot be bigger than the total volume of fluid which is 29 ml.

*Table 4: The composition of the digestive fluid in the apparatus, divided in four steps. *Acid or base needed to calibrate the pH level to pH < 2 is included in this volume. (Tysse 2014).*

Step	Added component	Volume [ml]	New total volume [ml]	pH	Time approximately before next step [min]	Comment
1	Milk	3,625	3,625	6-7	0	Mixed and pH measured outside the apparatus
2	Saliva	3,625	7,250	6-7	0	
3	HGJ	7,250	14,5	<2	30	All three components are mixed in the cup.
4	HDJ	14,5	29,0	6-7	60	Added to the mix in the cup

3.1.2 Volume control

To figure out the volume of the intestinal system, a very exact measurement of the intestinal volume was done. The result is given in table 5.

Table 5: This table shows all volumes in the intestine part. The length of the hose has been shortened.

Intestine part			
Part	**Dimensions [mm]**	**Volume [mm^3]**	**Volume [ml]**
Hose			
Diameter	3,17	9466,1	9,5
Length	1200		
Intestine glass			
Diameter	10	5024,0	5,0
Length	32		
Transition zone			
Big diameter	10	1797,7	1,8
Small diameter	3		
Length	15		
Membrane			
Diameter	12	11304,0	11,3
Length	50		
Total volume in hoses and membranes			**27,6**

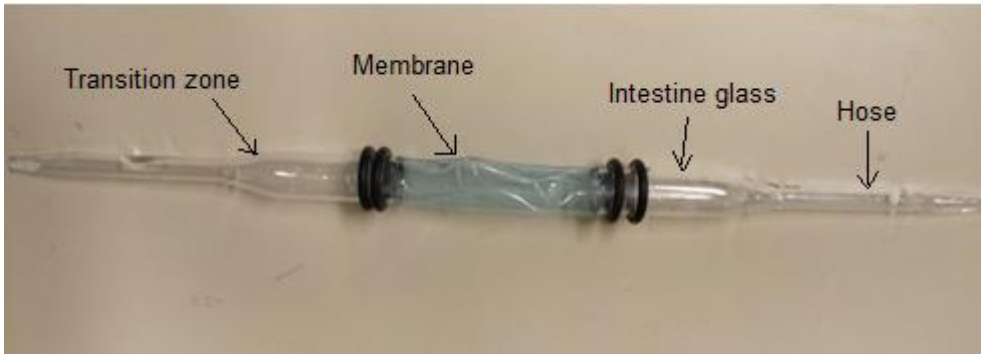

Figure 10: This picture shows all the parts that were considered when calculating the volume of the intestine.

The total volume is very close to 29 so it is necessary to check how high the fluid will stretch when the volume is only 1,4 ml. This is important to know because the hoses that goes into the stomach must reach below fluid surface. The right answer is (if the bottom of the stomach is planar) about 1,2 mm, but because of the practical difficulty of making the stomach, the bottom of the stomach is not planar, but stretches conically up into the stomach about 4 mm. This will increase the height of the fluid.

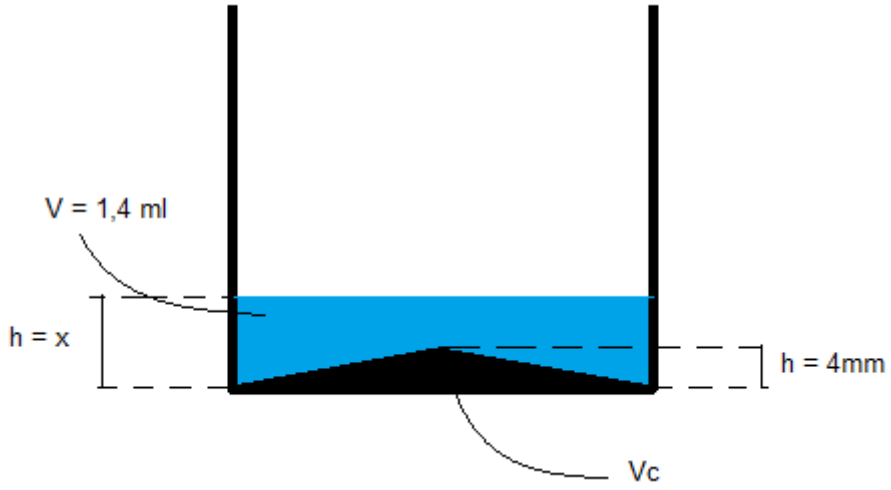

Figure 11: This picture illustrates how the inside bottom of the stomach reaches up into the volume of the stomach.

$$Vc = \frac{1}{3}Gh = \frac{1}{3}\pi r^2 h = \frac{1}{3}\pi * 18{,}75^2 * 4 = 1472\ mm^3$$

$$V = \pi r^2 h - Vc = 1{,}4\ ml = 1400 mm^3$$

$$h = \frac{1400 + 1472}{\pi * 18{,}75^2} = 2{,}6\ mm$$

2,6 mm is more than double of what we would have if the bottom of the glass was not conical. The conical bottom is actually a smart design because we deal with so small volumes.

3.2 Problem with membrane slipping of the glass

3.2.1 Possible solutions

3.2.2 Wider O-rings/multiple O-rings

To prevent the membrane from slipping off the glass, one idea was to get wider O-rings to ensure a greater contact area between the glass and the membrane which would increase the friction.

In the end it was decided to use multiple O-rings instead of using a lot of time on tracking down wider O-rings.

3.2.3 Bigger Buffer glass

The buffer glass made for prototype 1 was very small in inner diameter and even smaller when the O-rings were attached. This very point at which the O-rings were attached might have been a point of a relatively big pressure drop, causing the O-rings to slide long side the glass and eventually falling off. A bigger buffer glass was made as part of this solution.

3.1.2 O-ring mounting mechanism

To make the attachment of the membrane easier, a plastic tube with the same shape of the intestine glass, but bigger in diameter was 3D printed. This plastic tube is what is referred to as the O-ring mounting mechanism and is slided over the intestine glass, as shown in figure 12. The O-rings are rolled from the back end of the O-ring mounting mechanism and up the big diameter of the O-ring mounting mechanism. From there it is rolled off the O-ring mounting mechanism and on to the big diameter of the intestine glass. If a membrane is covering the tip of the big diameter of the intestine glass it will be caught between the O-ring and the intestine glass as intended.

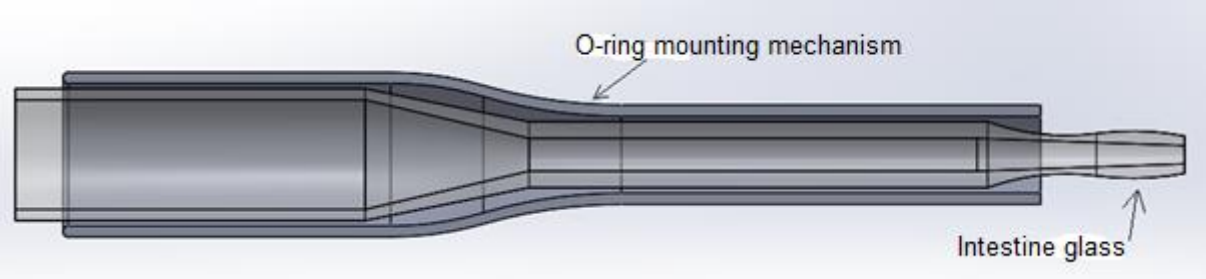

Figure 12: The picture shows the Intestine glass and O-ring mounting mechanism put together.

3.3 Diffusion through membrane

One of the biggest problems in the first prototype was the permeation of the colorant Evan's blue. The report of prototype 1 (Tysse 2014) states that the size of the pores (or the cut off size) in the membrane is 3,5 kDa. The particle size of Evan's blue is approximately 1 kDa. Nevertheless, testing in prototype 1 shows that there was no diffusion of the colorant. See "experimental work" for details on this topic.

Instead of using Evan's blue it was experimented with one amino acid called L-tryptophan and another phenolic compound called P-nitrophenol and this gave diffusion.

3.4 RC membranes

RC stands for *regenerated cellulose*, and are a cellulose-based dialysis membrane. These membranes are low flux membranes. They are also very thin and highly hydrophilic which means that the membrane surface is easily wetted (Neligan). The membranes can be used with dilute strong acids and bases, concentrated weak acids and bases, most alcohols and some mild or dilute organics, including DMSO. Standard RC can tolerate pH 2 - 12 and temperatures 4 – 121 °C. The membranes have a symmetric porosity (Spectrumlabs).

Table 6: The table gives a review of the membranes that have been tested in this thesis.

Part No.	Grade	MWCO	Flat width	Diameter	Volume or vol/length	Package
132110	Standard	3500 Da	18 mm	11,5 mm	1,1 ml/cm	Wet
128358	Standard	8000 Da	18 mm	11,5 mm	1,1 ml/cm	Wet
132680	Standard	12-14 kDa	45 mm	29 mm	6,4 ml/cm	Dry

3.5 Evan's blue

This is a blue colorant with the chemical formula; $C_{34}H_{24}N_6Na_4O_{14}S_4$ and a molecular weight of 960 g/mol, almost 1 kDa. The reason for choosing this feed in certain tests was to get a visual effect of the testing or to detect leakages.

3.6 L-tryptophan

L-Tryptophan has the molecular formula $C_{11}H_{12}N_2O_2$ which yields a MW of 204,23 g/mol. The density is 1,34 kg/liter (Chemicalbook.com). This solute comes as powder so it is very easy to make whatever concentration that is desired. The powder has no color and diffusion is therefore not as easily detected. L-tryptophan is not 100 % soluble in water which makes the mixing more difficult. Applying Eq. 1 gives a volume of 0,253 nm^3 with the accompanying radius of 0,392 nm which is the diameter of 0,784 nm.

3.7 P-nitrophenol

P-nitrofenol has the molecular formula $C_6H_5NO_3$, which yields a MW 139,11 g/mol. The density is 1,27 kg/liter (Chemicalbook.com). This solute was already mixed with water. The concentration of the compound is 1mM (millimolar). The solution has a yellowish color for easy detection of diffusion. Applying Eq. 1 gives a volume of 0,182 nm^3 with the accompanying radius of 0,352 nm which is the diameter of 0,704 nm.

3.8 Parts of the system

3.8.1 Stomach

The volume of the stomach is the first part to start with when making a new prototype in solidworks. It should contain the gastric and duodenal fluids, and also those fluids from food intake (saliva and milk). From (Tysse 2014) the volumes of the different fluids in the stomach are given in table 4 (see chapter 3.1.1). These values is adopted in this work as well.

The new stomach is transparent, so that it is possible to see through it and the diameter is increased to make it easier to place equipment inside. The height of the stomach is also smaller which will also make it easier to place equipment inside. See appendix A.

3.8.2 Hoses

The hoses that are used were picked out during development of the first prototype. Through testing (Tysse 2014), it was discovered that an inner diameter of 3,17 mm would prevent lumps (problem with milk products) to get stuck in the opening, while still obtaining a desired flow rate.

Table 7: The table shows previous result of testing of three different hoses (Tysse 2014). Milk was used as fluid.

Hose size i.d [mm]	Flow through	Lumps stuck	Concerns
1,6	No	Yes	No flow through, lumps stuck in the opening
3,2	Yes	Minimal	Although most of the lumps got through, some stayed stuck to the tube wall, when trying to empty the tube
8,0	Yes	No	Lumps stays stuck to the wall, the wetted perimeter was too small

3.8.3 Buffer glasses

The buffer glass that is used in this thesis has a bigger diameter than the buffer glass in the first prototype. The motive for this change was that the gap between the outer diameter of the "intestine" and the inner diameter of the buffer glass was very small.

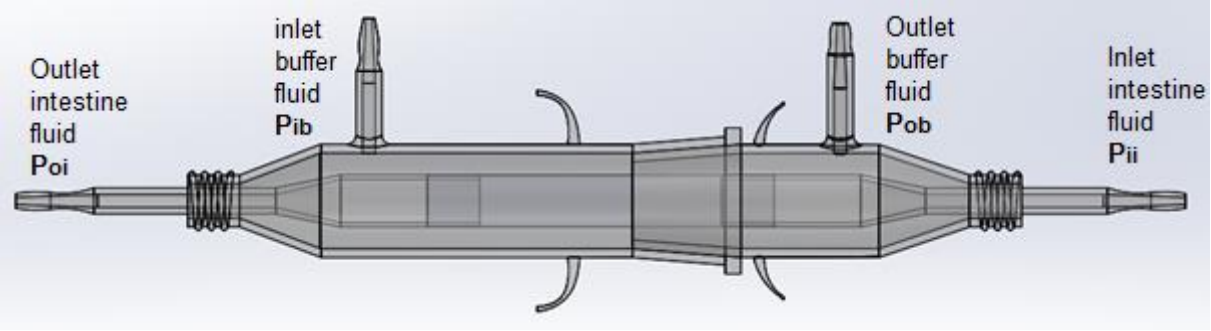

Figure 13: The gap between the buffer glass and small intestine is very small which causes a big pressure drop. This pressure drop will increase to an even higher level when the O-rings are attached.

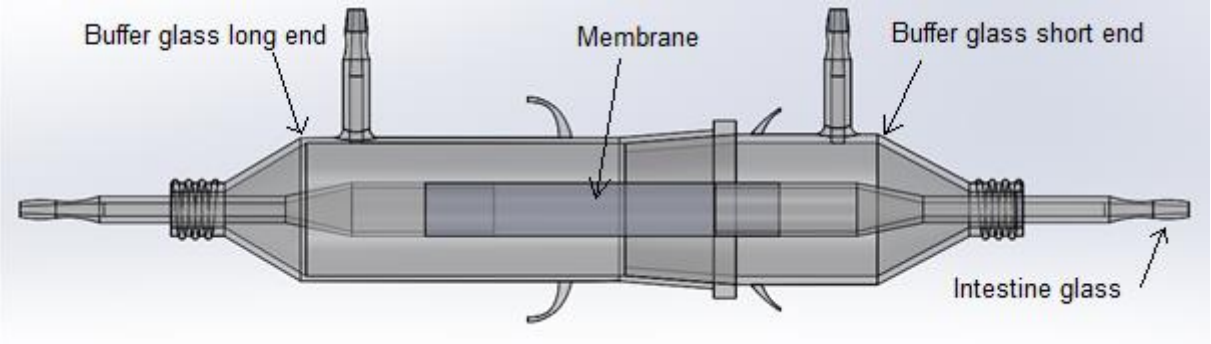

Figure 14: This picture shows the design of the new membrane unit. It shows that the gap between the buffer glass and the small intestine is bigger, thus leaving more room for the O-rings and decreasing the pressure drop.

Figure 14 shows the new buffer glass with bigger diameter which will decrease the pressure drop in throughout the glass. See appendix B and C.

3.8.4 Intestine glass

This part looks the same as it does in the first prototype. However it has also been made with a smaller inner diameter for the outlet opening. The reason for this is to try to get a bigger pressure inside the membrane so that the collapse of the membrane will be less. The negative side effect will possibly be that lumps get stuck in the small diameter, but this needs to be tested.

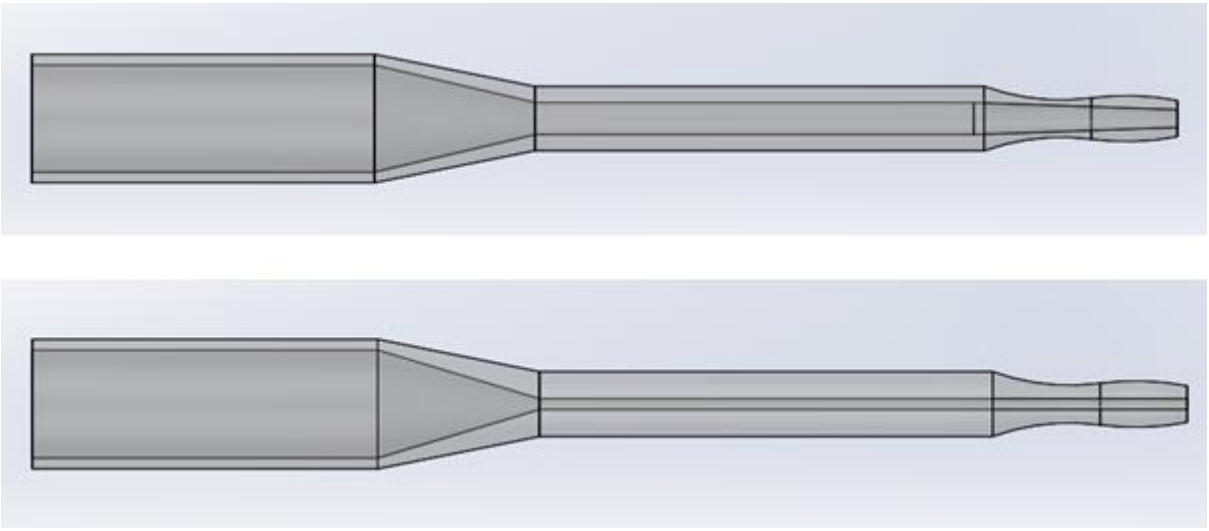

Figure 15: The upper picture shows the intestine glass with the original outlet diameter (3mm). The picture below shows the intestine glass with 1mm outlet diameter.

3.8.5 Water bath

The water bath functions as the source of heat. It should imitate the surrounding temperature of the stomach which is 37℃. The water bath is made rectangular so that looking through the glass is easier than when looking through a circular glass. The water bath also functions as a stand for all the equipment used in the testing of the system and is part of the reason for making it rectangular. This makes it easy to place the equipment around the stomach. See appendix D.

3.8.6 Centring brackets for water bath

To be able to place the water bath right in the centre of the rheometer probe it was necessary to make a centring mask. It was done by using the heating element of the rheometer because it is concentric with the probe. The heating element was thus used as a reference when making the "centring brackets for water bath". See appendix E.

3.8.7 Centring brackets for stomach

Since the stomach goes inside the water bath, this also needs to be concentric to the probe and the centring brackets make sure of this. It is not desirable to have too many things surrounding the stomach as that will decrease heat transfer from the water bath to the stomach. On the other side it is important to make sure that the stomach does not float up when water is added to the water bath. See appendix F.

3.8.8 PH mounting foundation

The mounting foundation is one of the parts that is attached to the side of the water bath. Its purpose is to hold the PH sliding mechanism and to serve as a platform for this sliding. See appendix G.

3.8.9 PH sliding mechanism

This part was made so that it was possible to change the position of the tip of the PH meter and to lower and raise it. Positioning marks (6mm apart) on the sliding arm were also made because it should be possible to place the arm exactly in the same place as previous tests. In this way the repetitively properties of the system is maintained. See appendix H.

3.8.10 PH holder

The PH holder is attached to the PH sliding mechanism, and also has the opportunity to slide so that it is possible to lower and raise the PH electrode. It is equipped with a small arm for making it easier to slide it. See appendix I.

3.8.11 DC motor mounting foundation

This part was originally made considering the option of rasing and lowering the DC motor propeller. The propeller is supposed to distribute heat in the water bath. A kind of angle elevation design was produced and is presented in the picture below. See appendix J for details.

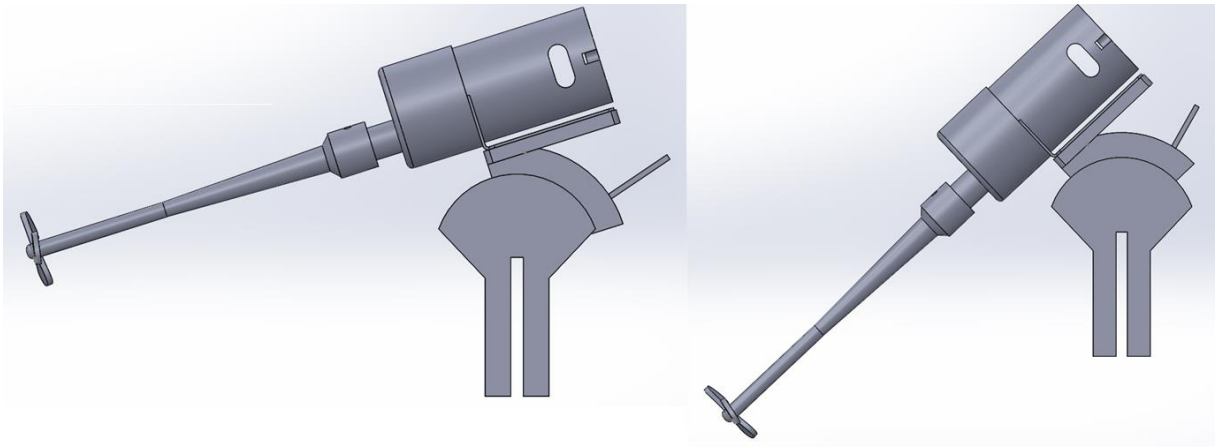

Figure 16: The situation to the left shows the propeller in an elevated position. The picture to the right shows the propeller in a lowered position.

3.8.12 DC motor holder

This is the part where the DC motor is attached and it is the part that rotates around the top of the DC motor mounting foundation. See appendix K.

3.8.13 DC motor propeller

The only function of this part is to ensure a good distribution of heat in the water bath. See appendix L.

3.8.14 Hose fixture for stomach and water bath

Two parts were made for leading the hoses down the “stomach”, so that they did not interfere with the rheometer propeller. One of the parts is attached to the water bath and the

other part is attached to the centring brackets of the stomach. The hose fixtures make sure as little as possible of the hoses are used and that they slide down the side of the inner diameter of the stomach. The propeller rotates without hitting the tubes. The hose fixtures decreases the amount of hoses that is used which is a good thing considering the small volumes available. See appendix M and N.

3.8.15 Buffer glass fixture 1 and 2

To make the system as compact as possible the buffer glass should hang on the outside of the water bath. Inside would be better, but the water bath was too small. A criteria was that the buffer glass should have an inclination to avoid the problem of air bubbles (Tysse 2014). The design is inspired by the design of May Helen Tysse last year for the same problem. See appendix O and P.

3.8.16 Buffer tank with lid

The buffer tank was designed considering the possibility of making a lower pressure inside the buffer circuit. The motive of doing this was to remove the problem of collapse. In that case it was necessary to close the circuit and therefore it comes with a lid. See appendix Q.

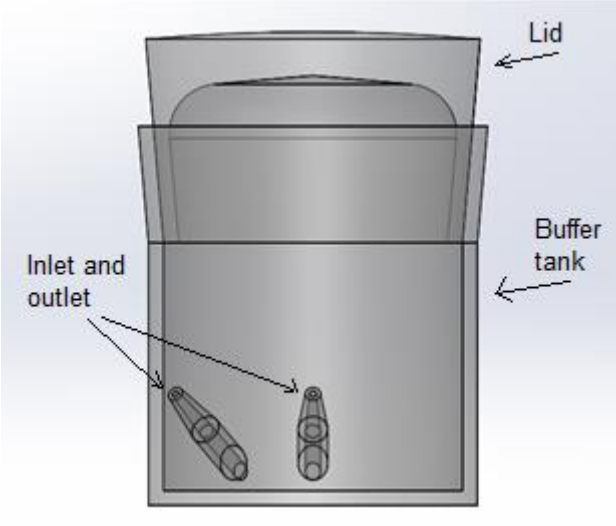

Figure 17: Picture of the buffer tank and lid.

4 User manual

Prototype II of an in vitro dynamic model of the stomach and small intestine

4.1 Parts

Table 8: This table consists of all parts used in the system and a numbering system.

Part nr.	Name	Abbreviation	Qty.	3D printed/glass blasted
1	Centring brackets for water bath		2	3D
2	Water bath		1	Glass blasted
3	Centring brackets for stomach		2	3D
4	Stomach		1	Glass blasted
5	Hose fixture for stomach		1	3D
6	Rheometer propeller	RP	1	3D
7	Rheometer propeller extension	RP extension	1	
8	Buffer tank with lid		1	Glass blasted
9	Hose fixture for water bath		1	3D
10	PH mounting foundation		1	3D
11	PH sliding mechanism		1	3D
12	PH holder		1	3D
13	DC Motor mounting foundation		1	3D
14	DC Motor holder		1	3D
15	DC Motor propeller		1	3D
16	Buffer glass fixture 1		1	3D
17	Buffer glass fixture 2		1	3D
18	Buffer glass long end		1	Glass blasted
19	Buffer glass short end		1	Glass blasted
20	Intestine glass		2	Glass blasted
21	Hose		5	
22	Membrane		1	
23	Hose connectors		4	
24	O-ring		4	
25	O-ring mounting mechanism		1	3D
26	Peristalsis		3	
Equipment nr:	**Type of equipment**		**Qty.**	
27	Peristaltic pump		1	
28	DC Motor		1	
29	Rheometer		1	
30	Cooler		1	
31	Spectrophotometer		1	
32	PH electrode		1	
33	Power supply DC motor		1	

4.2 Part numbering

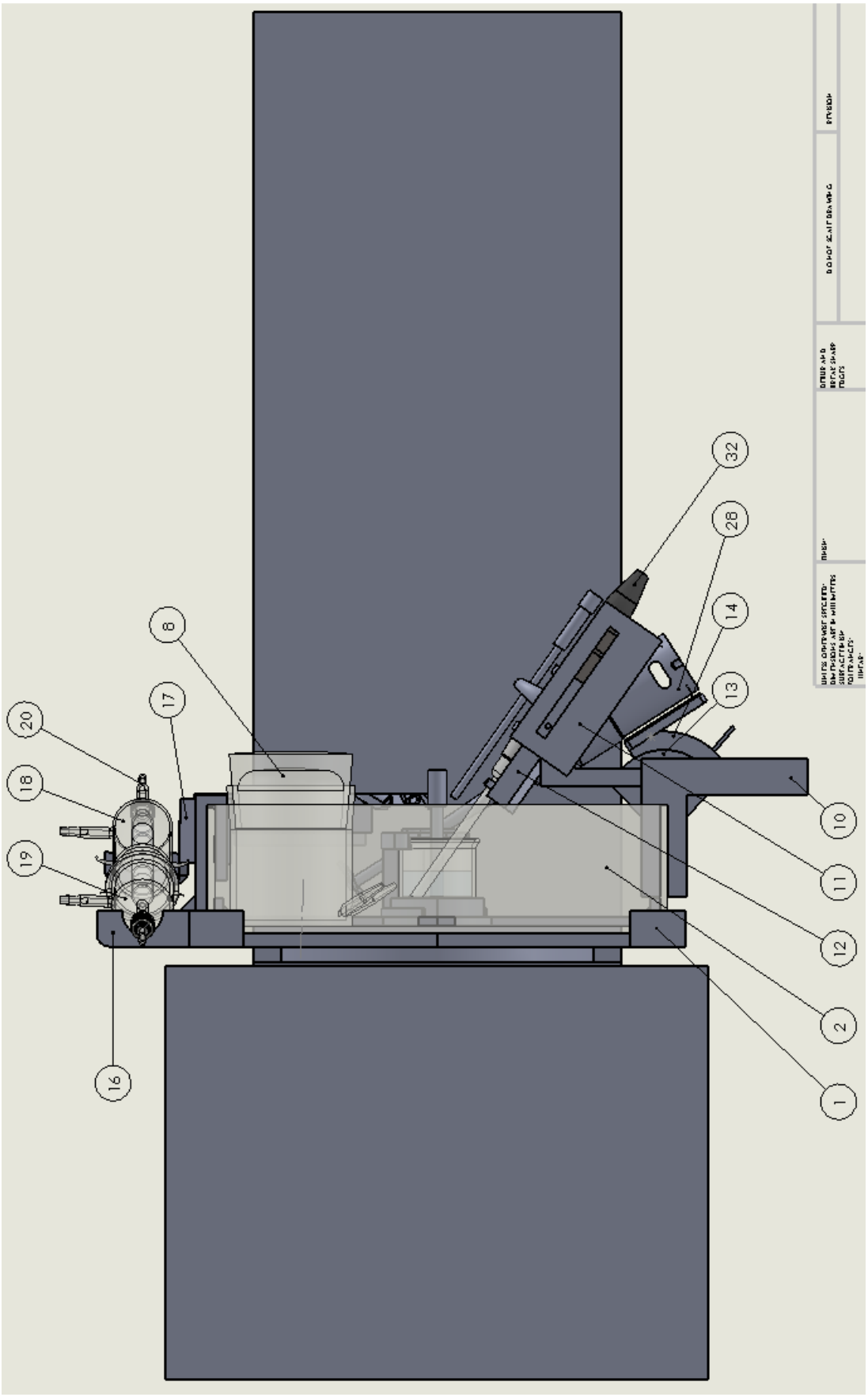

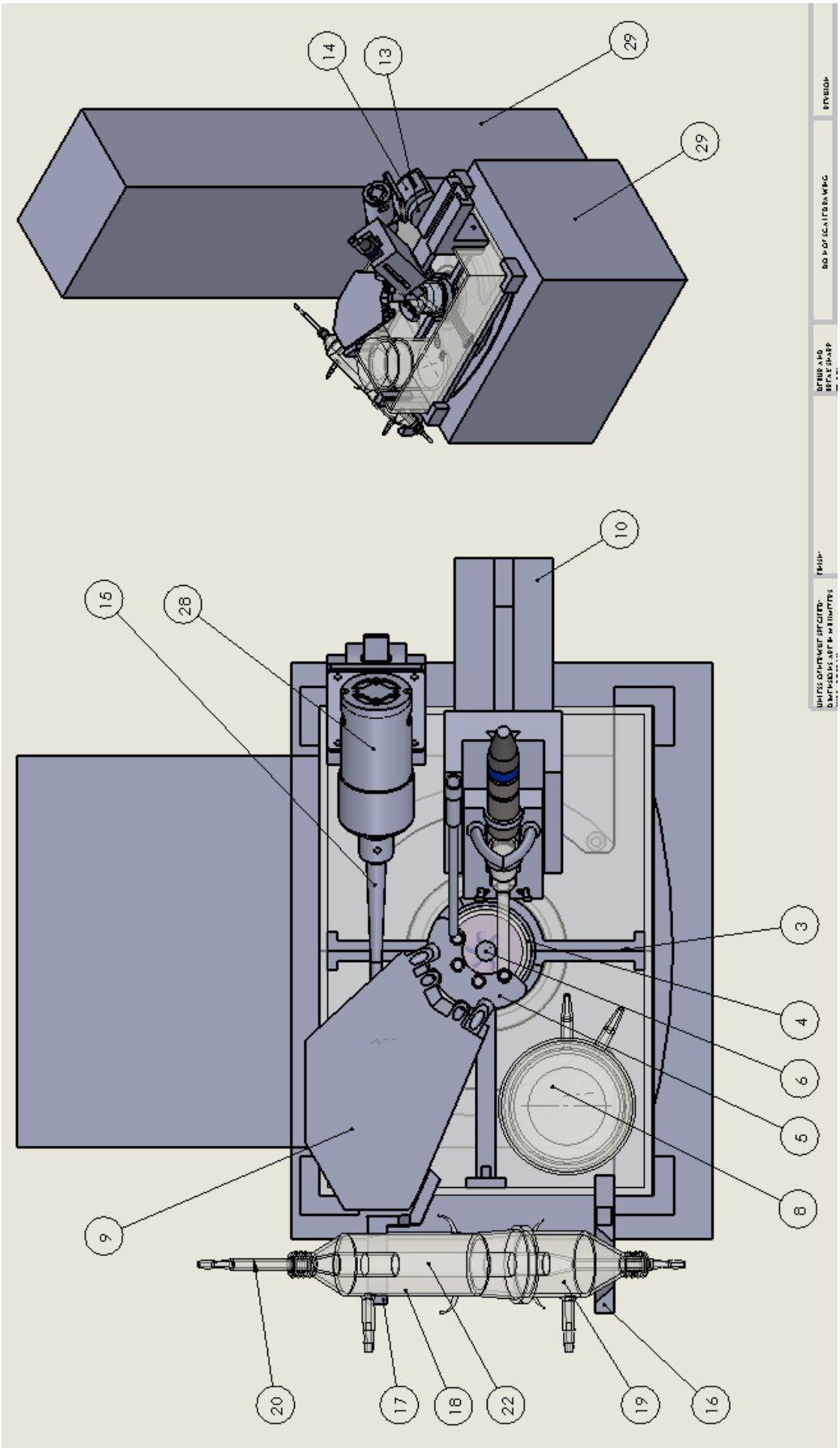
14
13
29
29
10
15
28
3
4
6
5
8
9
20
17
18
22
19
16

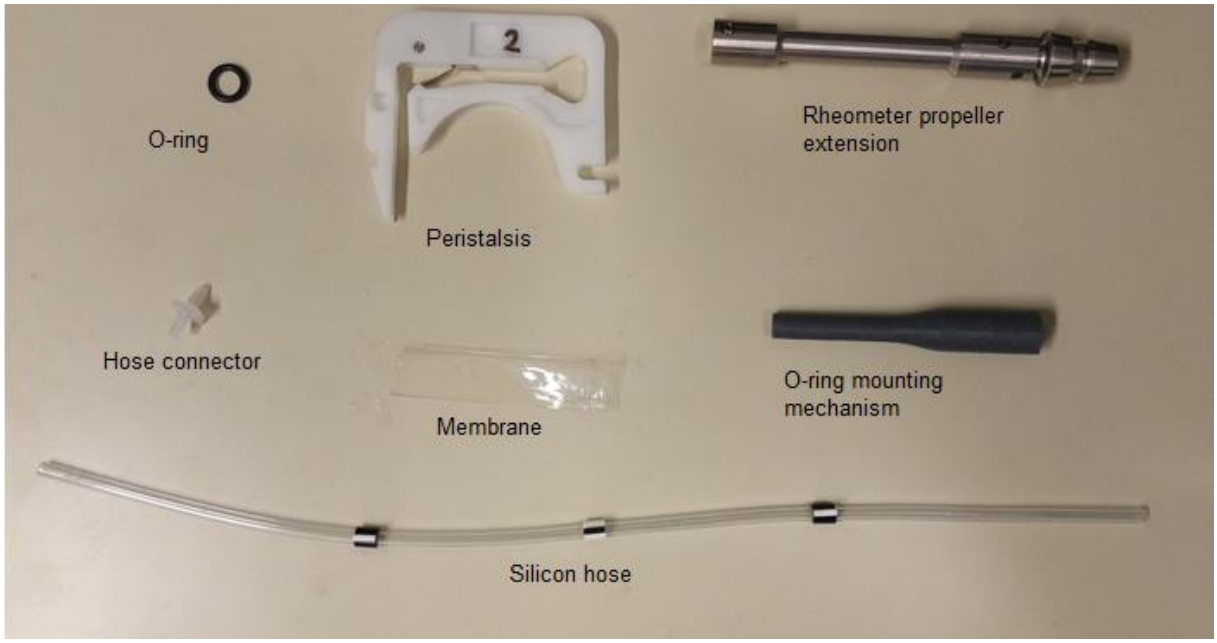

4.3 Setup guide

This setup guid is explicitly for testing with water and amino acids. When testing with milk, the adding of the fluids will be different than explained in this guid. The physical setup of the parts will be the same. By following this guide systematically, you make sure that everything is in order before starting the tests. T

4.3.1 Ready the UDS200 and Rheometer

1. Turn on Physica UDS200, the computer and Lauda Ecoline.
2. Login to the user Physica
3. Open UDS 200
4. File – open - stian – basic.orx
5. Let the system load (the UDS 200 displays “loading” while loading. It might take a few minutes)
6. Double click “MC200 stian” and let the system load (the UDS 200 displays “loading” while loading. It might take a few minutes)
7. Click initialization (this elevates/lowers the probe connector of the rheometer to its starting point).
8. Click lift position (this option elevates the probe connector to a certain point chosen by us. It can be changed under settings)

9. Wait for the probe connector to stop and attach the RP extension (metal shaft). It is easier to remove the RP extension when placing the hoses. The picture below shows a red ring around the RP extension. The prototype should not be connected at this point.
10. Add a thin layer of thermo conductive paste on the heat surface of the rheometer and put the prototype in place. It should look like this.

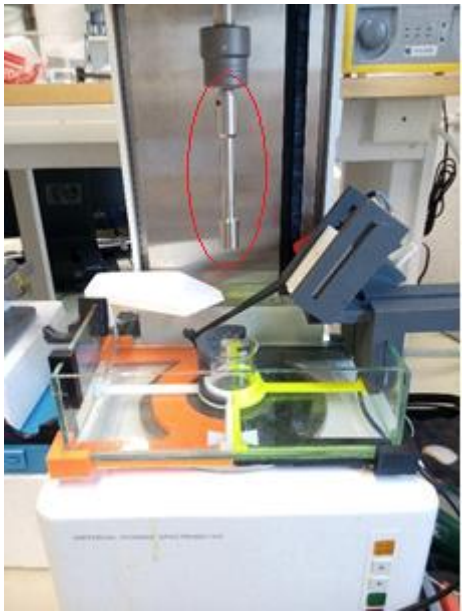

11. Fill the aquarium with water that is not too cold. This reduces the amount of time required to heat the water to 37 degrees.

Before proceeding, prepare a mixture for the feed (e.g. L-tryptophan), you should do it before proceeding to the next step, because some amino acids (in powder form) takes a lot of time to dissolve. Cut a piece of membrane at this point because it should lie in water for some minutes before put to use (see assembling the membrane unit for info on cutting membrane).

4.3.2 Ready the prototype for testing

1. Place the peristaltic pump and the water bath in place. The peristaltic pump should be elevated 27 cm from the bottom of the rheometer and placed as pictured here. If the prototype is used without the rheometer (that is the prototype is placed directly onto a table) it is not necessary to elevate the peristaltic pump. The important thing for saving the amount of hoses used, is that the bottom of the pump is at the same level as the bottom of the prototype.

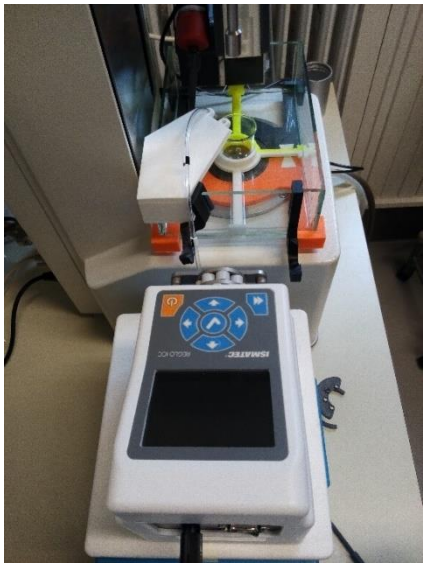

2. Connect the DC motor to the power supply

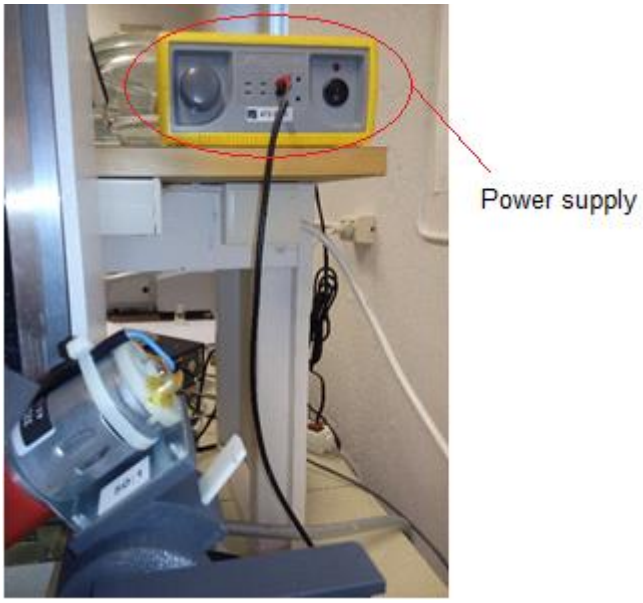

3. Connect hose 3 to a peristalsis part as shown in the picture and connect it to pump 3. Hose 3 is marked with the number 3 inside a plastic bag.

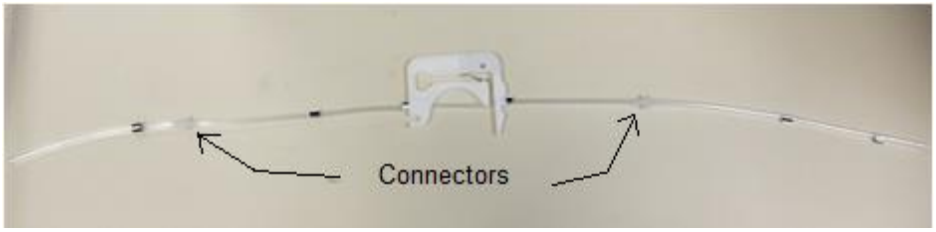

4. Connect hose 2 to a peristalsis part as shown in the picture and connect it to pump 2. Hose 2 is marked with the number 2 inside a plastic bag.

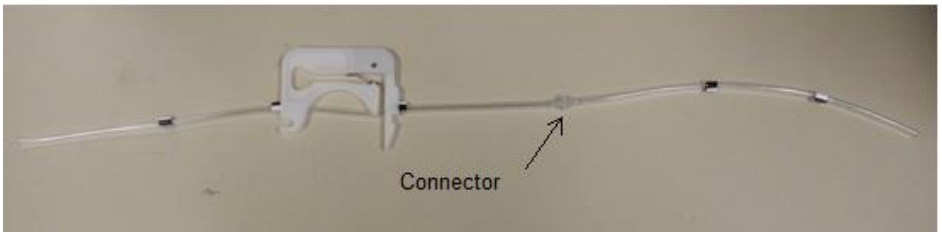

5. Connect hose 1 to a peristalsis part as shown in the picture and connenct it to pump 1. Hose 1 is marked with the number 1 inside a plastic bag.

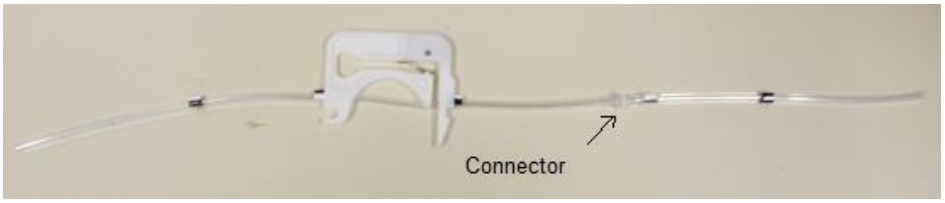

6. Place both ends of hose 3 as shown in the picture. The peristalsis that holds hose 3 is marked with the number 3. If not, remember that the outermost pump is pump 3.

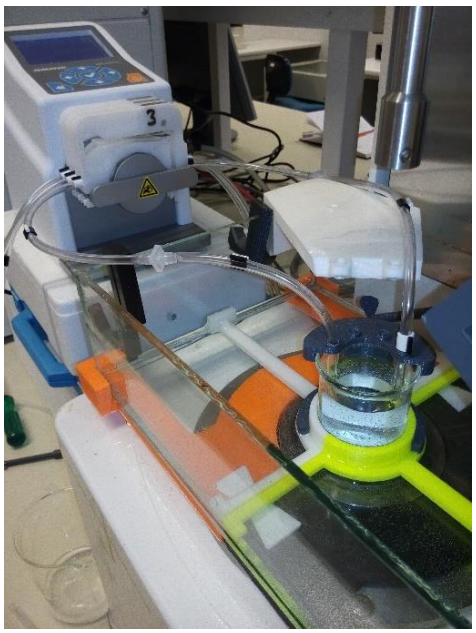

7. Place the long end of hose 2 as shown in the picture. The other end of hose 2 is connected to the membrane unit when it is involved.

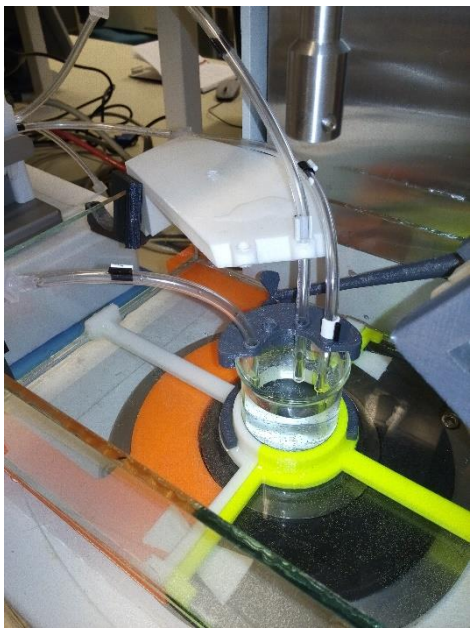

8. Run the long end of hose 1 through the hole of the “hose fixture for water bath” and connect it to the closest opening of the buffer tank. Take a new hose and connect it to the other opening of the tank (The free end of this hose is connected to the buffer glass later). Be careful so that the tank is not immersed in water without the hoses attached.

9. Before proceeding with this step, assemble the membrane unit (see assembling the membrane unit). Follow each step and when finished, place the membrane unit on the side of the water bath. Take the short end of hose 1 and connect it to the opening of the “buffer glass short end”. Take hose 2 and connect it to the intestine glass coming out of “buffer glass short end”. See picture below.

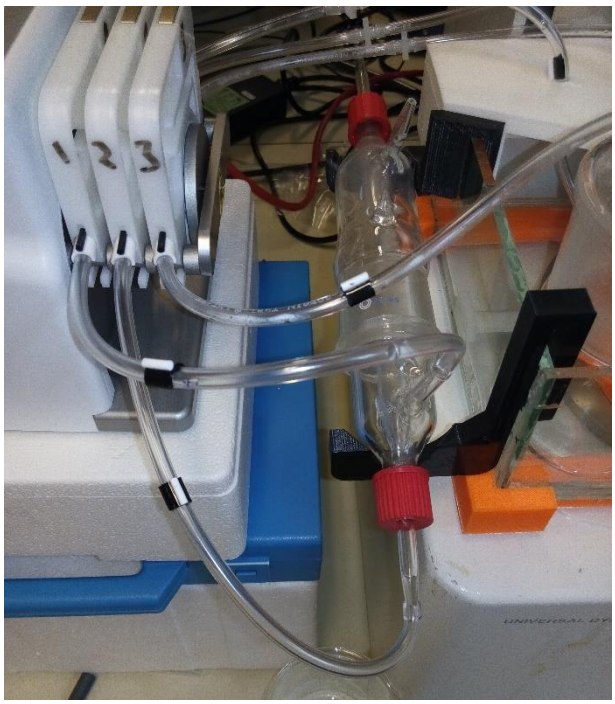

10. Slide a new hose through the last hole in the “Hose fixture for stomach” and connect it to the second intestine glass coming out of “buffer glass long end”. The free end hose that is coming out of the buffer tank is connected to the opening of “buffer glass long end”.


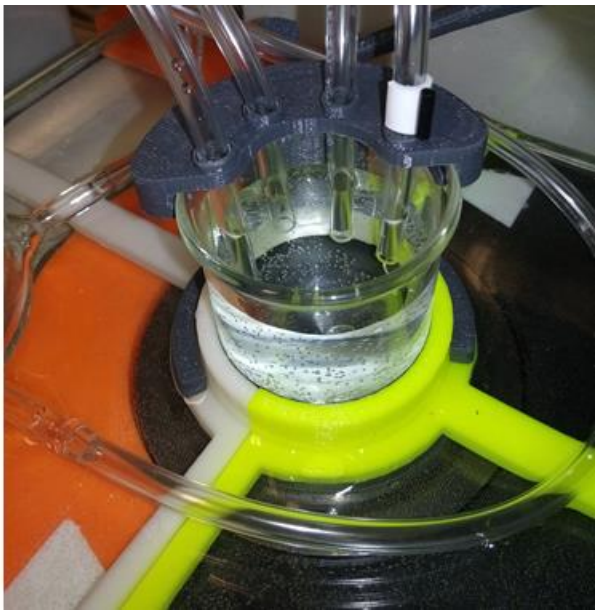

4.3.3 Assembling the membrane unit

This picture shows all the parts (except membrane) necessary for assembling the membrane unit.

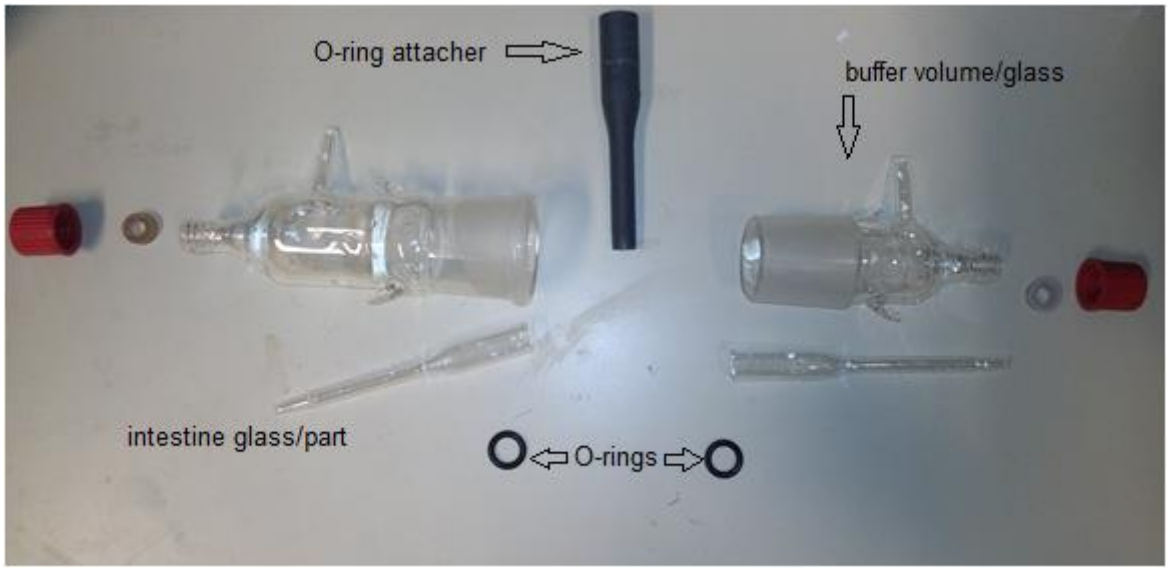

1. Fill each volumes (buffer tank and stomach) with their respective fluids. The buffer tank needs only water (150 ml) and the stomach is filled with 29ml of the fluid that was prepared during “Ready the UDS 200 and Rheometer”.

2. Rinse the membrane that was cut during “Ready the UDS 200 and rheometer”. The membrane gets dry very fast so keep a glass of pure water in the nearby.
3. Slide the membrane onto one of the glass intestines. Make sure everything is wet or else the membrane will not slide easily. It is easier to slide it from the small diameter end.
4. Place the two intestines big diameters concentric to one another and drag the membrane over the first intestine and onto the other. Slowly separate the two intestines until the membrane covers approximately 1 cm of each intestine (5 cm free membrane).
5. Use the O-ring mounting mechanism and one or two O-rings on each side to attach the membrane.
6. Now the intestine part is ready. Assemble it inside the buffer glass and place the membrane unit as showed in the picture below.

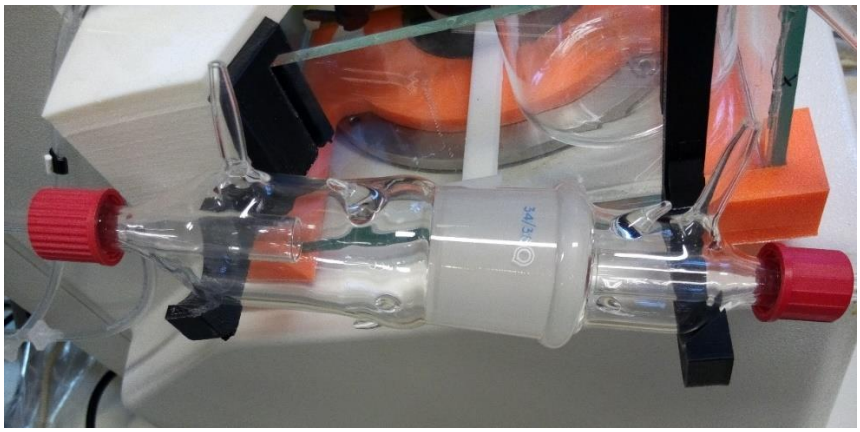

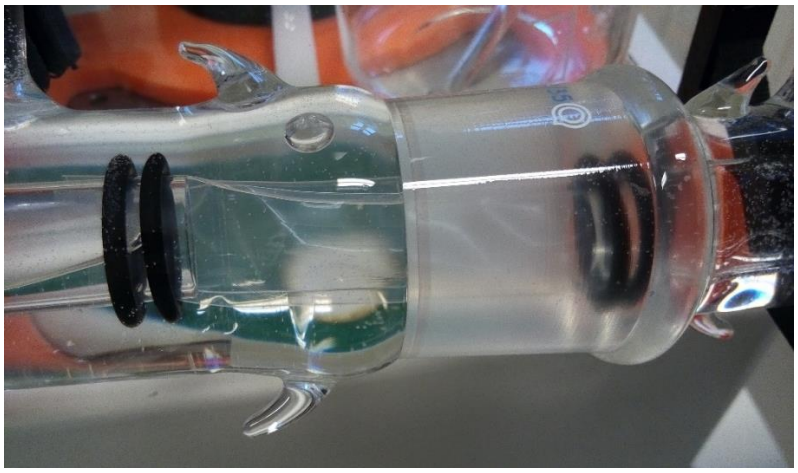

5 CAD simulation

5.1 Pressure drop

5.1.1 Pressure difference across the membrane

One of the problems in the first prototype was that the membrane collapsed, evidently because of the big pressure on the outside wall of the membrane. The volumetric flow rate that was used in the first prototype was 0,2 ml/s in both circuits (Tysse 2014). Judging from figure 18 the total pressure on both sides of the membrane seems to be equal and close to atmospheric pressure as expected. This should not result in any collapse.

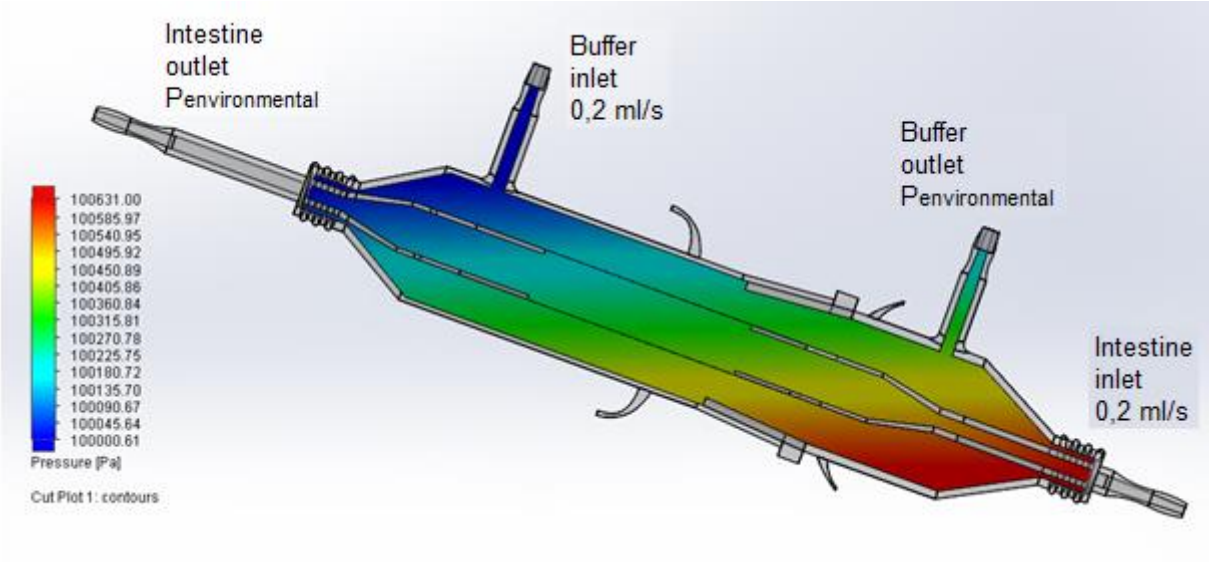

Goal Name	Unit	Value	Averaged Value	Minimum Value	Maximum Value
Total pressure inside membrane	[Pa]	100415	100415	100415	100415
Total pressure outside membrane	[Pa]	100464	100464	100464	100464

Figure 18: Pressure inside and outside the small intestine. Fluid flow in both circuits is 0,2 ml/s.

However the result of previous testing (Tysse 2014) showed that the membrane collapsed under such conditions. The Table in figure 18 shows that there is in fact a difference in pressure across the membrane, and that the pressure is slightly bigger in the buffer liquid. The difference is only 50 Pa which is very little, but the membrane is very soft, so only a small difference is required to bend it. The pressure difference is only a result of the static pressure difference in the membrane unit. Since the diameter of the buffer glass is bigger than the diameter of the membrane, the water surrounding the membrane will have a higher pressure on every point of the membrane.

5.1.1.1 Increasing the velocity of intestinal fluid

This simulation was only executed because it would be interesting to see how big the velocity of the intestinal fluid should be to prevent collapse. It was tried with an inlet mass flow of the intestinal fluid of 10 ml/s (50 times higher) while keeping the buffer velocity at 0,2 ml/s. This velocity of the intestinal fluid is of course too high, but will be tested in the dynamic testing only for the sake comparison. The result of simulation is given in table 9.

Table 9: This table shows the pressure difference across the membrane when increasing the intestinal fluid flow.

Goal Name	Unit	Value	Averaged Value	Minimum Value	Maximum Value
Total pressure inside membrane	[Pa]	102692	102691	102679	102698
Total pressure outside membrane	[Pa]	100464	100464	100464	100464

A test was also done by increasing the inlet mass flow to 2 ml/s (only 10 times higher). This resulted in a smaller pressure difference, but should be enough to keep the membrane from collapsing. Result is given in table 10.

Table 10: This table shows the pressure difference across the membrane when increasing the intestinal fluid flow.

Goal Name	Unit	Value	Averaged Value	Minimum Value	Maximum Value
Total pressure inside membrane	[Pa]	100523	100523	100523	100523
Total pressure outside membrane	[Pa]	100464	100464	100464	100464

Dynamic testing will prove which of the two velocities are sufficient. For the two tests where the intestinal velocity is increased, there is not given a picture of the membrane unit. As the fluid velocity in the membrane increases, the color inside the membrane will get more red (higher pressure) while the color outside the membrane will remain the same as in figure 18.

5.1.1.2 Reduction of cross sectional area of intestine

By reducing the cross sectional area of the outlet of the intestine we may keep the same velocity on both fluids (0,2 ml/s) and still get a higher pressure inside the intestinal wall. The outlet intestine was switched out with another intestine with smaller diameter. The results are given in figure 19.

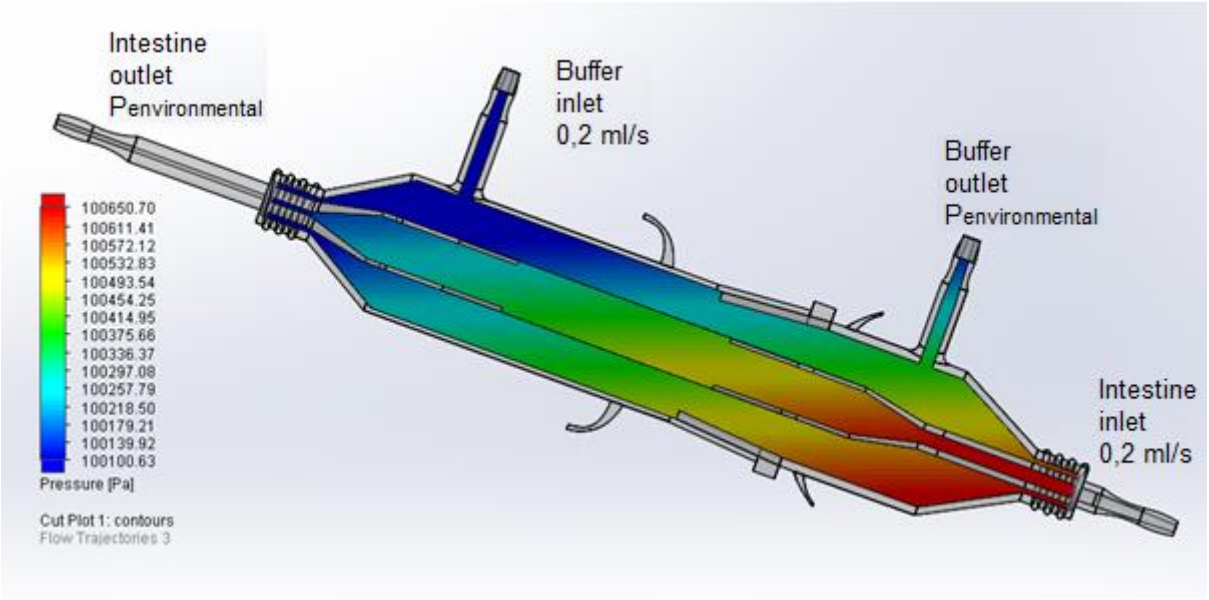

Goal Name	Unit	Value	Averaged Value	Minimum Value	Maximum Value
Total pressure inside membrane	[Pa]	100531	100531	100531	100531
total pressure outside membrane	[Pa]	100475	100475	100475	100475

Figure 19: By looking closely at this picture you can see that the diameter of the outlet of the intestine is smaller.

The smaller diameter of the outlet intestine causes a bigger pressure drop inside the membrane. This pressure drop is very well illustrated by the color inside the membrane. The small outlet diameter of the intestine will possibly have a negative effect on the fluid flow as lumps might get stuck in the opening. However when using only amino acids solved in water it should work fine, because we will get no coagulation and therefore no lumps will occur.

5.1.1.3 Increasing the outlet diameter of the buffer

This test was done to see if it was possible to further decrease the buffer pressure outside the membrane wall. The outlet diameter of the buffer was made bigger and the narrowing the same as the inlet (3 degrees). The result are given in figure 20.

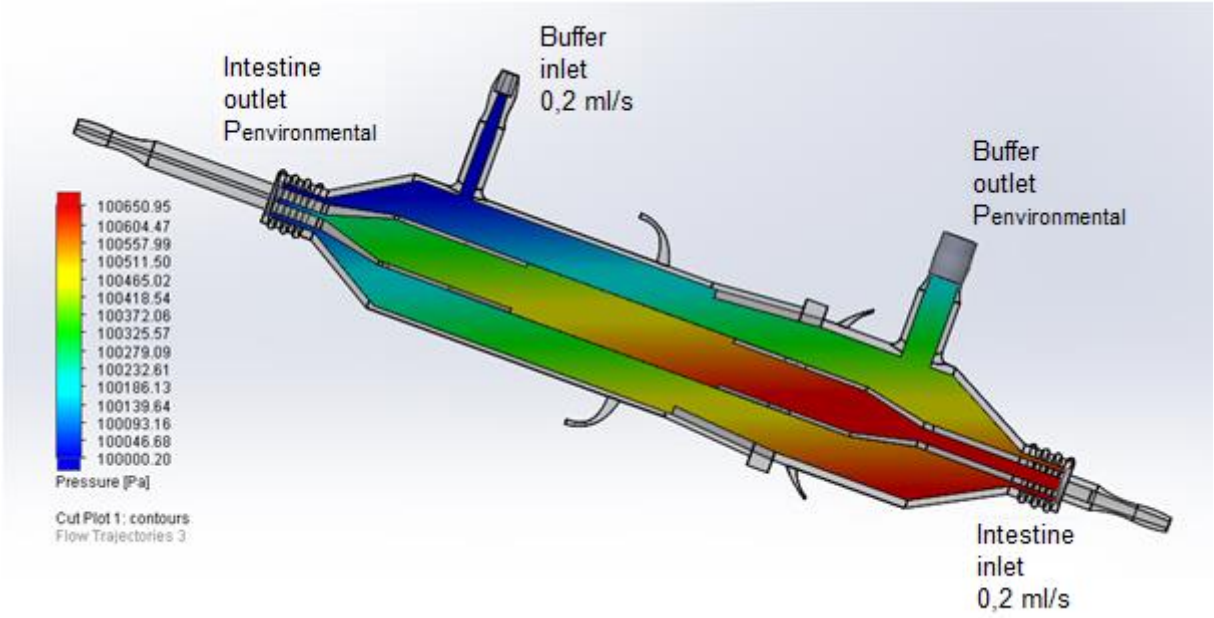

Goal Name	Unit	Value	Averaged Value	Minimum Value	Maximum Value
Total pressure inside membrane	[Pa]	100633	100633	100633	100633
Total pressure outside membrane	[Pa]	100473	100473	100473	100473

Figure 20: The fluid flow in both circuits is 0,2 ml/s.

The buffer inlet was also rotated 180 degrees to see if this could have an impact on the buffer pressure, but the difference between the two setups were insignificant. By increasing the buffer outlet diameter the pressure difference becomes even bigger than for the other cases with the same fluid flow.

5.2 Diffusion

5.2.1 Particle simulation of L-tryptophan

The particle simulation was executed as an attempt to make a model of the system in solid works. To have a model of the system in solid works, would be a good way to compare real life diffusion to that in a CAD program and even prepare future testing on the computer.

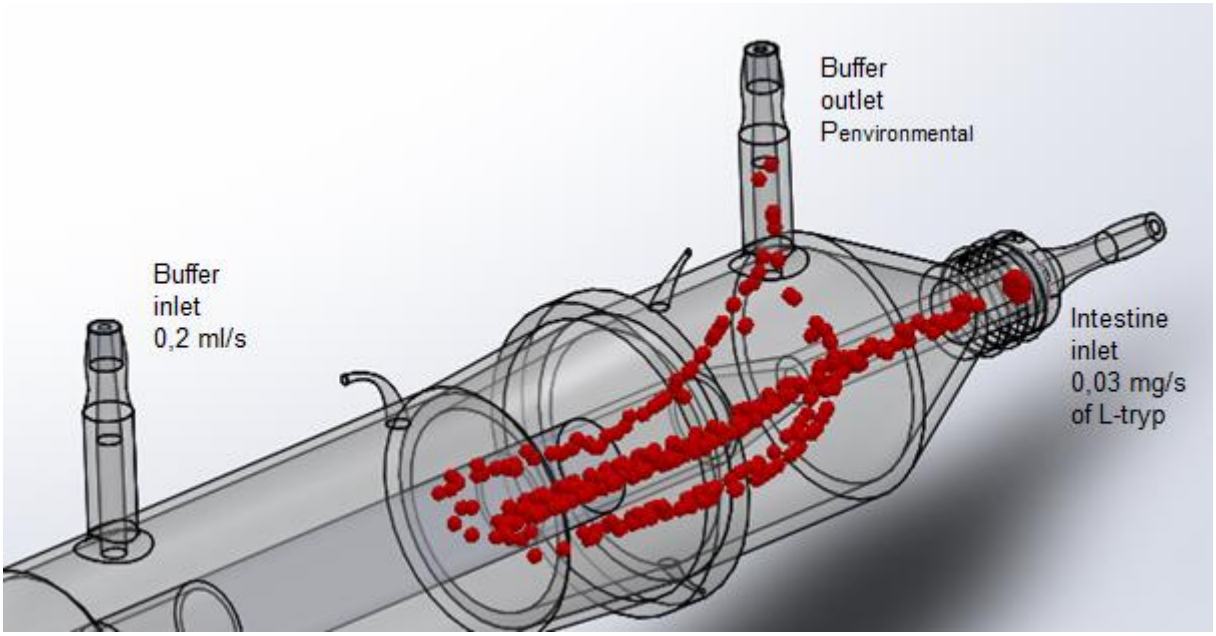

Figure 21: This is a picture of a particle simulation done in solidworks.

5.2.2 Results and discussion

As presented in figure 21, all the particles enter the buffer fluid as soon as they reach the membrane. This is not a logical behaviour of cross flow filtration (see chapter 2.10). The diffusion of particles should show a more even distribution through the length of the membrane, where some particles diffuse and others don't. Although a lot of time was spent on doing these simulations with different conditions, the results was always as presented in figure 21.

6 Experimental work

6.1 Introduction static testing

Test 1-17 are all tested in a similar manner. It is always a membrane involved and always a liquid (feed) inside this membrane. The concentration of solute is always higher inside the membrane than in the liquid surrounding the membrane. The liquid surrounding the membrane is referred to as the buffer liquid. The feed will, if it manage, permeate through the membrane and mix with the buffer liquid. Samples will always be taken from the buffer liquid for analysing in the SPM.

6.2 Test 1-6

The first six tests were all executed with the same physical setup, but with different conditions.

6.2.1 Purpose

The purpose of these tests were to trouble shoot the results of previous testing (Tysse 2014) and to try different conditions for getting Evan's blue to permeate. At this stage it was important to understand what went wrong in the first prototype.

6.2.2 Materials and methods

All six tests were executed by using a cylindrical glass tube with a membrane folded over the bottom edge of the tube, creating a barrier for the feed inside the tube. The feed (Evan's blue or water) is supposed to permeate through the membrane and into the buffer liquid. See figure 22 for setup.

The setup to the left shows a test where the concentration difference of Evan's blue across the membrane is the driving force for diffusion. Since the two liquids are at the same level of height, the concentration gradient will be the only physical driving force for separation. The setup to the right shows a clear difference in the height between the two liquids and a pressure gradient occurs. This pressure gradient should push the feed through the membrane.

Because of dents that appeared on the membrane when folding it over the glass tube, it was tried to close these pores by attaching a double sided tape between the membrane and the glass. The idea was that the tape should work as soft interlayer that would completely close all openings.

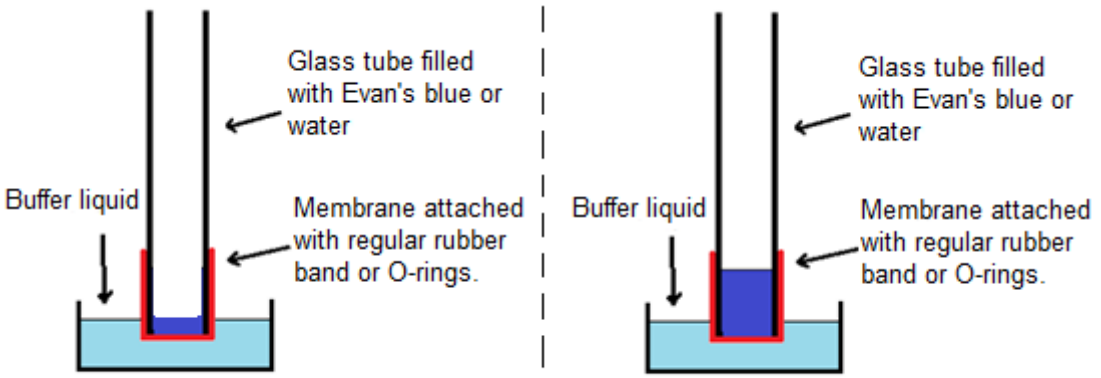

Figure 22: This figure shows the physical setup of test 1-6. Testing was executed with pressure- and concentration difference. Different type of feed and different method for attaching the membrane to the glass was put at assessment.

6.2.3 Results and discussion for test 1-6

The results of test 1-6 were all unanimous in that no diffusion occurred. It seemed as if the Evan's blue molecules were too big or that the chemical properties between membrane and Evan's blue does not favour diffusion. Even the water did not permeate through the membrane during "pressure gradient test". The double sided tape worked as expected and there were no leakages after attaching it. It can be argued that the use of a double sided tape can inflict with the results of the ABS values if the sticky material on the tape is solved in the feed or buffer. Since we deal with so small volumes it should be taken extra care as to what chemicals are added.

6.3 Test 7

6.3.1 Purpose

To make sure the time frame did not have anything to do with the results of test 1-6, a three day test was put at assessment.

6.3.2 Materials and methods

Two membranes (8 kDa and 12-14 kDa) was filled with Evan-s blue, closed in both ends and put in two different beakers of water throughout the weekend.

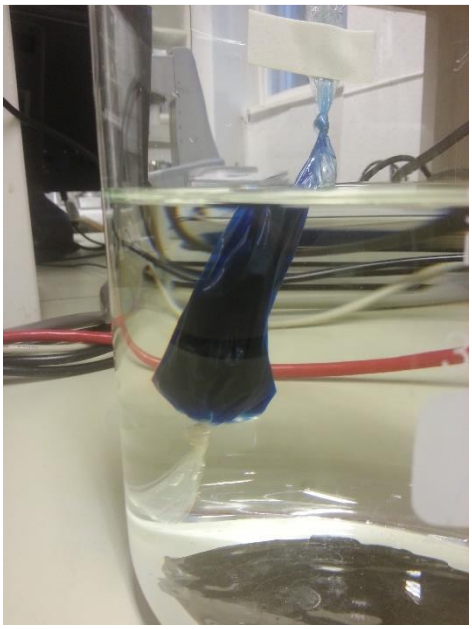

Figure 23: This picture is taken three days after initializing the test.

6.3.3 Results and discussion

Even after three days of testing, there were no diffusion. The most likely explanation to this result is the chemical properties of Evan's blue and that it is not suited for RC membranes. The size should not be a hindrance for diffusion, see chapter 6.4.3.1 *(M. Cassidy, [personal communication, 28 jan. 2015]).*

6.4 Test 8

6.4.1 Purpose

The result of the previous test lead to experimentation with one amino acid and another phenolic compound as feed in subsequent tests. The purpose was to test other types of feed and compare the permeability to that of Evan's blue which was zero.

6.4.2 Materials and methods

L-tryptophan and one phenolic compound called P-nitrophenol was used as feed. These components are much smaller than Evan's blue (see chapter 3.5 - 3.7) and so diffusion should be more favourable for this solution. Only the 8 kDa membrane was used. 1mM of P-nitrophenol and an arbitrary amount of L-tryptophan was put in the membrane and the membrane was sealed at both ends. It was then put in half liter of water for one hour.

In this test the membranes were sealed with an orange pinch. To make sure the pinch did not harm the membrane in any way, a third membrane containing Evan's blue was tested for leakages. If Evan's blue suddenly permeated in this test it would be because of leakages caused by the pinch.

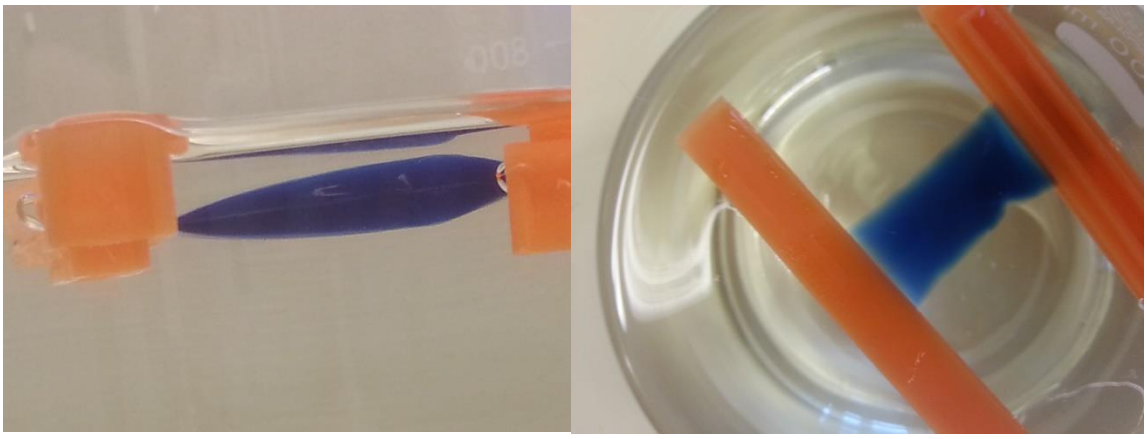

Figure 24: The picture to the left is taken from the side of the beaker and the picture to the right is taken from above. It shows the membrane with Evan's blue sealed at both ends with an orange pinch. The membrane was not harmed by the pinch.

6.4.3 Results and discussion

6.4.3.1 Test 8, P-nitrophenol

After only one hour it was clear that something had diffused because of the changing color of the buffer liquid. The ABS values detected in the SPM were too high to measure reliable concentrations.

6.4.3.2 Test 8, L-tryptophan

L-tryptophan has no color so the samples from this test had to be run through the SPM to detect solute. The SPM detected a lot of compound which is proof of permeation also for this compound.

6.4.3.1 Test 8, Evan's blue

The results from the "pinch test" of the Evan's blue showed no leakages and the membrane seemed fine after inspection. However after washing the membrane thoroughly the color of the Evan's blue was still attached to the membrane which is an indicator that molecules are stuck within the pores. This is a form of fouling, see chapter 2.5.

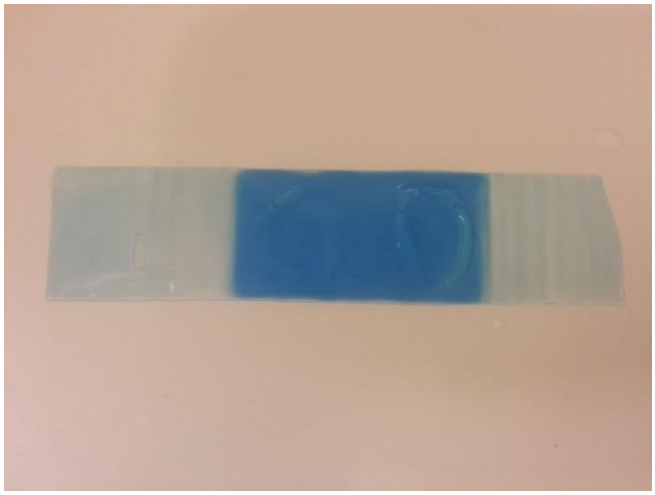

Figure 25: This picture shows that the color of Evan's blue is difficult to wash away. This is an indicator of fouling.

In association with this result Spectrum labs was contacted to get a better understanding of why molecules that are 3-4 times smaller than the pores do not permeate. After some communication the following email arrived.

> *"The 3.5 kDa MWCO will retain 960 D (Evan's blue) by about 70-80% and the 8 kDa MWCO will retain 960 D by about 50-60%. The 12-14 kDa MWCO will retain 960 D by about 10-20%.*
> *However, as I mentioned, we have found a strange phenomenon in which some molecular property of dyes (Evan's blue) do not allow them to pass through the membrane in general.*
> *So using amino acids should definitely be an improvement. Keep in mind that you will need to use a MWCO of at least 50-100 X larger than the MW of the molecular species that you wish to eliminate (pass) through the membrane. So a 12-14 kDa MWCO should be sufficient to remove amino acids ranging from 90 – 150 Daltons".*

(M. Cassidy, [personal communication, 28 jan. 2015])

These facts clearly states that at least 20-30% of Evan's blue should have permeated through the 3,5 kDa membrane and even more for the other membranes. In chapter 2.5 it is explained that fouling may happen after only a few minutes. This may be the case for Evan's blue only that it happens immediately and judging from figure 25 it seems plausible.

6.5 Test 9

6.5.1 Purpose

This test was executed to see what would be the biggest concentration of L-tryptophan and P-nitrophenol that will give ABS values of about 1. Values high above 1 may not give reliable values.

6.5.2 Materials and methods

Two separate concentrations of 100 mg/liter of L-tryptophan and 139 mg/liter P-nitrophenol was diluted and measured in the SPM until the ABS value was about 1. L-tryptophan comes as powder and is therefore easy to mix to a desired solution. P-nitrophenol on the other hand is already diluted, so the feed concentration will always be 139 mg/liter.

6.5.3 Results and discussion

6.5.3.1 L-tryptophan at 220 nm

A concentration of 3 mg/liter gave an ABS value of approximately 1 for L-tryptophan at 220 nm. This means that the buffer liquid should not contain more than about 3 mg/liter of that substance in order to get reliable measurements. Later tests show that 5-6 mg/liter might be an acceptable level of L-tryptophan.

6.5.3.2 L-tryptophan at 280 nm

A concentration of 20 mg/liter gave an ABS value of about 1 for L-tryptophan at 280 nm. This means that the buffer liquid should not contain more than about 20 mg/liter of that substance in order to get reliable measurements

6.5.3.3 P-nitrophenol

Diluting P-nitrophenol at a ratio of 1:10, gives an ABS value of exactly 1. The buffer liquid should not have a higher concentration than 13,9 mg/liter. The feed will always be 1mM or 139 mg/liter because it is already diluted.

6.6 Test 10

6.6.1 Purpose

Test 10 was about making standard curves for the relevant wavelengths of L-tryptophan and P-nitrophenol, to be used as a conversion curve from ABS values to concentration (mg/liter), See chapter 2.15. The relevant wavelengths of L-tryptophan is 220 nm and 280 nm. The aromatic side chain of amino acids absorbs at 220 nm and the actual amino acids absorbs at 280 nm.

6.6.2 Materials and methods

6.6.2.1 L-tryptophan at 220 nm

A solution of 6 mg/liter was diluted as shown in table 11. Also the ABS value greater than 1 is considered because it is not that high above one and it is not deviating from the straight line (see figure 26).

6.6.2.2 L-tryptophan at 280 nm

A solution of 20 mg/liter was diluted as shown in table 12. The ABS values are the mean value of two tests (see figure 27).

6.6.2.3 P-nitrophenol

A solution of 13,9 mg/liter was diluted as shown in table 13. The wavelength that is most absorbed is that of 400 nm.

6.6.3 Results and discussion

6.6.3.1 L-tryptophan at 220 nm

Table 11: This table relates concentration to ABS values for the amino acid L-tryptophan at 220 nm.

Concentration [mg /liter]	ABS	Wavelength [nm]
6	1,212	219
3	0,637	219
2	0,436	219
1,5	0,334	219
0,75	0,188	219
0,375	0,107	218

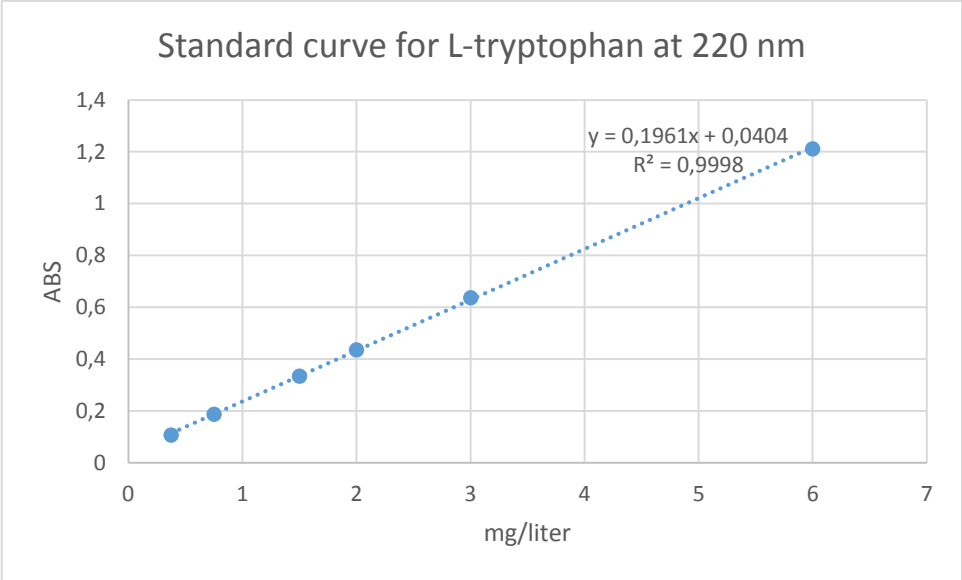

Figure 26: This plot shows a very good result for a standard curve with a root mean square error of less than 0,02 %.

As can be seen from the graph the linear relationship between concentration and ABS values are strikingly good, which means that Beer Lamberts Law can be used for determining the concentration. See Eq. 25.

6.6.3.2 L-tryptophan at 280 nm

Table 12: This table relates concentration to ABS values for the amino acid L-tryptophan at 280 nm.

Concentration [mg/liter]	ABS	Wavelength [nm]
20	0,5615	280
10	0,269	280
5	0,1385	280
2,5	0,0665	280

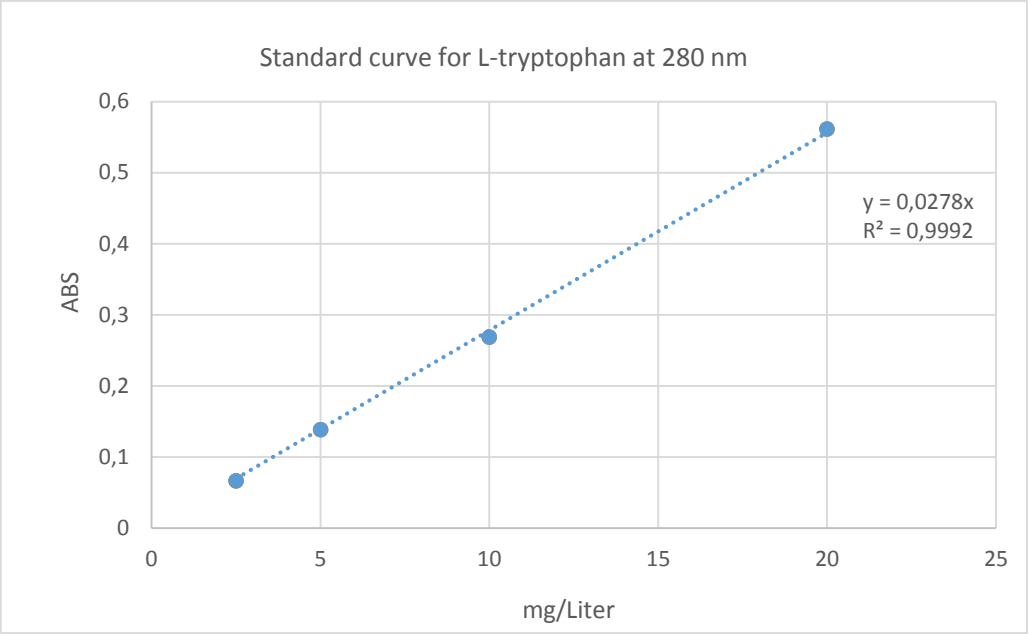

Figure 27: This plot shows a very good result for a standard curve with a root mean square error of less than 0,08 %.

Also in this plot the standard mean deviation is very small, so it would be possibly to use Eq 25 to figure out the concentration.

6.6.3.3 P-nitrophenol at 400 nm

Table 13: This table relates concentration to ABS values for the phenolic compound P-nitrophenol at 400 nm.

Concentration [mg/liter]	ABS	Wavelength
13,9	1,100	398
9,27	0,858	400
6,95	0,729	401
4,63	0,507	398
3,475	0,400	399
2,78	0,326	398
1,74	0,216	398
1,39	0,206	398

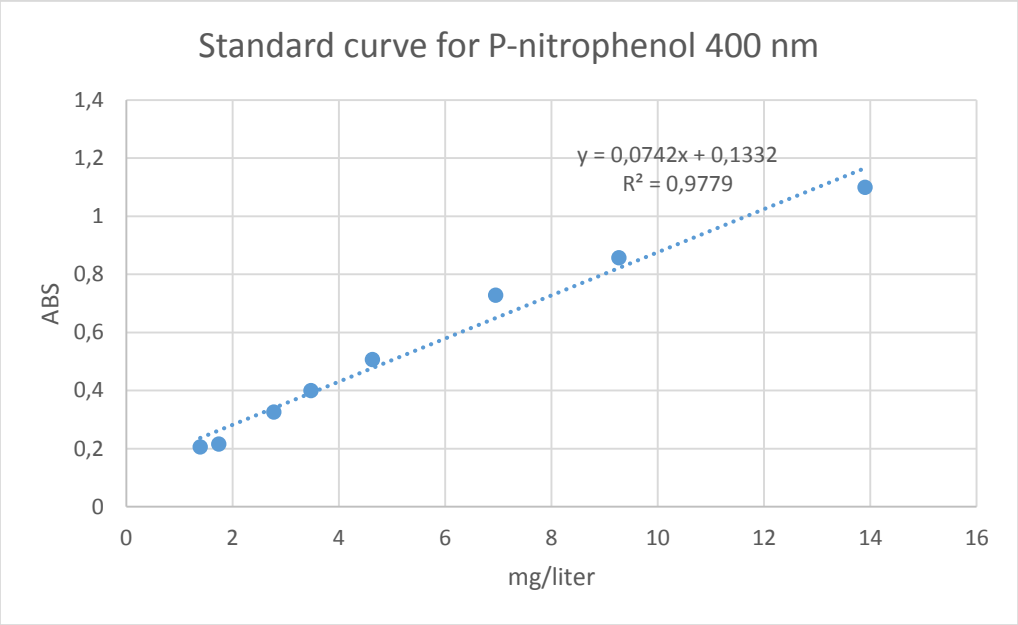

Figure 28: This plot also presents a good result for P-nitrophenol. Less than 3 % error.

Figure 28 presents a nice correlation between the plots and the straight line. The line does not however go through origo which is strange because at zero concentration it is expected that the ABS value is also zero. By forcing the trendline to go through origo, the standard mean deviation gets three times bigger (9%). That trend line is not presented.

6.7 Test 11

6.7.1 Purpose

The purpose of this test was to determine a suitable volume and concentration of the feed and a suitable volume for the buffer liquid for the static testing. This had to be done because it was a big difference in the amount of solute needed to get desirable ABS values for wavelengths 220 nm and 280 nm of L-tryptophan. P-nitrophenol is already diluted and is therefore not considered in test 11.

6.7.2 Materials and methods

As L-tryptophan has an accepted value of 3 mg/liter (the true value is actually between 3-6 mg/liter) for absorption at 220 nm, it should be considered as the highest acceptable value in the buffer liquid (permeate side) at the end of the test. How much solute is to be added in the feed depends on the volume of the feed and the buffer liquid. To illustrate this, figure 29 shows how distribution of molecules happens after a while. If time = several hours, has a concentration

of 3 mg/liter and a volume of 0,1 liter, then the amount of solute is 0,3 mg. At time = zero, 0,3 mg of solute is trapped inside the membrane with a volume of 0,002 liter. That yields a concentration inside the membrane of 150 mg/liter. To get a volume of 0,002 liter in the membrane, they are cut at a length of 7 cm.

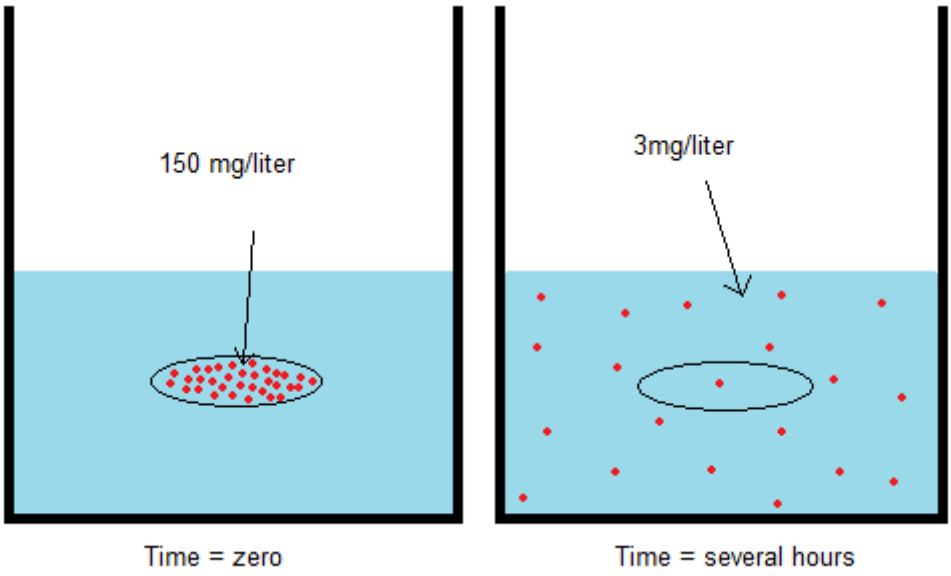

Figure 29: The concentration difference across the membrane will lead to molecules permeating into the buffer liquid and obtaining equilibrium.

This concentration of the feed (150 mg/liter) is theoretically correct if the duration of a test is several hours and the goal is a buffer liquid concentration of 3 mg/liter. However these permeation tests last only for 1 hour which is not enough time for the amount of solute (0,3 mg) to permeate through the membrane (as experimenting has shown). This means that the feed should have a higher concentration than 150 mg/liter, see next section.

6.7.3 Results and discussion

Table 14: Results from static experimenting of L-tryptophan and P-nitrophenol is presented in this table.

	L-tryptophan				P-nitrophenol	
Membrane	3,5 kDa	8 kDa	3,5 kDa	8 kDa	3,5 kDa	8 kDa
Feed concentration	1500 mg/liter	1500 mg/liter	1500 mg/liter	1500 mg/liter	139 mg/liter	139 mg/liter
Max ABS wavelength	0,971 220 nm	1,453 220 nm	0,211 280 nm	0,536 280	0,117 400 nm	0,333 400 nm
Duration	60 min	60 min	30 min	30 min	60 min	60 min

About 1500 mg/liter has proven to be a good concentration in the feed for obtaining ABS values that are within the range of 0-1,5. For the wavelength 220 nm it is higher than desired, but it makes sure that readings of wavelength 280 nm is obtained. This implies that the volume of the feed is 0,002 liter and that the buffer volume is 0,1 liter.

The low ABS values of P-nitrophenol is a result of the low concentration that was available. L-tryptophan was available as powder and therefore much easier to make higher concentrations.

6.8 Test 12-16

6.8.1 Purpose

The goal of these tests will be to find the diffusion coefficient of the membranes. Different membranes, different buffer volume and different feed concentration is tested to see if there will be changes to the diffusion coefficient. Some deviation is expected because of method and workmanship, but it should be approximately the same because diffusion coefficient is not dependent on concentration gradient (Norby). By Fick's first law it is expected to obtain a curve looking something like that in figure 30. The picture to the left shows that the rate of change in concentration in the buffer liquid flattens out as time passes. This is due to the flux that gets smaller and smaller as the concentration gradient gets smaller (see Eq. 10). The picture to the right shows the same curve, but with flux on the y-axis and the concentration in buffer liquid on the x-axis. When the concentration in the buffer liquid increases, the concentration gradient decreases and the flux will also decrease as shown in this figure.

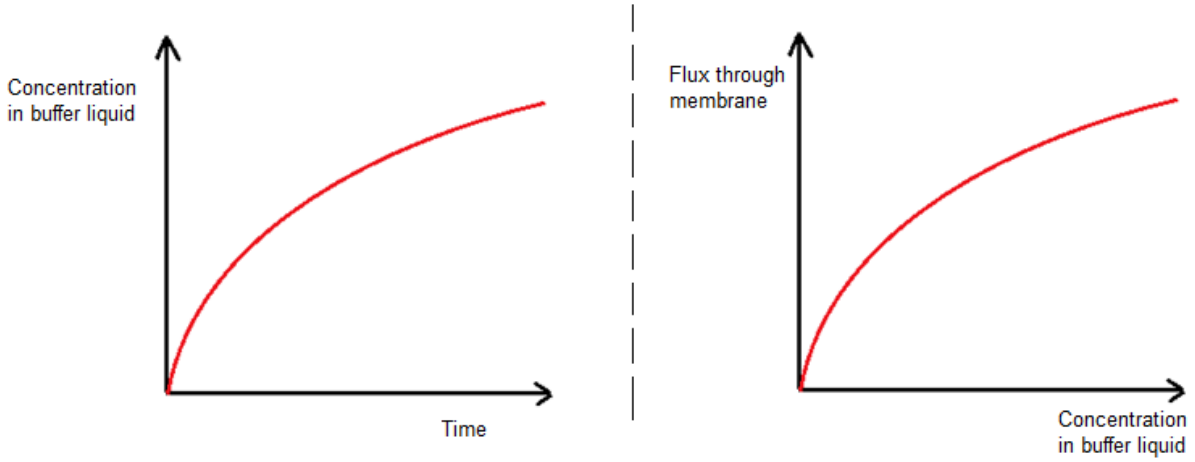

Figure 30: The figure compares the same situation with different units.

6.8.2 Materials and methods

The procedure of testing is the same for every test. That is, a membrane containing the feed is put in a buffer volume for 30-60 minutes. Changes made to the feed concentration for L-tryptophan or the buffer volume is given in the tables for each test.

6.8.2.1 L-tryptophan

From test 11 it was discovered that a feed concentration of 1500 mg/liter is good for detecting the two different wavelengths of L-tryptophan. 150 mg/liter is measured and put in a beaker of 0,1 liter water (this yields the concentration of 1500 mg/liter). A 7 cm long piece of membrane is cut and the mixed solution is put inside the membrane. The membrane is sealed with an orange pinch on both sides and put in a beaker containing 0,1 liter of pure water. Samples will be taken every 5^{th} minute and later analysed in the SPM.

6.8.2.2 P-nitrophenol

This compound is already diluted and the concentration is 139 mg/liter. 0,002 liter of P-nitrophenol is put in a membrane and that membrane is put in a beaker containing 0,1 liter of pure water for half hour up to one hour. Samples will be taken every 5^{th} minute and later analysed in the SPM.

6.8.3 Results and discussion

The results of tests 12-16 are presented in chapter 6.20 because it is easier to compare every test when they are all put in one table. As explained these results will give the diffusion coefficients for every test.

6.9 Test 17

6.9.1 Purpose

The thickness of the membrane will have a big effect on the permeability according to equation 11. In order to get as reliable diffusion coefficients as possible, it was asked from the membrane provider that they take measurements of those membranes relevant to this thesis. Three specimens of each membrane were tested and an average result obtained. The results are given in table 15.

6.9.2 Results and discussion

Table 15: This table gives the average values of the membrane thickness test provided by Spectrum labs.

Part	Average thickness (mm)	STD
Part# 132110 S/P7 3.5 kDa 18mm	0,0485	0,005
Part# 128358 S/P7 8 kDa 18mm	0,0642	0,012
Part# 132680 S/P2 12-14 kDa 45mm	0,0391	0,002

Spectrum labs informed *(M. Cassidy, [personal communication, 16 feb. 2015])* that membrane thickness is not a critical physical specification for them and that they do not measure or have an established thickness tolerance range. This means that two specimen of the same membrane may differ in thickness and therefore the results show an average value for the thickness.

6.10 Test 18

6.10.1 Purpose

To build an accurate model of the system, one of the most important factors is the properties of the membrane, and knowing how they affect diffusion. By looking at the membranes in the microscope, the goal was to identify the pores, but this proved to be difficult.

6.10.2 Materials and method

Spectrum Labs were contacted to find useful data on the porosity, but the provider of the membrane do not have any data on the size of the pores of their membrane, nor do they know the quantity of those pores. Since the information obtained from Spectrum Labs were difficult to use, a test was executed by looking at the membrane through a microscope.

6.10.3 Results and discussion

From personal communication with the membrane company, the following email explains their definition of porosity of the RC membrane.

> *"In regard to the membrane porosity, since the membrane is essentially a spongy matrix consisting of varying-sized interconnecting openings (much like a sponge), we do not have a practical method to directly measure membrane porosity. Instead we indirectly determine the membrane porosity as a function of the retention performance. This is expressed as a MWCO (Molecular Weight Cut-Off) which means the APPROXIMATE solute size that is retained by APPROXIMATELY 90% in a dialysis period of 17 hours.*

Lastly, I am not at liberty to disclose our MWCO retention test method since this is company proprietary information".

(M. Cassidy, [personal communication, 11 mar. 2015])

6.10.4 Results from microscope

Figure 31 shows one photo of the membrane in the magnification 100X and 3 photos at 200X magnification.

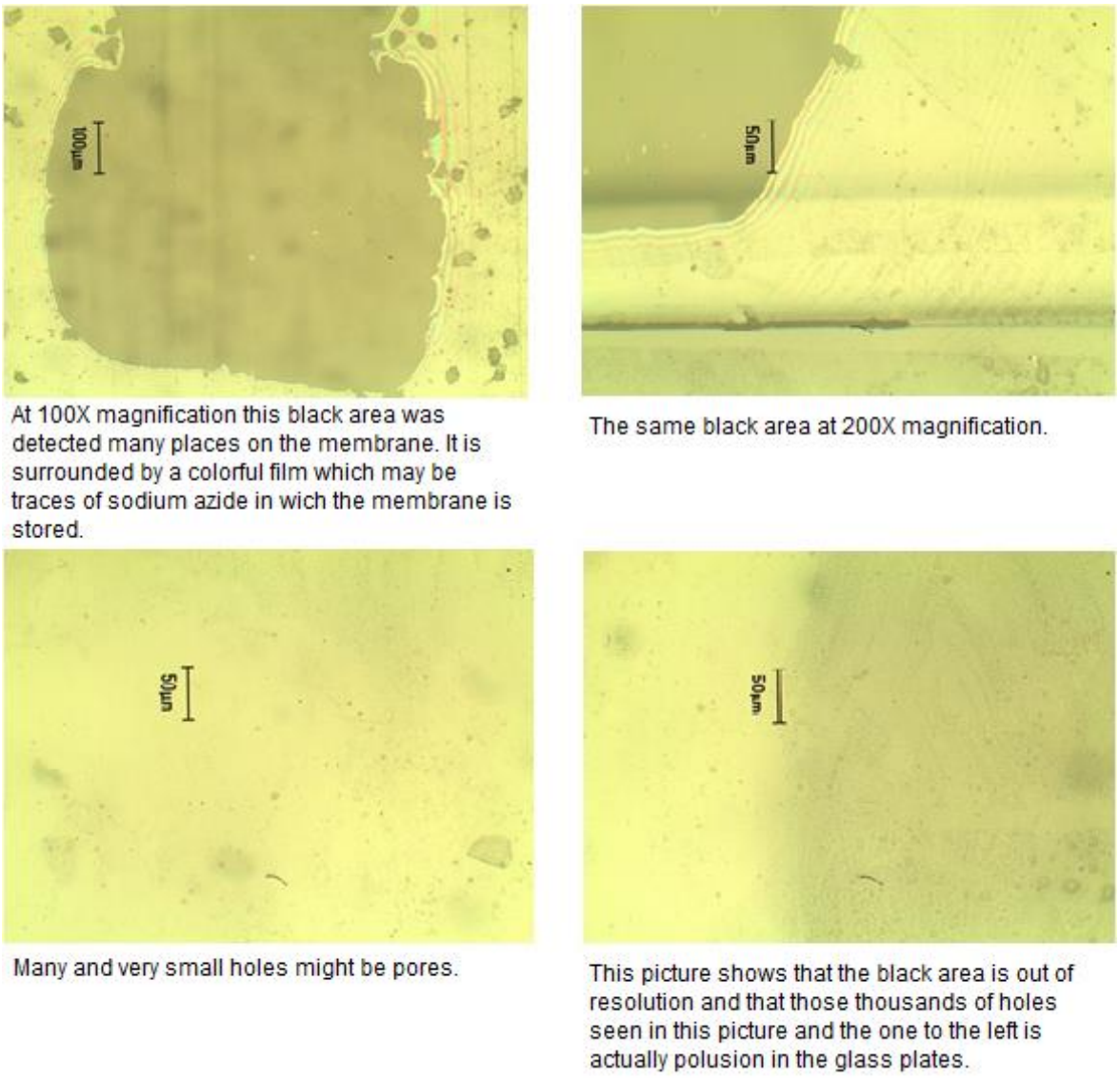

Figure 31: This figure shows pictures of the membrane taken with a microscope. The microscope was not powerful enough, or it might be that the type of microscope setup is not suitable for looking at this membrane.

The results in this test was that no pores were detected through the microscope. The explanation given by Spectrum is the nearest to give a visualization of the "pores". The fact that the membrane is much like a sponge might increase the tortuosity of the membrane because pores are interconnected. By Eq. (14) this should decrease the effective diffusivity causing the membrane to be less permeable. This is also consistent with the fact that this is a low permeable membrane (Neligan).

6.11 Introduction to dynamic testing

The dynamic testing of the membrane involves the in-vitro model that was built specifically for this thesis. These tests are executed to resemble the natural processes in an in-vivo system more accurately than the static testing. The dynamic testing is the most important tests because it includes all the components of the system. Like the static testing, samples are always taken from the buffer liquid and analysed in the SPM. The same standard curves are used to get the concentrations.

6.11.1 Purpose

The purpose of these tests are to compare the diffusion coefficient from the dynamic testing to the static testing and to test the usability of the system. Not only the diffusion coefficient is important, but also the temperature of the liquids and the precision that is required for a dynamic prototype. The membrane collapse and its ability to stay attached to the intestinal glass will also be put at test.

6.12 Test 1

6.12.1 Purpose

The purpose of the first test was to assemble everything together, prototype and membrane unit with the membrane attached. To make a membrane collapse test and make sure the membrane stayed on the intestinal glass during the test.

6.12.2 Materials and method

Three different flow velocities were tested to see how the collapse of the membrane responded to those velocities. According to Eq. 21, the velocity should have a big saying on the pressure drop in a circular tube. The configuration of the tests was both counter-current flow and co-

current flow. The intended flow regime for the actual testing is counter-current. The maximum velocity that were tested in the flow simulation was not possible to test in the practical experiment because of the maximum volume flow rate of the peristaltic pump. Instead the maximum flow rate was tested (see table 17). For the minimum flow rate, a low value was chosen.

Table 16: Flow regime 1 is counter-current.

FLOW	ml/s
Buffer inlet flow	0,2
Intestinal inlet flow	0,2

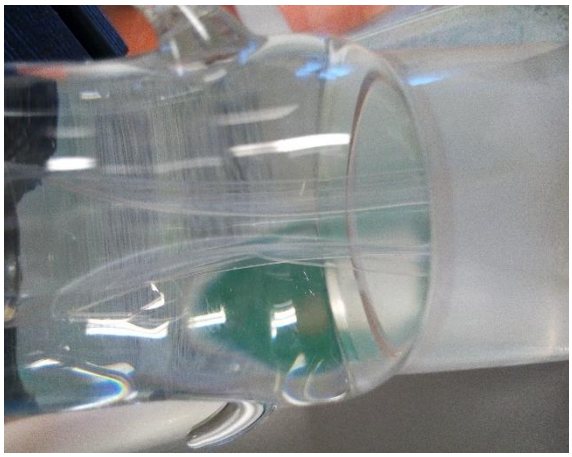

Figure 32: This figure shows flow regime 1.

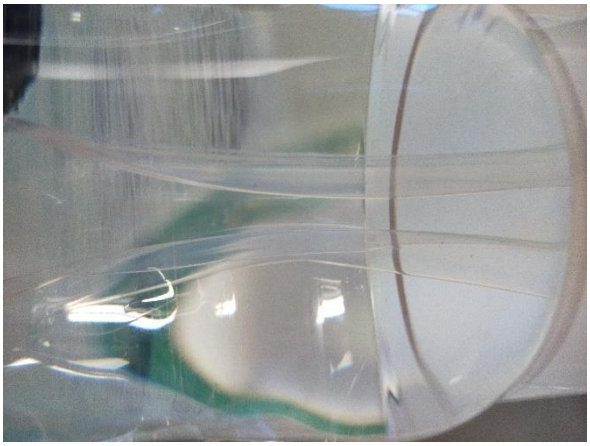

Figure 33: This figure shows flow regime 2.

Table 17: Flow regime 2 is counter-current.

FLOW	ml/s
Buffer inlet flow	0,2
Intestinal inlet flow	0,457

Table 18: Flow regime 3 is counter-current.

FLOW	ml/s
Buffer inlet flow	0,2
Intestinal inlet flow	0,083

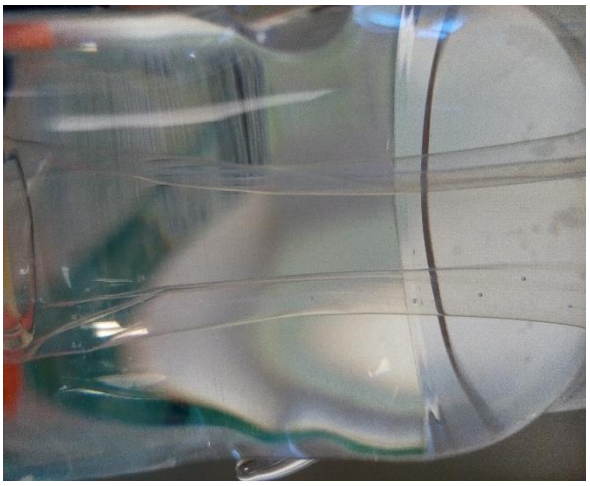

Figure 34: This figure shows flow regime 3.

6.12.3 Results and discussion

As expected the membrane collapsed during testing, otherwise the equipment worked fine. The membrane stayed attached to the intestine glass for the duration of the test (1 hour). The membrane collapsed in all three flow regime, but the collapse is not severe and is not dependent on which way the fluid flows. The fact that the collapse is not severe leaves a big area of the membrane available for diffusion, but not at optimum. It is the last flow regime that gives less collapse which is not to be expected because of the low flow in the intestinal circuit.

6.12.4 Later tests

Experimenting with the system showed that by turning on the pump for the inner circuit before turning on the pump for the buffer circuit will have a positive effect on the membrane collapse. See figure 35.

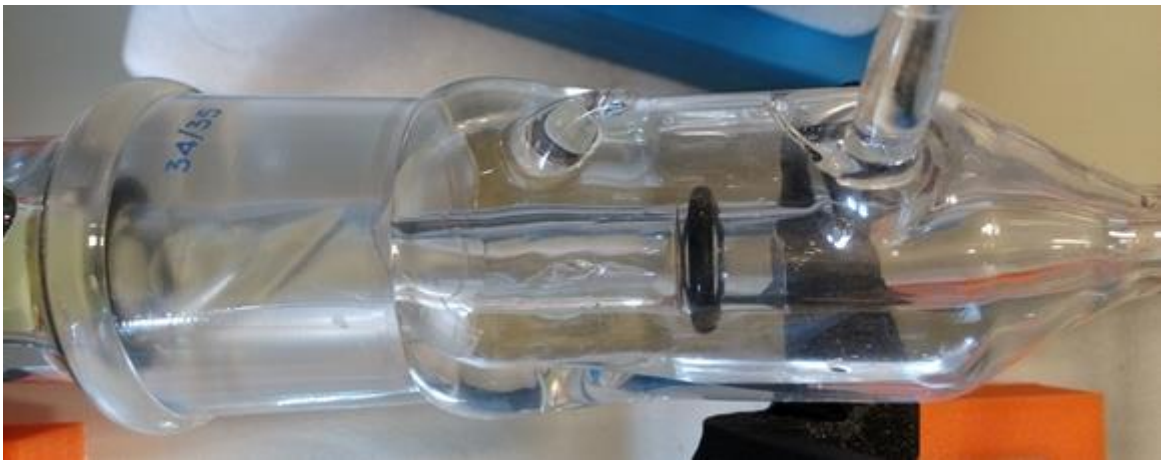

Figure 35: This figure shows the membrane collapse in a small test for functionality. Inside and outside the membrane water flows.

6.13 Test 2

6.13.1 Purpose

The purpose of this test was to get some data on the diffusivity of the membrane during dynamic testing. Only the prototype and the peristaltic pump was used for this test. At the end of the test the membrane was tested for leakages with Evan's blue.

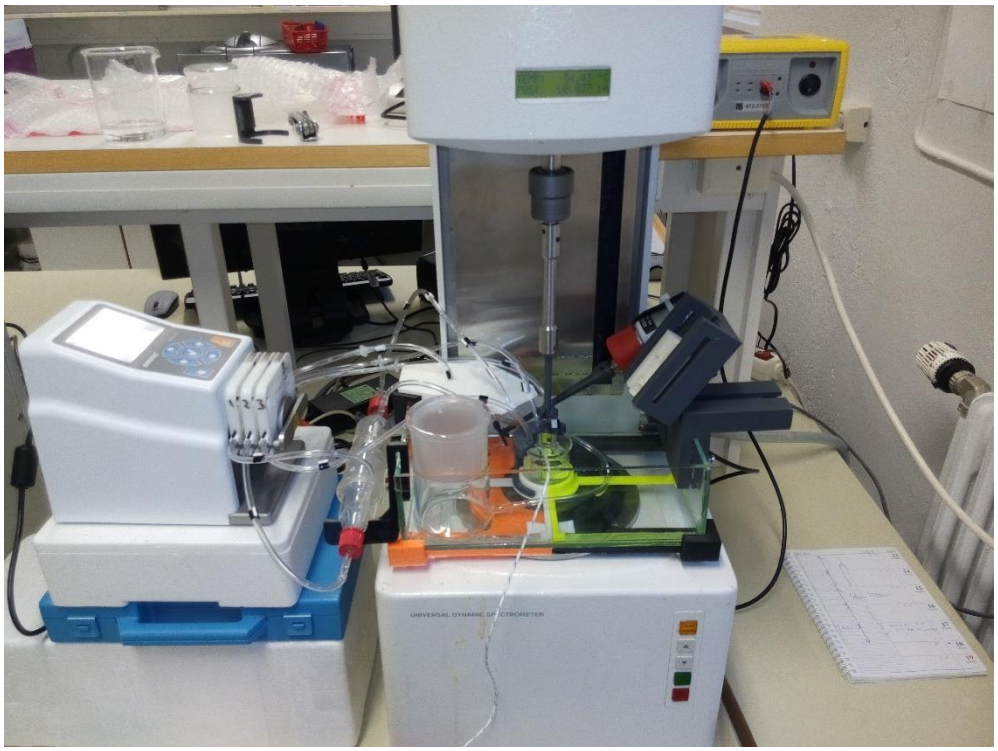

Figure 36: This picture shows the peristaltic pump working together with the prototype and membrane unit.

6.13.2 Materials and methods

1500 mg/liter was used as concentration in the feed and pure water was used as buffer liquid. Since we are using the prototype, the feed will now be added to the stomach. The hoses will circulate the feed from the stomach and over the membrane as in cross flow filtration and back to the stomach. See chapter 2.10 for information about cross flow filtration. The duration of the test was 1 hour, the flow rate of the feed was 0,2 ml/s and the flow rate of the buffer liquid was 0,33 ml/s.

6.13.3 Results and discussion

The testing was very successful. However, the regular concentration of 1500 mg/liter was used with a feed volume of 29 ml and a buffer volume of 100ml. This resulted in high ABS values because the feed was 14,5 times higher than that of the static testing and the buffer volume was the same. Therefore the potential concentration in the buffer got bigger. No Evan's blue leakage was detected after 1 hour testing which shows that the O-rings close the opening between the intestinal glass and the membrane.

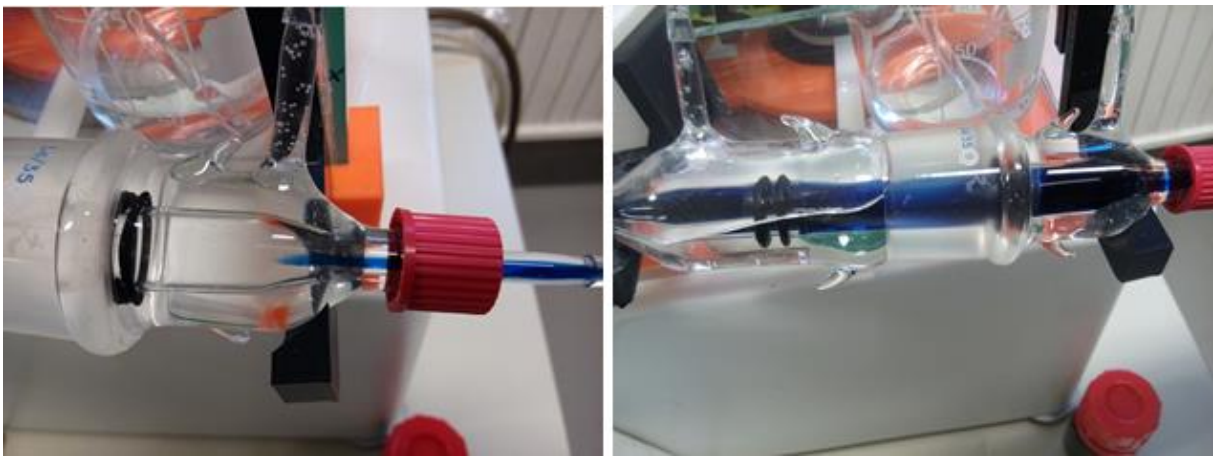

Figure 37: The picture to the left shows how Evan's blue enters the intestinal area where the membrane is. This flow is creeping. The picture to the right is taken approximately one hour later and as can be seen, there are no Evan's blue in the buffer liquid.

Since we have a bigger feed volume (29 ml) we need to adjust the concentration in the feed. The buffer volume is kept at 100 ml. After two hours of testing the buffer volume should not contain more than:

$$30\frac{mg}{liter} * 0{,}1\ liter = 3\ mg$$

$$The\ volume\ of\ the\ fluid\ is\ 29\ ml$$

$$\frac{0{,}1liter}{0{,}029liter} = 3{,}45$$

$$The\ concentration\ in\ the\ membrane\ needs\ to\ be\ 3{,}5\ times\ higher$$

$$than\ the\ potential\ concentration\ \left(\frac{3mg}{0{,}1liter}\right)in\ the\ buffer\ liquid$$

$$A\ solution\ of\ 3{,}5 * \frac{3mg}{0{,}1liter} = 105\ mg/liter$$

6.14 Test 3

6.14.1 Purpose

The purpose was to find a diffusion coefficient.

6.14.2 Materials and methods

A solution of 150 mg/litre (ten times lower than that of the static testing) was used as feed. In the calculation above, 105 mg/litre is the minimum value, but it is easier to measure 150 mg/litre. Samples were taken every 10^{th} minute and analysed in the SPM. The buffer volume was 100 ml.

6.14.3 Results and discussion

ABS values for both 220 nm and 280 nm were detected and was used to find diffusion coefficient. The highest ABS value was 1,220 at the wavelength 220 nm which is acceptable. One problem with keeping a buffer volume of 100 ml is the need of getting samples during the tests. 100 ml is not enough to take samples and still have enough buffer liquid for the membrane unit. In the next test the buffer volume should be increased to 150 ml.

6.15 Test 4

6.15.1 Purpose

The purpose of this test was to find a diffusion coefficient.

6.15.2 Materials and method

The feed concentration in this test was 150 mg/liter and the buffer volume was 150 ml.

6.15.3 Results and discussion

The buffer volume of 150 ml proved to be a little too big for an early distribution of solute in the buffer liquid. This resulted in no ABS readings to very low ABS readings the first 30 minutes of the test and no readings of ABS at wavelength 280 nm before 50 minutes had passed. Therefore ABS values at wavelength 280 nm was not included in this result.

6.16 Test 5 and 6

6.16.1 Purpose

The purpose was to fine diffusion coefficient.

6.16.2 Materials and method

These tests were executed with a feed concentration of 200 mg/litre and a buffer volume of 150 ml. The other conditions were the same as before.

6.16.3 Results and discussion

Two tests were executed in each test (5 and 6). The ABS readings were very good for these two tests.

6.17 Test 7

6.17.1 Purpose

The purpose of this test was to see how well the water bath reacted to the heating element of the rheometer. The goal was to find a temperature of the heating element that would stabilise the temperature in the water bath at 37˚C.

6.17.2 Materials and method

The temperature of the water of both the stomach and the water bath should be 37˚C. A thin layer of thermo conductive paste was added to the heating surface and the prototype was placed onto the rheometer. The Water bath was filled with 1,5 litres of water and the stomach was filled with approximately 29 ml of water. Temperature sensors were placed in the stomach and in the Water bath. The idea was that a certain temperature (>37˚C) of the heating element would stabilize the temperature of the stomach and the Water bath.

6.17.3 Results and discussion

With a heating surface of 70˚C on the heating element, the temperature in the stomach stabilizes at 36-37℃ (2 hour testing) which is known to be normal in a human body. However, because

of the bigger surface of the water bath the temperature never reaches 37˚C, but stabilizes on a much lower level at approximately 29℃. This is 8℃ lower than the desired value.

Figure 38: The picture to the left shows T1 and T2 where T1 is for the stomach and T2 for the water bath. The picture to the right shows the temperature sensor (blue wire in the stomach).

6.18 Test 8

6.18.1 Purpose

This test was executed as part of the product development process. The test consist of testing the use of the user manual.

6.18.2 Materials and method

Two summer internships at NMBU were asked to setup the prototype as explained in the user manual without any help. It should be mentioned that they are not studying to be engineers, they are not part of this thesis nor trained in assembling this kind of equipment. It was an advantage to have them test the user manual because they did not have a technical background.

6.18.3 Results and discussion

Only a few minor changes had to be made in order for a completely new user to setup the prototype. The feedback was that the user manual was very straightforward.

6.19 Dynamic fluid calculations for water

The purpose of calculating these values is to give the future user of this system the possibility to further develop the mathematical model of the system. Either by using the calculated dimensionless numbers in this thesis or to compare with new values will be of interest.

6.19.1 Reynolds number

This number is calculated both for the hoses and the membrane. In the membrane unit it is expected that the flow is fully developed which may not be far from the truth since we have so low velocities. See figure 37, left picture.

6.19.1.1 Hoses (3,17 mm diameter)

$$R_e = \frac{D\bar{V}\rho}{\mu} = \frac{0{,}00317m * 0{,}025m/s * 1000kg/m^3}{0{,}720 * 10^{-3}kg/(m * s)} = 110$$

6.19.1.1 Membrane (10 mm diameter)

$$R_e = \frac{D\bar{V}\rho}{\mu} = \frac{0{,}01m * 0{,}0025m/s * 1000kg/m^3}{0{,}720 * 10^{-3}kg/(m * s)} = 34{,}7$$

These values for the Reynold number suggest laminar flow (see chapter 2.12.2) which is exactly what we got. See figure 37.

6.19.2 Schmidt number

In order to estimate this number, it was necessary to calculate considering the lowest and highest average diffusion coefficient obtained from dynamic testing. The units of the diffusion coefficient has been changed to fit the other units of the equation.

6.19.2.1 Lowest value of Sc

$$Sc = \frac{\nu}{D_v} = \frac{\mu}{\rho D_v} = \frac{0{,}720 * 10^{-3}kg/(m * s)}{1000kg/m^3 * 4{,}67 * 10^{-11}m^2/s} = 15417$$

6.19.2.2 Highest value of Sc

$$Sc = \frac{\nu}{D_v} = \frac{\mu}{\rho D_v} = \frac{0{,}720 * 10^{-3} kg/(m * s)}{\frac{1000kg}{m^3} * 1{,}09 * 10^{-10} m^2/s} = 6605$$

In these calculations, it is the effective diffusion coefficient that is considered for estimating the Schmidt number. Eq. 9 states that it is actually the diffusion coefficient, D_v, which should be considered, but not enough information about the membrane is given to calculate D_v. Therefore we use the effective diffusion coefficient. Obtained values of Sc is within the desired range of 10^2 to10^5. See chapter 2.7.3.

6.19.3 Graetz number

The Graetz number is only calculated for the membrane because it is here we have diffusion that is of interest. Graetz number is calculated considering the high and the low value of Schmidt number.

6.19.3.1 Membrane (10 mm diameter)

$$Gz = \frac{\pi}{4} Re\ Sc\ \frac{D}{L_t} = \frac{\pi}{4} * 34{,}7 * 15417 * \frac{0{,}01}{0{,}5} = 8403$$

$$Gz = \frac{\pi}{4} Re\ Sc\ \frac{D}{L_t} = \frac{\pi}{4} * 34{,}7 * 6605 * \frac{0{,}01}{0{,}5} = 3600$$

6.19.4 Sherwood number for laminar flow

$$Sh = 1{,}76 Gz^{0{,}33} = 1{,}76 * 8403^{0{,}33} = 34{,}7$$

$$Sh = 1{,}76 Gz^{0{,}33} = 1{,}76 * 3600^{0{,}33} = 26{,}2$$

Appendix U shows a graph of Sherwood number as a function of Graetz number. The Sherwood number extends to the value 21 which is a little lower than what we obtained in our calculations. However the logarithmic x-axis of appendix U does not show values low enough considering the calculations of Graetz number. For example by taking 1/8403, we get 0,00012. This values is not shown on the x-axis of appendix U. By extending the graph it is possible to compare our values with the graph in appendix U. The error is not much and therefore it can be concluded that our calculations of these dimensionless numbers are pretty accurate.

6.20 Results of experimental work

6.20.1 Static results

The static results of test 12-16 are presented as diffusion coefficients. These coefficients are presented both as an average value and as a time dependent value. The average value is not the best way to present the data when explaining the mathematical model for each membrane, but is a good indicator that the tests give very much the same values. The time dependent diffusion coefficients shows the trend line for each test and compare them to each other.

6.20.1.1 Average diffusion coefficient

The static testing of both L-tryptophan with different start concentration and P-nitrophenol gives almost the same diffusion coefficient, which is a good thing because diffusion coefficient is supposed to be independent of concentration gradient (Norby). The average thickness of the different membranes is taken into account. Table 19 shows that the diffusion coefficient is the same for both 3,5 kDa and 8 kDa membrane. It is also worth mentioning that the diffusion coefficient found is the effective diffusion coefficient because it is found by testing. That means the tortuosity, porosity and constrictivity has contributed to these values.

Table 19: This table shows the average diffusion coefficient for each static test.

Test	MWCO kDa	Solute	Wavelength [nm]	Average effective diffusion coefficient [cm^2/h]
13a	3,5	(L-tryp)	220	1,83E-04
13b	3,5	(L-tryp)	280	2,69E-04
14	3,5	(P-nit)	400	6,53E-04
15a	8	(L-tryp)	280	1,55E-03
15b	8	(L-tryp)	220	7,83E-04
15c	8	(L-tryp)	220	6,96E-04
15d	8	(L-tryp)	280	1,81E-03
16	8	(P-nit)	400	2,08E-04
17	8	(L-tryp)	220	5,09E-04

6.20.1.2 Time dependent diffusion coefficient for 3,5 kDa membrane

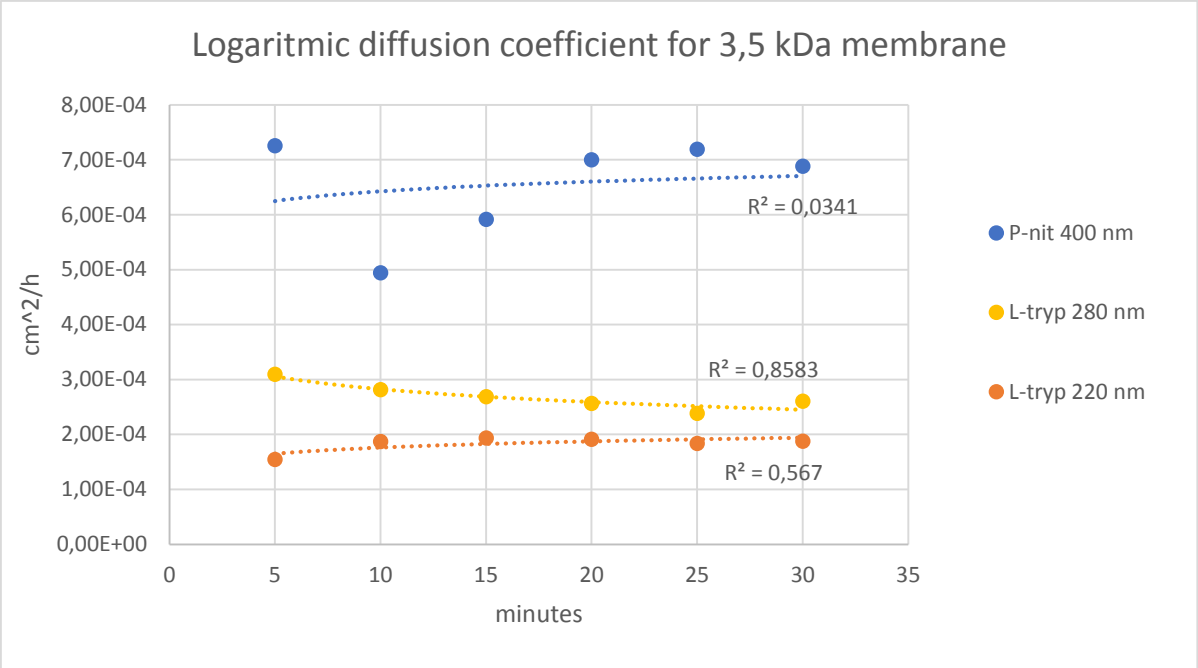

Figure 39: This figure shows how the diffusion coefficient for different molecules changes over time through a 3,5 kDa membrane during static testing.

The static tests done with a 3,5 kDa membrane where fewer than that for 8 kDa membrane. The results does not give a definite pattern as to how the membrane behaves towards different molecules. The time dependent diffusion coefficient is not calculated for these tests since they vary too much.

6.20.1.3 *Time dependent diffusion coefficient for 8 kDa membrane*

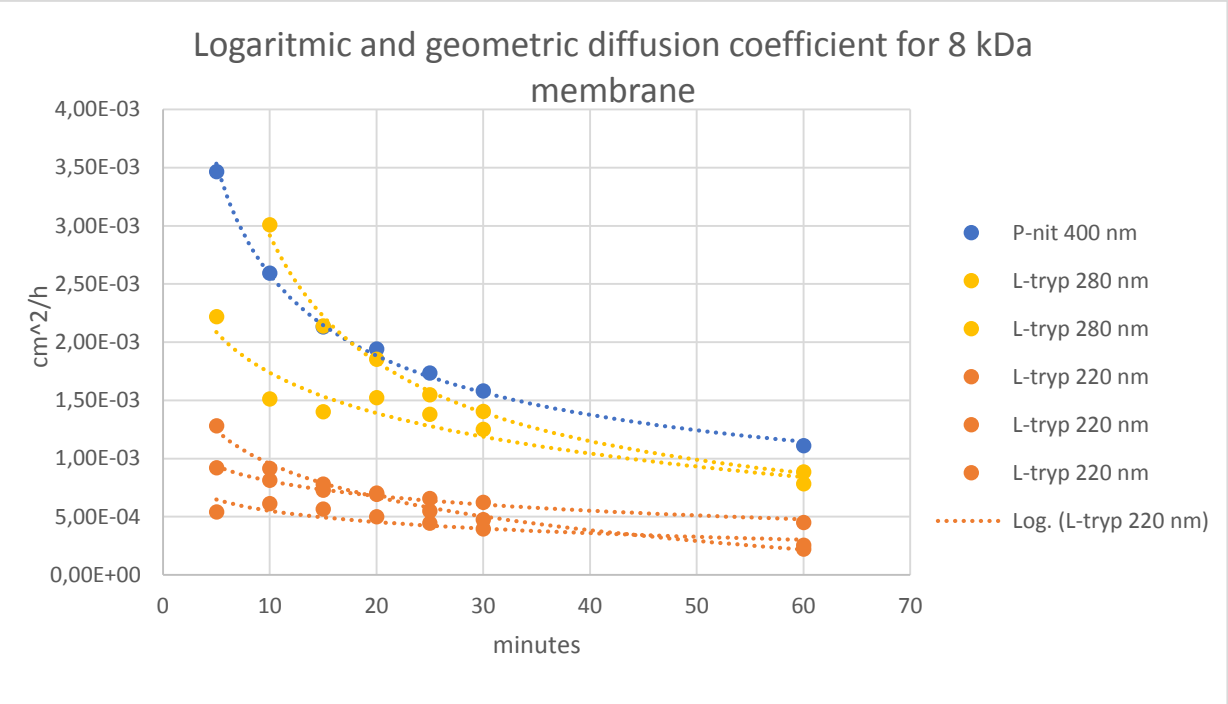

Test	Color	Trendline	Diffusion coefficient as product of time
15a		Logarithmic	$D_e = -0{,}0005\ln(t) + 0{,}0029$
15b		Logarithmic	$D_e = -0{,}0004\ln(t) + 0{,}0019$
15c		Logarithmic	$D_e = -0{,}0002\ln(t) + 0{,}0012$
15d		Geometrical	$D_e = 0{,}0137t^{-0{,}672}$
16		Geometrical	$D_e = 0{,}0073t^{-0{,}454}$
17		Logarithmic	$D_e = -0{,}0001\ln(t) + 0{,}0009$

Figure 40: This figure shows how the diffusion coefficient for different molecules changes over time through an 8 kDa membrane during static testing. The color represents testing of different wavelength.

This figure shows a clear different between the diffusion coefficient for the 8 kDa membrane considering L-tryptophan at wavelength 220 nm and 280 nm. L-tryptophan at 280 nm seems to have better permeation properties than L-tryptophan at 220 nm. P-nitrophenol at 400 nm shows the same tendency as L-tryptophan at 280 nm. The two upper trendlines correlate best with a geometrical formula and the rest correlate best with a logarithmic. The low effective diffusion coefficient is explained that the membrane is a low permeable membrane.

6.20.2 Dynamic results

6.20.2.1 Average diffusion coefficient

Table 20: This table shows the average diffusion coefficient for each dynamic test.

Test	MWCO kDa	Solute	Wavelength [nm]	Effective diffusion coefficient [cm^2/h]
3	3,5	(L-tryp)	220	2,18E-03
3	3,5	(L-tryp)	280	3,92E-03
4	3,5	(L-tryp)	220	1,68E-03
5	8	(L-tryp)	220	3,04E-03
5	8	(L-tryp)	280	2,21E-03
6	8	(L-tryp)	220	2,76E-03
6	8	(L-tryp)	280	1,81E-03

6.20.2.2 Time dependent diffusion coefficient for 3,5 kDa membrane

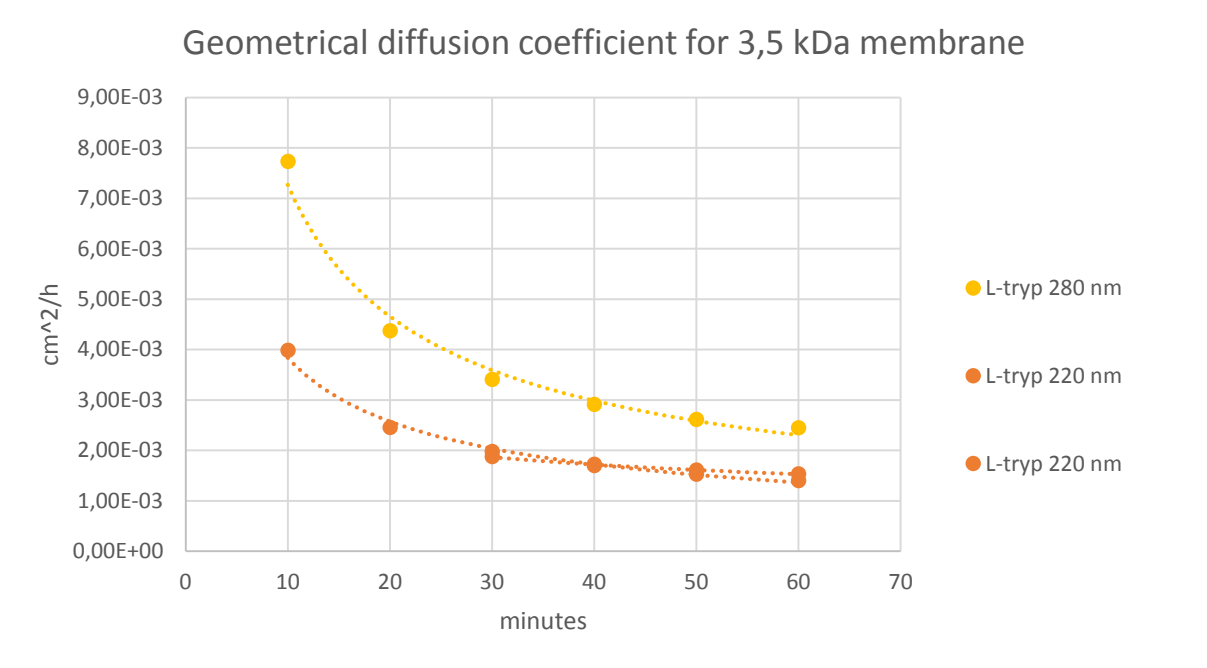

Test	Color	Trendline	Diffusion coefficient as product of time
3		Geometrical	$D_e = 0{,}0145t^{-0{,}577}$
3		Geometrical	$D_e = 0{,}0319t^{-0{,}642}$
4		Geometrical	$D_e = 0{,}005t^{-0{,}289}$

Figure 41: This figure shows how the diffusion coefficient for different molecules changes over time through a 3,5 kDa membrane during dynamic testing. The mathematical expression for each is also given.

Permeation of L-tryptophan at 280 nm and 220 nm show the same tendency as the static testing where 280 nm is favourable. 280 nm is for amino acid and 220 nm for the aromatic side chain.

6.20.2.3 Time dependent diffusion coefficient for 8 kDa membrane

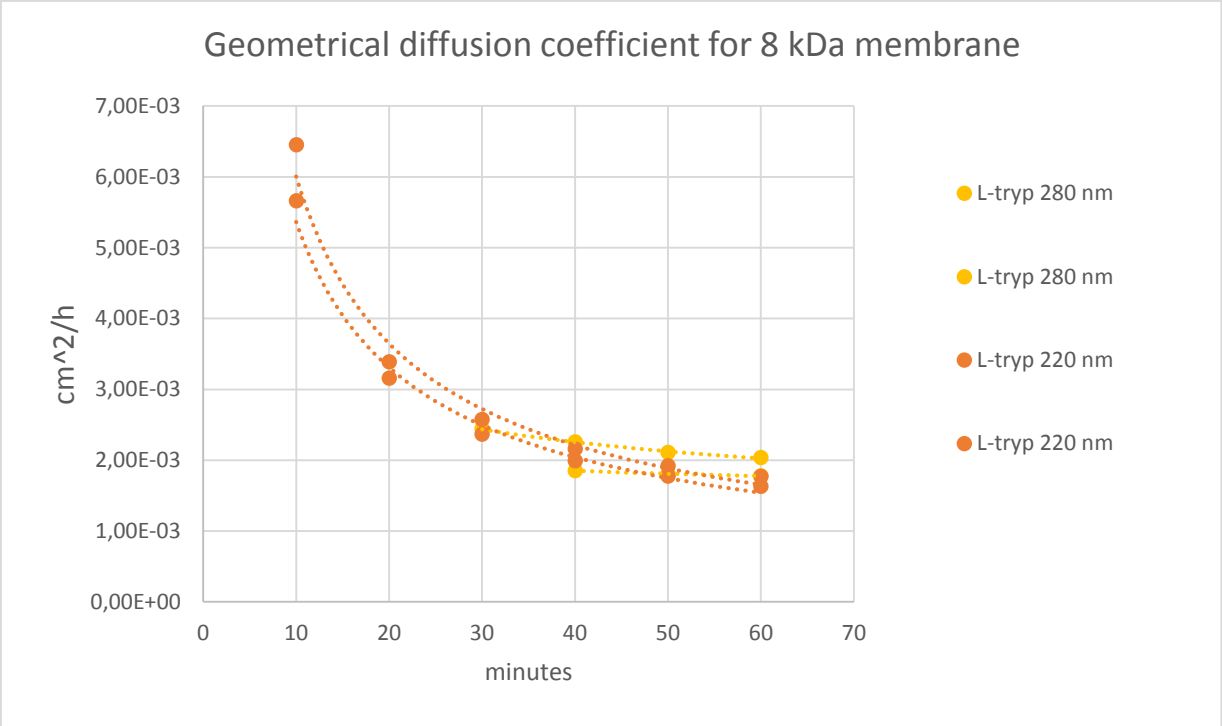

Test	Color	Trendline	Diffusion coefficient as product of time
5		Geometrical	$D_e = 0{,}0315t^{-0{,}720}$
5		Geometrical	$D_e = 0{,}0061t^{-0{,}268}$
6		Geometrical	$D_e = 0{,}0267t^{-0{,}697}$
6		Geometrical	$D_e = 0{,}0027t^{-0{,}099}$

Figure 42: This figure shows how the diffusion coefficient for different molecules changes over time through an 8 kDa membrane during dynamic testing. The mathematical expression for each is also given.

In this case we cannot say that there is a difference between permeation of amino acids and the aromatic side chains. The table in figure 42 shows that the equations for the time dependent diffusion coefficient is much alike and the plotting of the result show the same.

7 Problems encountered

7.1 Volume limitations

Increasing the diameter of the stomach drastically decreased the height of the fluid inside. This was no surprise, but made it more difficult to pump fluid out of the glass and to fit the PH meter inside the stomach for monitoring. Since 29 ml is the maximum amount of HGJ and HDJ together, the hoses and membrane unit had to be made very small. This caused some practical problems because of distances between the pump and the prototype. The length of the membrane had to be shortened from 10 cm to 5 cm, to be able to fill the volume with HGJ and HDJ, see chapter 3.1.2.

7.2 Communication

UiO GBD is a very small department of only two people and my perception was that they had a lot to do all the time. My method when ordering new parts were always to be available to questions from UiO GBD regarding my orders. This was explicitly emphasized in the mails. I never received any questions about the orders, and sometimes the parts were not made according to the drawings. In total, these communication problems postponed the initialization of the testing by two weeks. Thanks to the flexibility of Terje Hansen at UiO GBD, it was no longer than two weeks.

7.3 Stand for motor

The possibility of rotating the motor at some degrees was impossible after installing the "hose fixture for water bath". The stand for the motor was one of the first part that was made and as development of other parts improved, the rotational option was impossible and also unnecessary. By rotating the "DC motor holder "only a few degrees, resulted in a big displacement of the tip of the propeller because of the small radius of the "DC motor holder".

7.4 Limits to what can be produced

7.4.1 Frosted glass

Frosted glass on the big end diameter of the intestine glass would give a rougher surface. To have a rougher surface between the membrane and the intestine glass would definitely

increase the friction coefficient and prevent the membrane from falling off. This would probably have been a smart design, but the practical challenge for the UiO GBD was that the glass broke during this stage of designing. Ultimately it was not made because of these challenges.

7.4.2 Water bath

The water bath that was made in the glass blowing department of UiO, was not made according to those measurements that was given. The reason for this was that they did not have the right equipment for making it exactly as the drawing. This resulted in that more time was spent on making new "centring brackets for water bath" and "centring brackets for stomach".

7.5 Heating of water bath

Since the plastic used to print the different parts is not a good conductor of heat, it was difficult to raise the temperature in the water bath to 37 degrees. This had also to do with the small surface of the heating element which is not suitable for heating as it is at this point.

7.6 Dynamic testing

One problem with the dynamic tests was that it took a long time for some solutes to be detected in the buffer liquid. This was not exclusively for one solute, but for both the amino acid and the side chain. This resulted in trendlines that did not span over the entire testing period. For the majority of the dynamic tests, it was always a substance that did not appear before 30-40 minutes after initialization of test.

7.7 Particle simulation

A lot of time was spent on doing this particle simulation which consisted in simulating diffusion through the membrane in solidworks. There were no tutorial on how to simulate cross flow filtration in solidworks which made it even harder to deal with.

8 Discussion and future work

8.1 Diffusion coefficient

The experimental work lead to a mathematical expression for the diffusion coefficient for almost all cases. Some results were good and represented very well the experimental tests, whereas other tests did not give a representative picture. The results of the dynamic testing was more stable than the results of the static testing.

8.1.1 Static testing

In the static testing the results from using a 3,5 kDa membrane did not produce trendlines good enough to estimate the diffusion coefficient. It became clearer that these results were not representative when looking at the other tests. For example in all other cases of this thesis, the diffusion coefficients drops as time passes, but for the static testing with 3,5 kDa membrane two out of three trendlines show an increase in diffusion coefficient which is not logical when taken into account the development of fouling and concentration difference (see chapter 2.5 and 6.8.1). These are two factors that weakens diffusion over time. It is not critical to do more static testing to get better result because the system will be dynamic.

For the 8 kDa membrane all the results show a decrease in the diffusion coefficient over time. It is also a clear difference between the diffusion of substance that absorbs light at 220 nm and 280 nm. As described in chapter 2.16 the substance absorbing at 280 nm is typical for amino acids and substance absorbing at 220 nm is the side chain of those amino acids. Another discovery made from these permeation tests is that the diffusion coefficients that lie above a certain value follow a geometrical trendline, while diffusion coefficients that are lower follow a logarithmic trendline. This means that for the lower values of diffusion coefficients, the change is also lower. The permeation of substance that absorbs light at 280 nm seems to be bigger than for substance that absorbs at 220 nm which is strange (see chapter 8.1.2). This is also the case for testing with 3,5 kDa membrane. The limit or value where the trend line changes from being logarithmic to geometrical is uncertain but there seems to be more of a transition zone judging from figure 40.

8.1.2 Dynamic testing

The dynamic testing with the 3,5 kDa membrane gives about 10 times higher diffusion coefficients compared to the static testing with the same membrane and solute. This is also to be expected because the flux is expected to increase when two fluids flow counter current with a membrane between one another instead of no fluid flow (Tysse 2014). The development of the diffusion coefficient seems to follow a more representative curve (see figure 41). The fact that permeation of one substance (280 nm) in this membrane is greater than another is strange because the understanding so far about aromatic amino acids is that they have an aromatic side chain attached to it. So if one aromatic amino acid permeates through the membrane, then so should the aromatic side chain. This gives reason for asking two questions. Is there a difference in size of the amino acid and the aromatic side chain that gives these results or are there maybe pollutions among the amino acids?

For the 8 kDa membrane all the diffusion coefficients seem to be just as big (see figure 42), and follow almost the same path which has a geometrical trendline. Like in the first dynamic test (3,5 kDa membrane) there are some substances that is not detected before 30-40 minutes. However for the 8 kDa membrane this applies to the amino acid and not the aromatic side chain.

All the dynamic tests show that the trendlines follow a geometrical path and that this leads to a more rapid decrease in the diffusion coefficient. For the 3,5 kDa membrane the aromatic side chain is not represented in as great quantity as the amino acids, but in the 8 kDa membrane they are alike. This gives reason for thinking that the aromatic side chain does not permeate as easily as the amino acids and perhaps that they are not bound together as one molecule.

8.1.3 Testing the diffusion coefficient

By putting the diffusion coefficient into Eq. 11 or 18, the flux between each sample is plotted. The accumulation of permeate can be plotted in another diagram and compared to the experimental testing. This has been done, and the results are deviating. Some results correlate better with the practical testing, but the majority deviates a lot and the tendency is that the estimated value is higher than the experimental. The reason for this is explained that the equation used for calculating the diffusion coefficient does not reflect the physical shape of the membrane which is cylindrical. It represents one dimensional flux, whereas practically we see

a two dimensional and radial flux. The one dimensional flux considers a bigger membrane area than the actual area in the practical testing.

8.2 Deformation of membrane

Practically, it didn't seem as raising the fluid flow had an impact on membrane collapse. The membrane collapse seemed to be random and not necessarily an effect of fluid velocity. This can be explained by Eq. 21 where the pressure drop is dependent on the square of the velocity of the fluid. The velocity is very low and therefore will not have a big impact on this pressure drop.

The practical result of deformation testing was not in harmony with the simulation of pressure drop across the membrane. The simulation showed that by increasing the intestinal flow, the intestinal pressure got higher and the membrane should not collapse. The experimental testing showed the opposite.

Experimentation with turning on the pump for the intestinal fluid before turning on the pump for the buffer fluid showed that a pressure was build up in the intestinal fluid. This kept the membrane from collapsing, see figure 35.

Another way to solve the problem of membrane collapse might be to lower the pressure inside the buffer circuit. A prototype of a new buffer glass has been constructed in solid works, but has not been physically made or tested. It might be a problem with this solution because the pump is set to move a certain amount of fluid per time and this yields a pressure. It is uncertain if this pressure can be lowered by lowering the total amount of pressure inside the buffer liquid, but it should be tested.

8.3 Temperature control

The temperature in the dynamic model did not reach acceptable values in the water bath. Only in the intestinal fluid the temperature kept 37℃ during 2 hours testing. Another hating source is required to maintain the temperature of the water in the water bath at 37℃, alternatively it could be an idea to make a bigger heating surface on the rheometer. This could for example be done by using metal as the material in the "centring brackets for water bath". This will distribute the heat much faster than the 3D plastic. In this case the "centring brackets for water bath" can cover the entire bottom surface of the water bath. To keep the heat loss to a

minimum it may be a good idea to have plastic walls surrounding the water bath. This plastic has low heat conducting properties and would help in raising the temperature in the water bath.

8.4 DC motor mounting foundation

This part (part 13 table 8, user manual or appendix J) makes it possible to tilt the propeller at intervals of 14 degree angles. It also makes it possible to raise the propeller out of the water with this tilting solution. The problem with the design is the angle of 14 degrees that is too much. Practically it is only possible to keep the propeller at one specific angle. By tilting the "DC motor holder" (part 14 table 8 or appendix K) it either bumps into the bottom of the water bath or it is raised out of the water. The scenario where it is raised out of the water is desirable, but the "hose fixture for water bath" (part 9 table 8 or appendix N) gets in the way.

8.5 Hose fixture for water bath

The design of this part should be changed so that it does not get in the way of the "DC Motor propeller" (part 15 table 8 or appendix L).

8.6 Buffer glass short end

The angle of 20 degrees at which the membrane unit is tilted causes a problem with filling up the buffer glass. Before the buffer glass is filled up so that it covers the membrane, it flows out of the buffer outlet because it is at a lower level. The solution to this can be to design a bigger outlet diameter that extends a couple of centimetre before it is drafted inwards to an opening of 3 mm diameter.

The outlet diameter is also a question as to whether it should be bigger or not. A bigger diameter would definitely decrease the pressure inside the buffer volume which is a good thing regarding membrane collapse (see CAD simulation), but it would demand a bigger hose at the buffer outlet. A bigger hose does not fit in the peristaltic pump as the biggest possible is 3,17 mm (Tysse 2014). In this case a new pump is needed.

8.7 Tilting the membrane unit

The case of tilting the membrane is a solution that was adopted from the first prototype (Tysse 2014) because it removed the air bubble around the membrane. In this thesis the buffer glass has been made bigger and the problem of air bubble disappeared. The “buffer glass fixture 1 and 2” (part 16 and 17 table 8 or appendix O and P) tilts the membrane unit 20 degrees. They were made before considering the positive effects of a bigger buffer volume, but is actually not necessary in this thesis for tilting the membrane unit. They are however necessary for holding it. It is recommended that new “buffer glass fixture 1” is redesigned so that it does not tilt the membrane unit.

8.8 PH sliding mechanism

This component has a big development opportunity because at this point it is not too flexible as to how it can be moved. It only moves in two planes which are in and out towards the centre of the water bath and up and down towards the centre at an inclination of 55 degrees. A new part has been made in solidworks that makes it possible to change this angle from 0-90 degrees. At 90 degrees it would be possible to get further down into the stomach for measuring PH at an early stage of testing.

8.9 The mixing steps

The mixing of milk and saliva is done in the stomach with the propeller as a mixing tool. When the HGJ is added, the hoses of pump 3 is attached to the stomach for circulating the fluid. For this step it is probably not necessary to use a pump for circulating the fluid, but to continue with the propeller as the mixing mechanism. This reduces the amount of parts around the stomach and also the complexity of the system.

8.10 Future work

Some proposals to future work has already been suggested in the previous sections of this chapter, and most of them deal with prototyping. Future work that is more related to the use of the system, should focus on applying knowledge about daily consumptions of nutrients to the system and see how the performance is. Chapter 2.11 gives a description of common nutrients which can be of help in future simulation.

9 Conclusion

A mathematical model of the diffusion coefficient is presented in this thesis. It shows that the diffusion coefficient is time dependent and follows a downward pattern. This pattern has a geometrical or logarithmic trend. The equation that was used for calculating the diffusion coefficient is based on one dimensional flux, whereas the physical membrane has a two dimensional and radial flux. However the diffusion coefficient presented in this thesis can be used to make rough estimates of experimental results.

The prototype has become portable and is not only applicable for use with the rheometer. It has also become more compressed in the sense that all the parts of the prototype is assembled close together.

The heating element of the rheometer is not big enough to heat the water in the "water bath" to acceptable values. The materials that are used for making all "centring brackets" has also a negative effect on the heat distribution from the heating element to the "water bath".

The solution with membrane collapse is promising, but should be tested in a more extensively matter before concluding that it is the solution. However, the CAD simulation presents methods for regulating the pressure across the membrane.

The design of most parts work well together and only small changes are necessary to make them fulfil their purpose. However the finished model makes it possible to do repetitive testing without having to interact with vital parts of the model.

Last but not least, the user manual made for the prototype presents and explains all developments made for this model and makes it easy for a new user to assemble the model.

10 References

BERG, G. B. v. d., RACZ, I. G. & SMOLDERS, C. A. (1989). Mass transfer coefficients in cross-flow ultrafiltration. *Elsevier Science Pulblishers B.V*.

Çengel, Y. A. (2003). *Heat transfer : a practical approach*. 2nd ed. Boston: McGraw-Hill. xxvii, 932 p. pp.

Chemicalbook.com. *L-tryptophan*. Available at: http://www.chemicalbook.com/ProductChemicalPropertiesCB3750054_EN.htm (accessed: 02.03).

Chemicalbook.com. *P-nitrophenol*. Available at: http://www.chemicalbook.com/ProductChemicalPropertiesCB7852550_EN.htm (accessed: 02.03).

Cussler, E. L. (2009). *Diffusion : mass transfer in fluid systems*. 3rd ed. Cambridge ; New York: Cambridge University Press. xvii, 631 p. pp.

Devle, H., Andresen, C. F., Rukke, E., Vegarud, G., Ekeberg, D. & Scüller, R. (2012). Rheological Characterization of Milk during Digestion with Human Gastric and Duodenal Enzymes. *Department of Chemistry, Biotechnology and Food Science, Norwegian University of Life Sciences, Ås, Norway*, 20.

Eijsink, V., Gulbrandsen, T., Isaksen, T., Naas, A. & Kokkim, E. (2014). *Anvendt og eksperimentell biokjemi Laboratoriekurs*, vol. 9. Ås: Norges Miljø- og Biovitenskapelige Universitet.

Fogler, H. S. (2006). *Elements of chemical reaction engineering*. 4th ed. Prentice Hall PTR international series in the physical and chemical engineering sciences. Upper Saddle River, NJ: Prentice Hall PTR. xxxii, 1080 p. pp.

H, V., D, B., A, P. & T, K. (1988). Milk lipid globules: Control of their size distribution. 85.

Harold, E. P. (2009). Size and shape of protein molecules at the nanometer level determined by sedimentation, gel filtration and electron microscopy. *US National Library of Medicine*.

Heldman, D. R. (2003). *Encyclopedia of agricultural, food, and biological engineering*. New York: Marcel Dekker. xvi, 1184 p. pp.

Holzer, L., Wiedenmann, D., Münch, B., Keller, L., Prestat, M., Gasser, P., Robertson, I. & Grobety, B. (2012). The influence of constrictivity on the effective transport properties of porous layers in electrolysis and fuel cells. *Springer Science+Business Media New York 2012*.

Lekang, O.-I. (2013). *Aquaculture engineering*. Second Edition. ed. Chichester, West Sussex, UK: Wiley-Blackwell. xv, 415 pages pp.

Logan, B. E. (2012). *Environmental transport processes*. 2nd ed. Hoboken, N.J.: Wiley.

McCabe, W. L., Smith, J. C. & Harriott, P. (2005). *Unit operations of chemical engineering*. 7th ed. McGraw-Hill chemical engineering series. Boston: McGraw-Hill. xxv, 1140 p. pp.

Modules, C. *Graetz*: COMSOL Modules. Available at: http://www.rpi.edu/dept/chem-eng/WWW/faculty/plawsky/Comsol%20Modules/Graetz/Graetz_new.html (accessed: 10.5).

Neligan, P. *Critical Care Medicine Tutorials*. University of Pennsylvania. Available at: http://www.ccmtutorials.com/renal/rrt/page4.htm (accessed: 25.02.15).

Norby, T. *Defects and Reactions*. Department of Chemistry, U. o. O. (ed.).

Salas-Bringas, C., Rukke, E., T, D., Vegarud, G., C, A. & Scüller, R. (2014). Developing an In-Vitro Dynamic Model of the Stomach and Small Intestine for Milk Products with Rheological Monitoring.

Scmid, F. (2001). Macromolecules: UV-visible Spectrophotometry. *Macmillan Publishers Ltd*.

Spectrumlabs. *standard regenerated cellulose membrane*. Available at: http://www.spectrumlabs.com/dialysis/SpectraPorSeven.html?Pn=132110; (accessed: 25.02.15).

Tysse, M. (2014). *Developing an In-Vitro Dynamic Model of the Stomach and Small Intestine for milk Products-First Prototype*. Faculty of Environmental Sciences and Technology, Department of Mathematical Sciences and Technology: Norwegian University of Life Sciences

Ulleberg, K. E. (2011). *In vitro digestion of caprine whey proteins by human gastrointestinal juices: Effect of whey hydrolysates and peptides on in vitro cell responses*. Ås: Norwegian University of life sciences, Department of Chemistry, Biotechnology and Food Science.

Appendix A

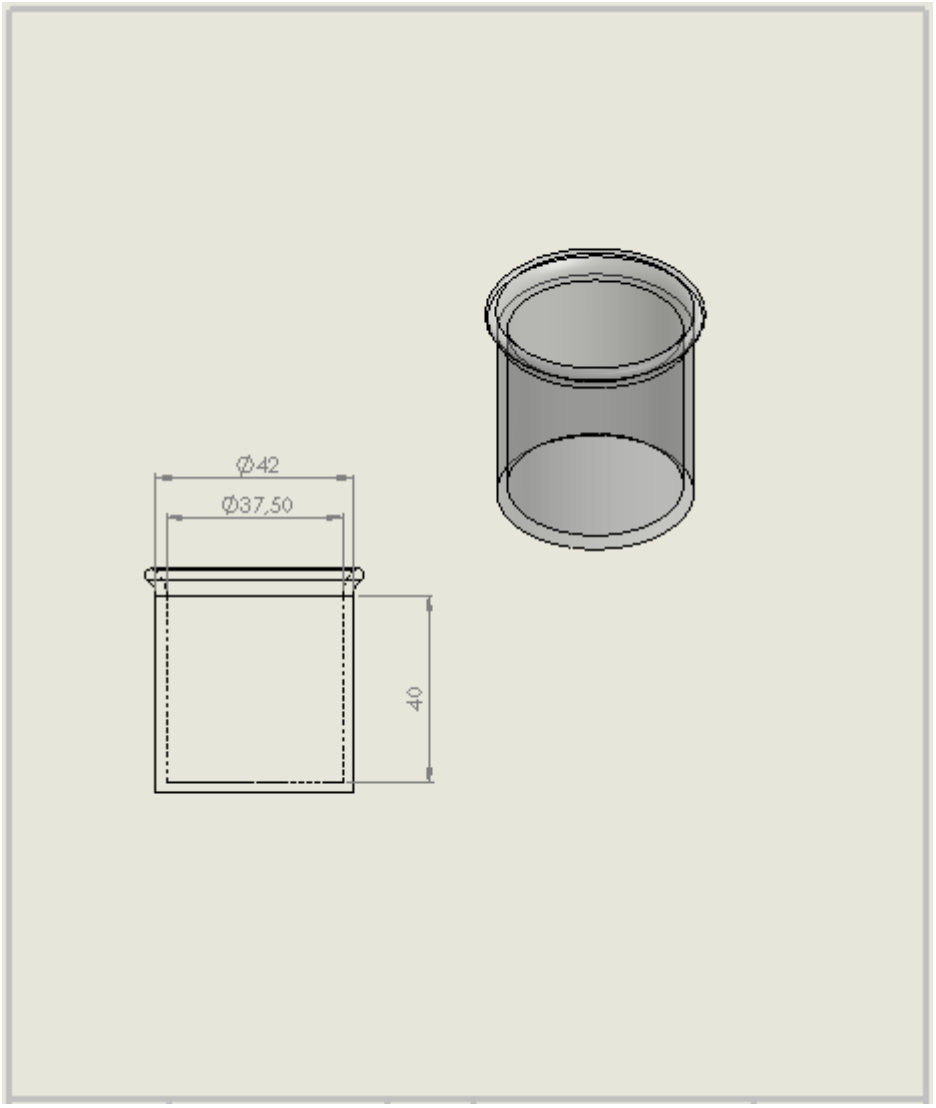

Figure 43: Drawing of the «Stomach» with dimensions.

Appendix B

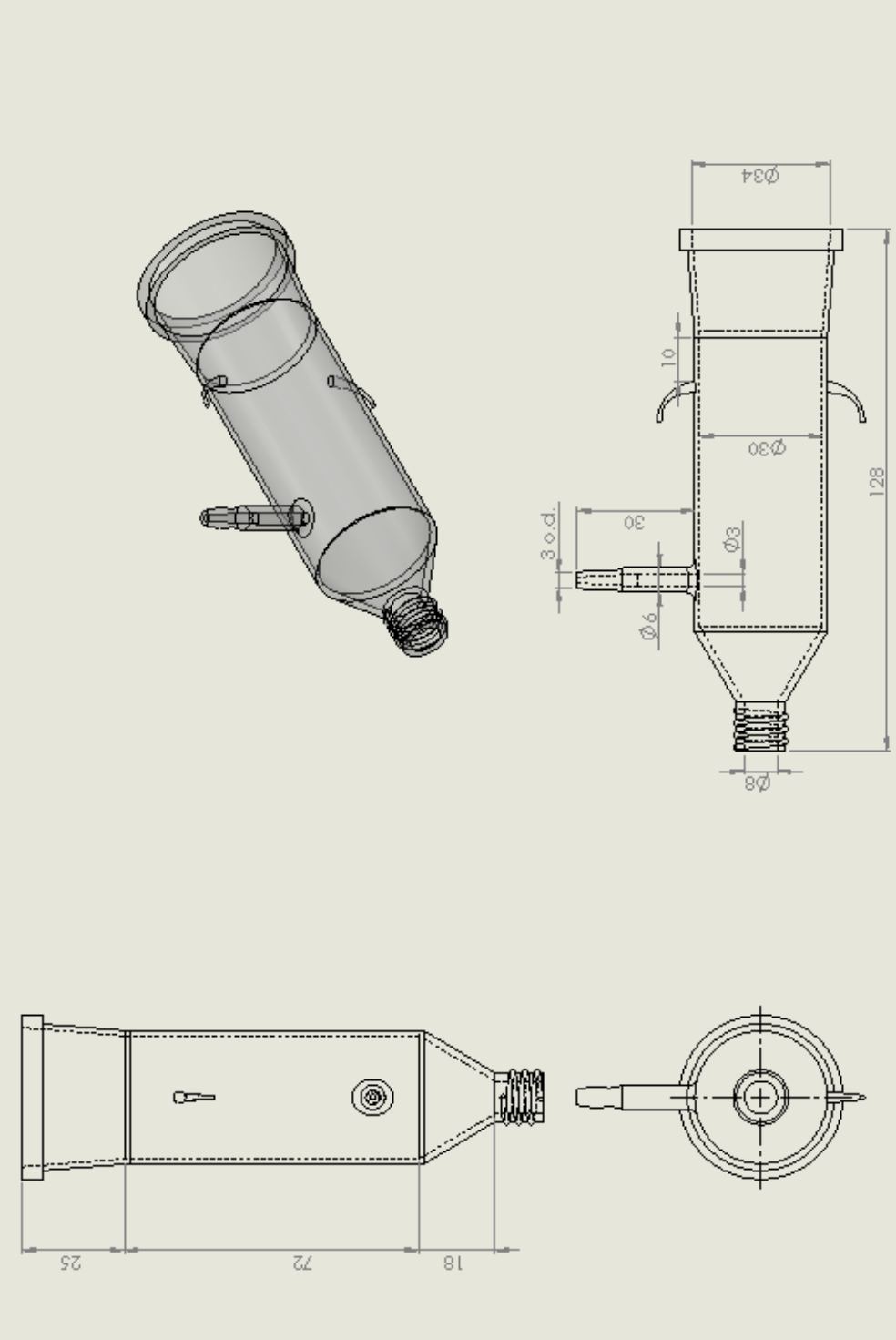

Figure 44: Drawing of the «Bufferglass long end» with dimensions.

Appendix C

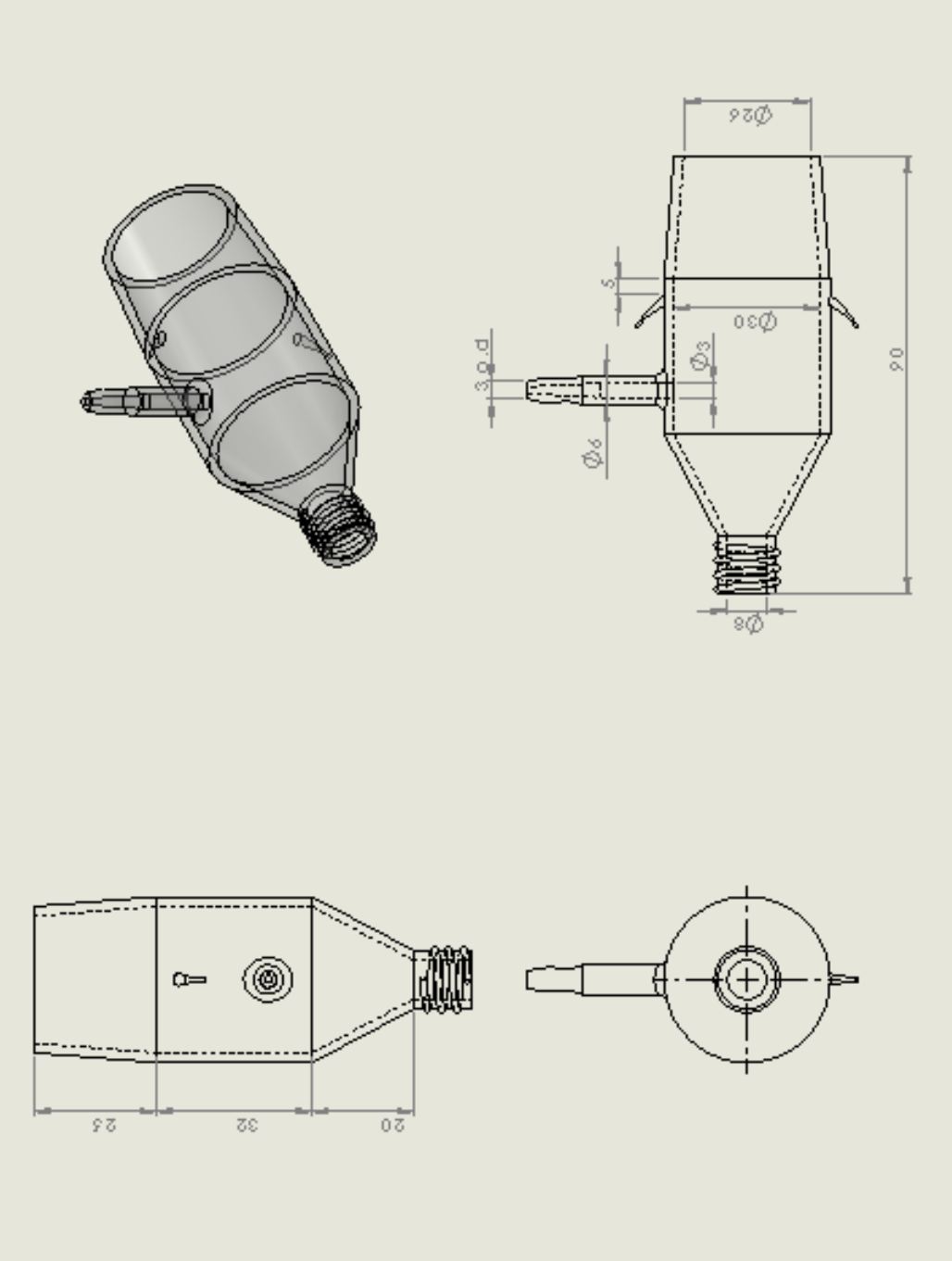

Figure 45 Drawing of the «Bufferglass short end» with dimensions.

Appendix D

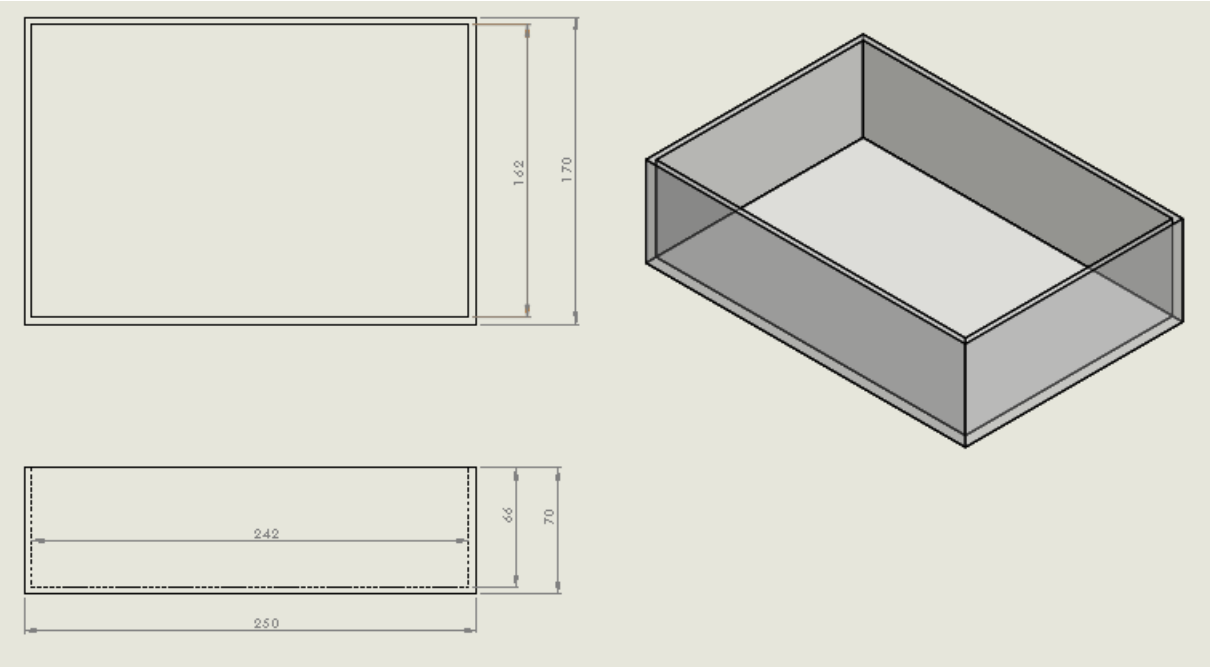

Figure 46: Drawing of the «Water bath» with dimensions.

Appendix E

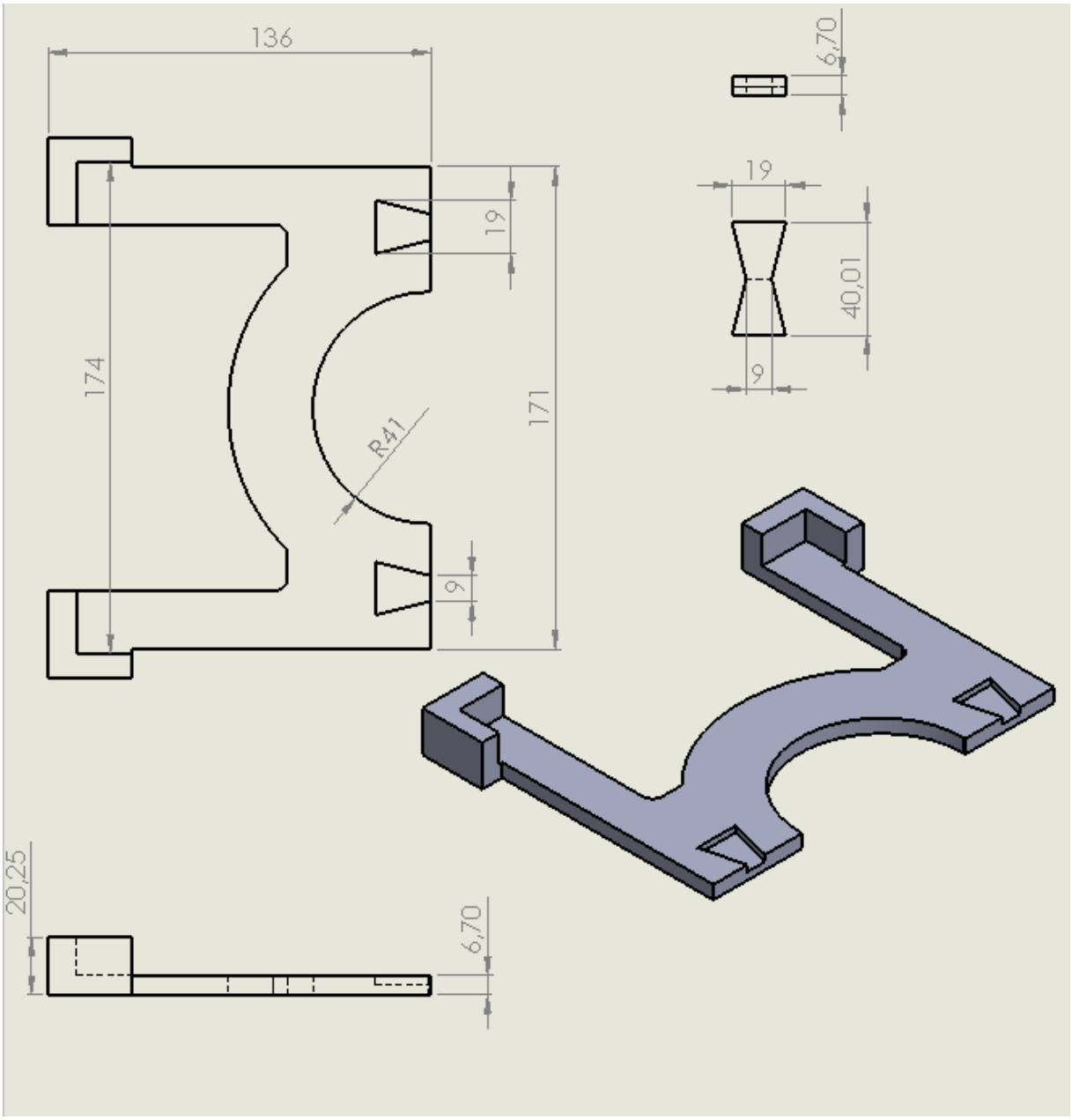

Figure 47: Drawing of the "Centring brackets for water bath" with dimensions.

Appendix F

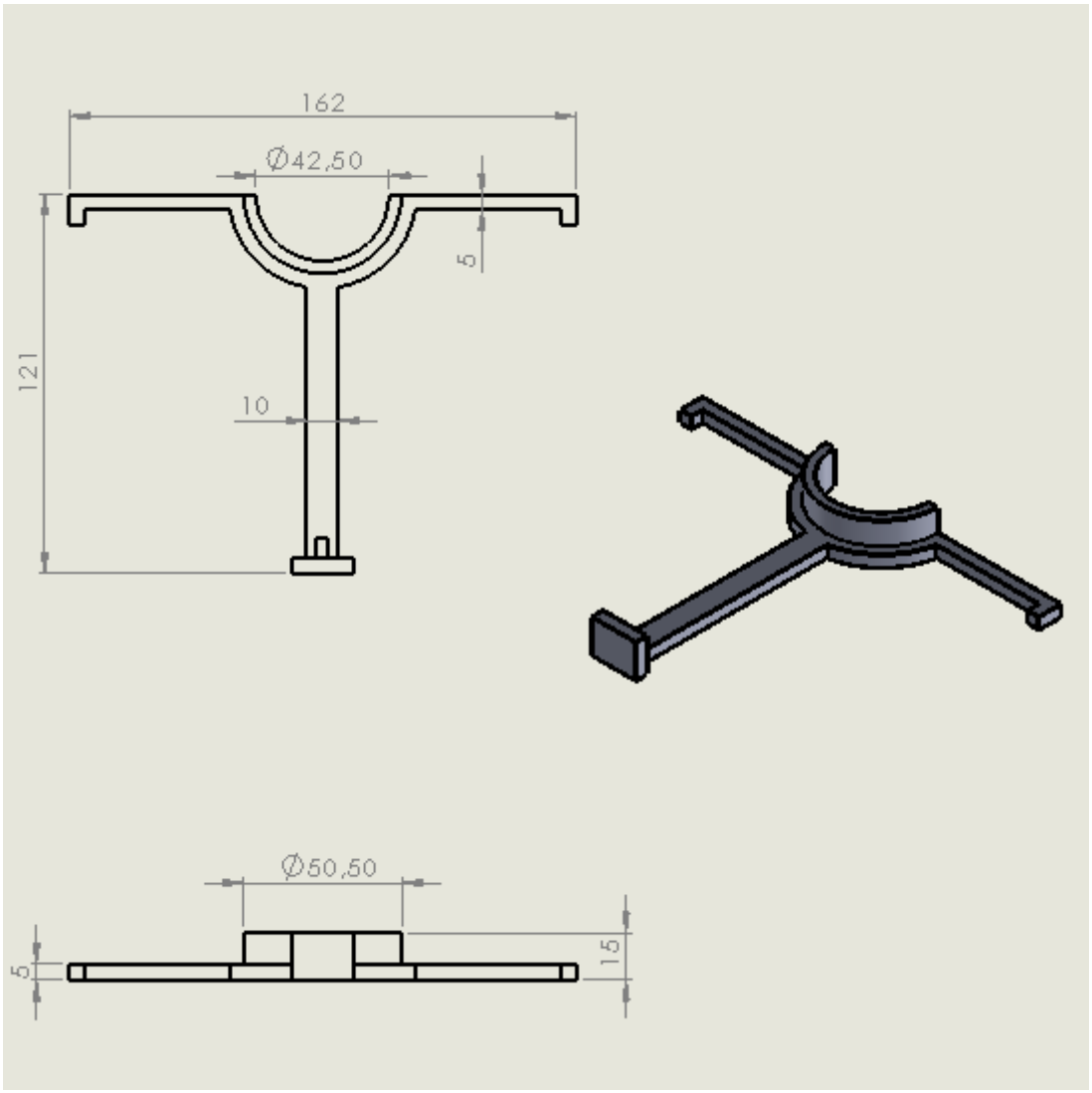

Figure 48: Drawing of "Centring brackets for stomach" with dimensions.

Appendix G

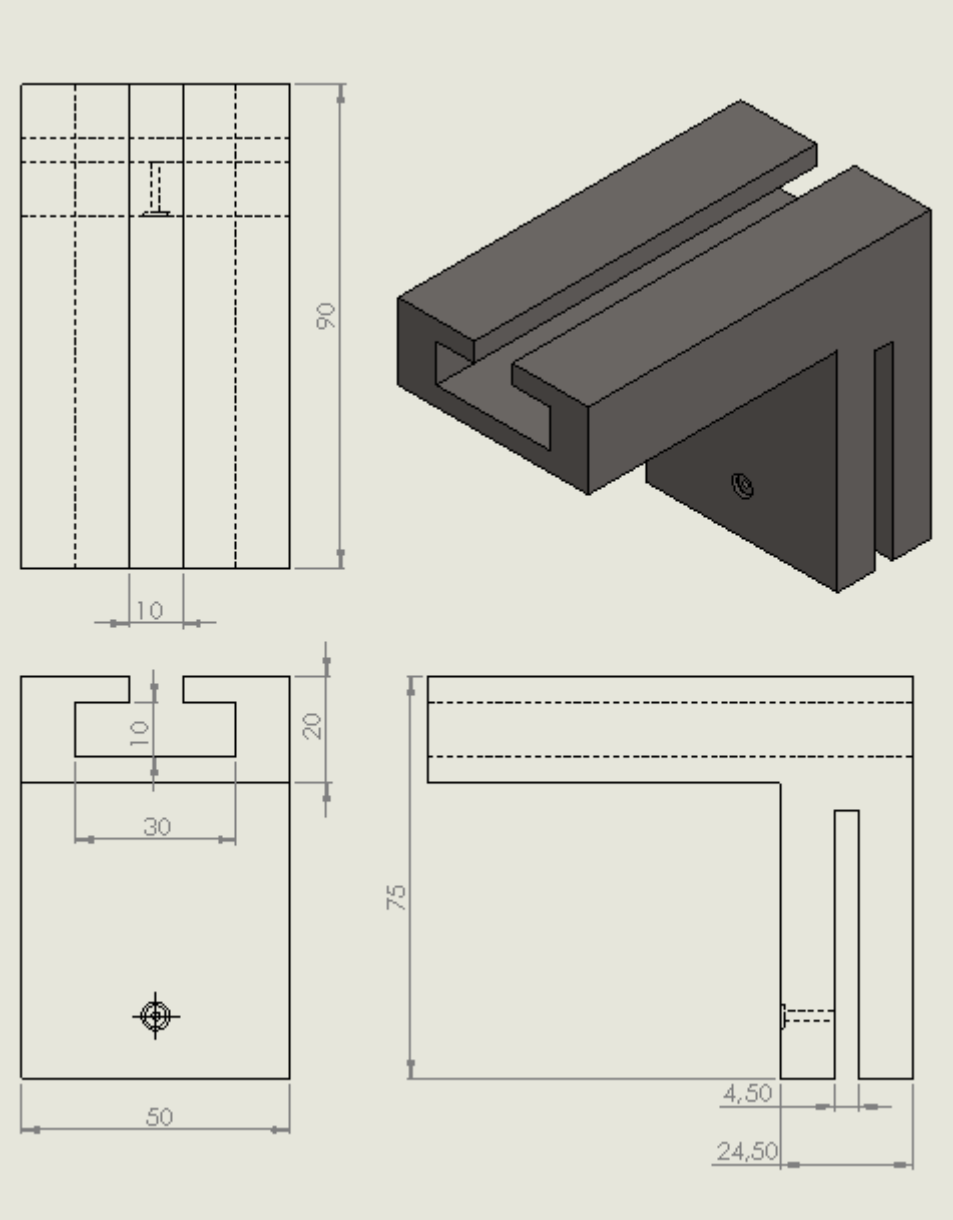

Figure 49: Drawing of the "PH mounting foundation" with dimensions.

Appendix H

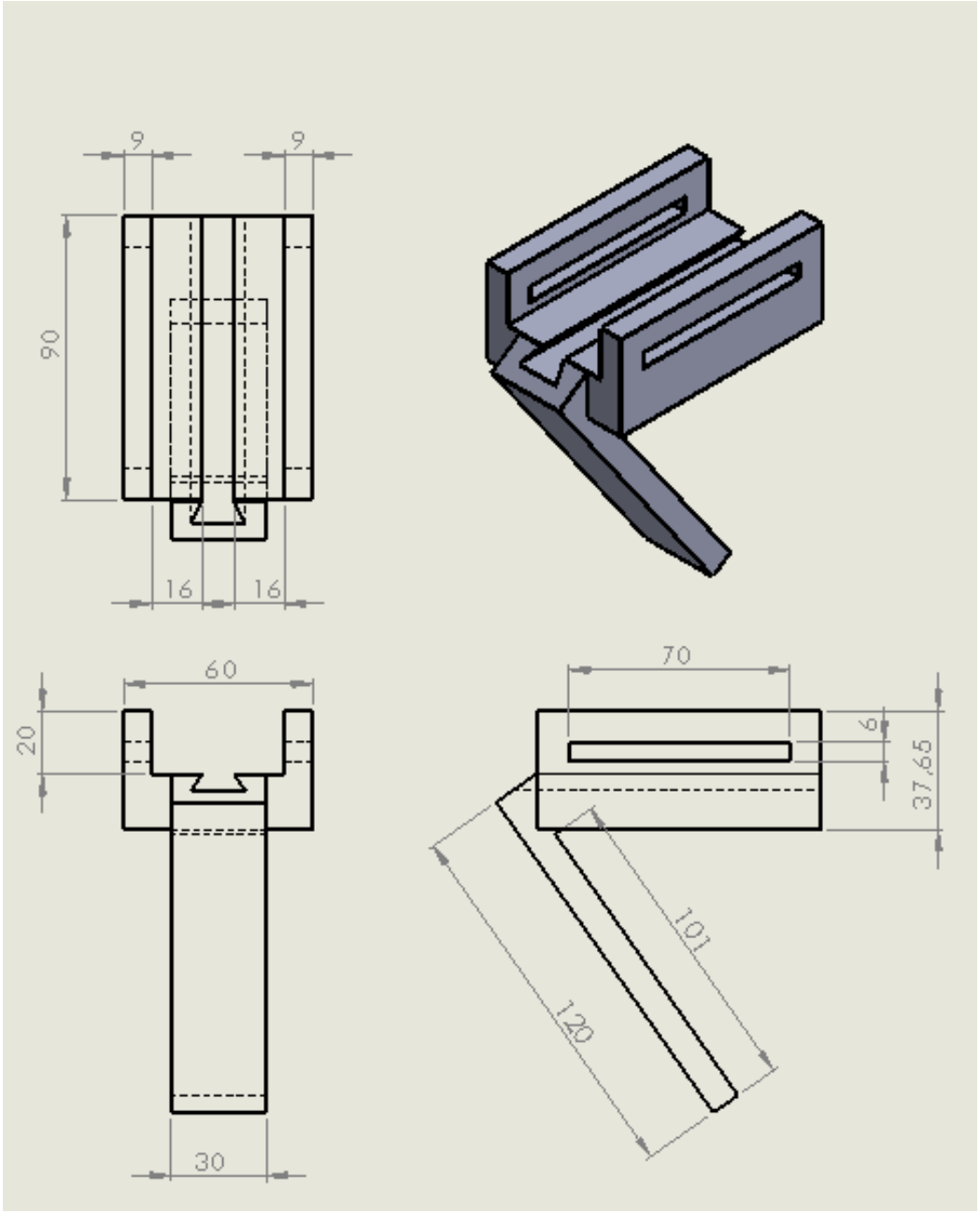

Figure 50: Drawing of the "PH sliding mechanism" with dimensions.

Appendix I

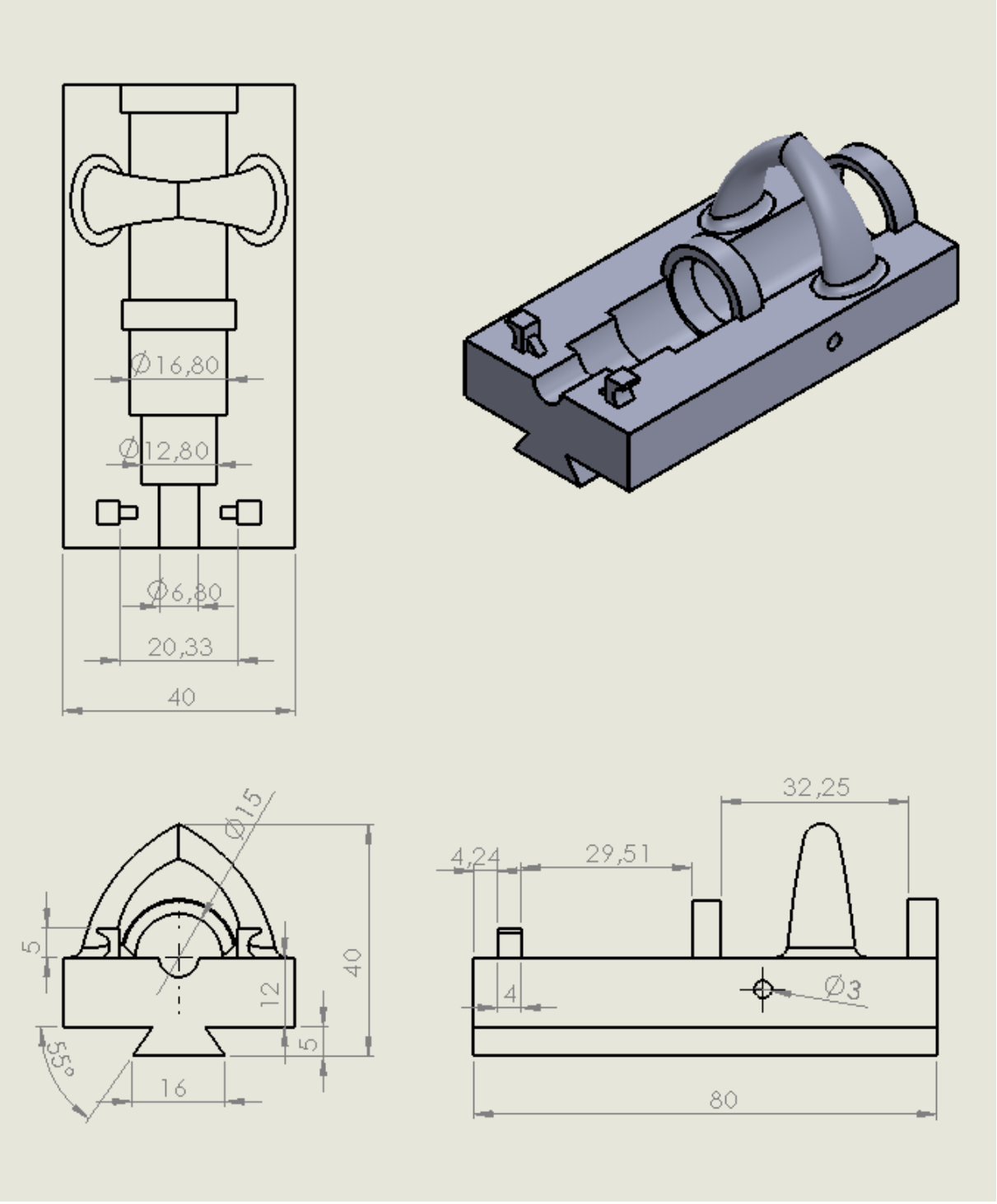

Figure 51: Drawing of the "PH holder" with dimensions.

Appendix J

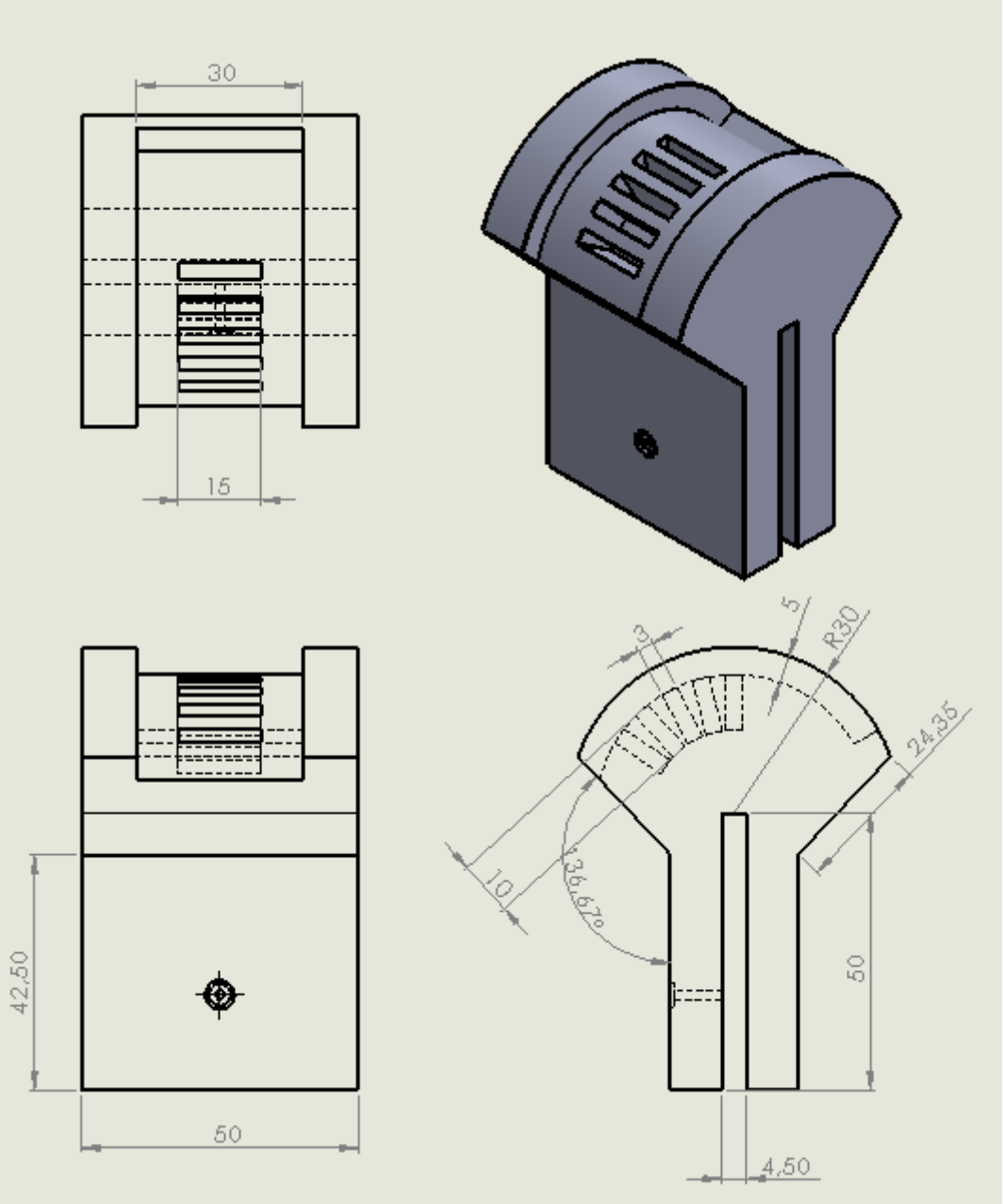

Figure 52: Drawing of the "DC motor mounting foundation" with dimensions.

Appendix K

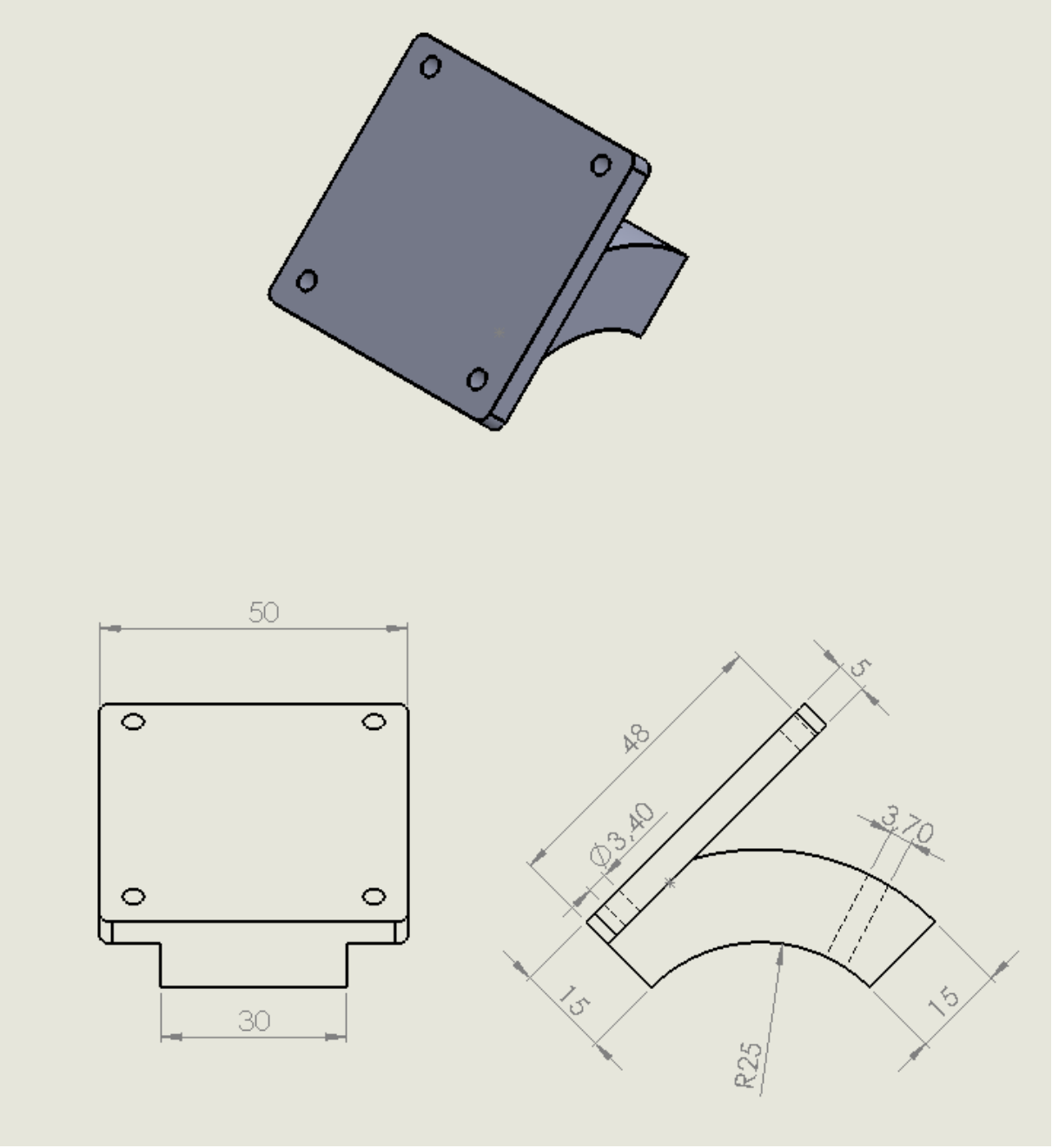

Figure 53: Drawing of the "DC motor holder" with dimensions.

Appendix L

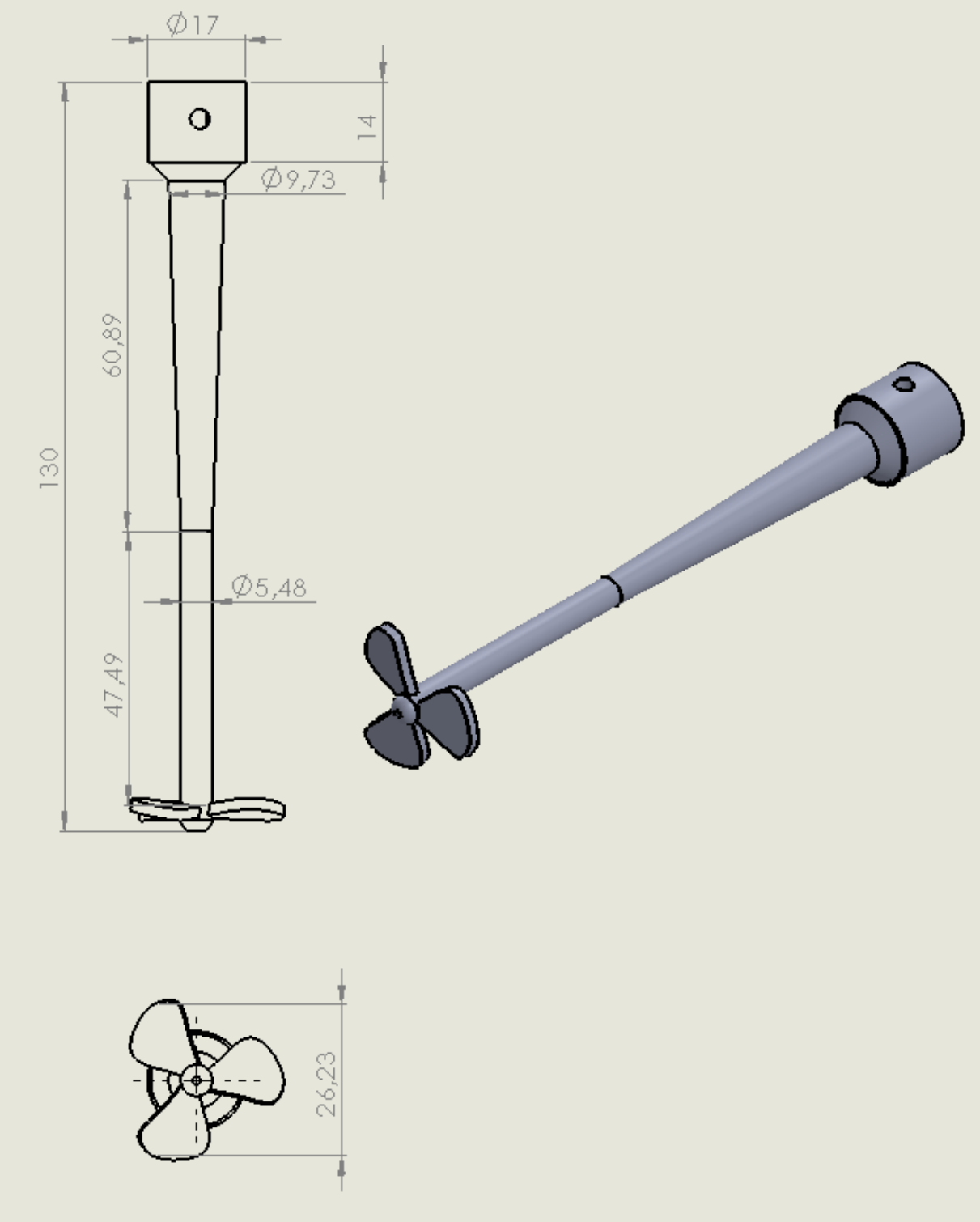

Figure 54: Drawing of the «DC motor propeller» with dimensions.

Appendix M

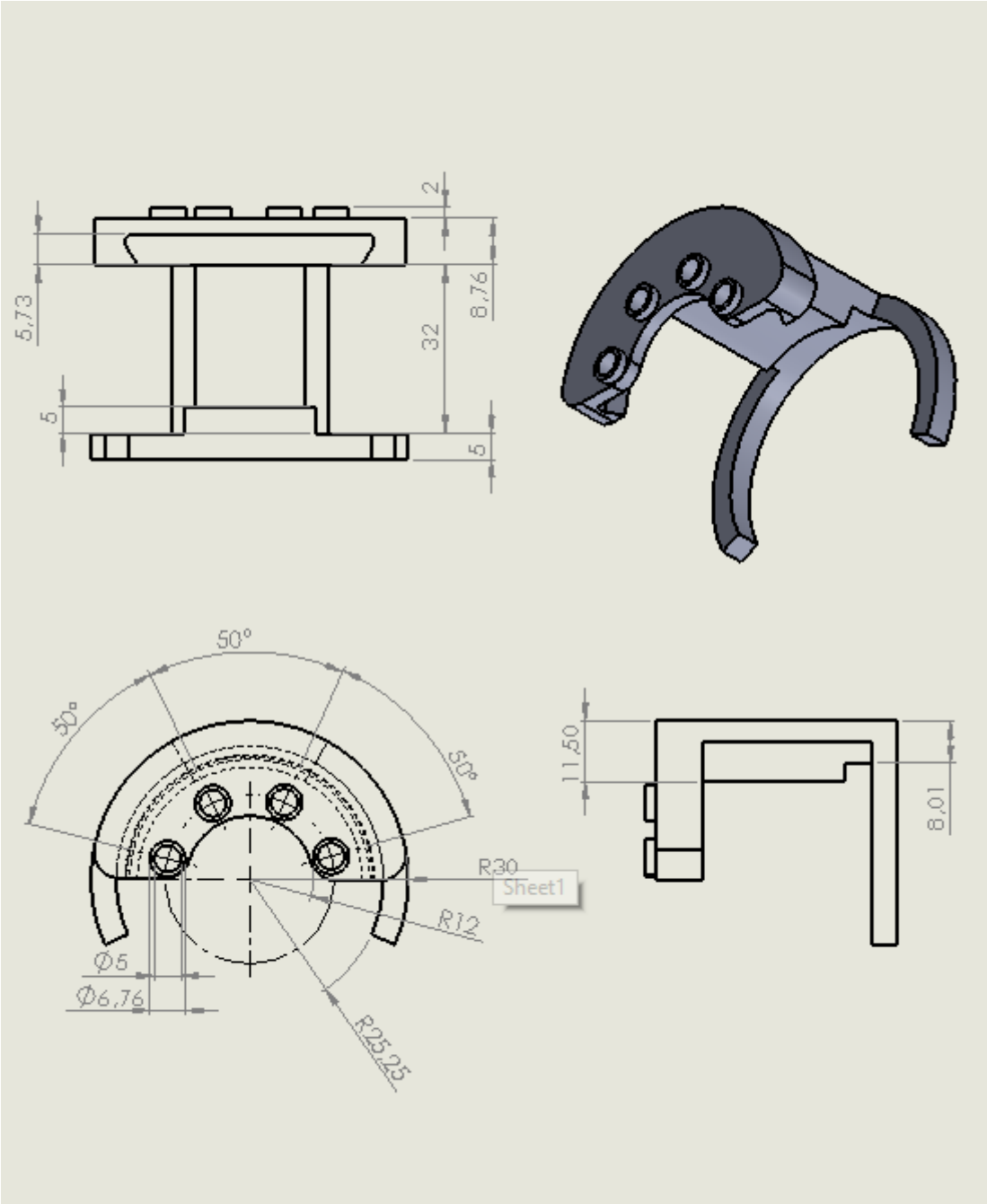

Figure 55: Drawing of the «Hose fixture for stomach» with dimensions.

Appendix N

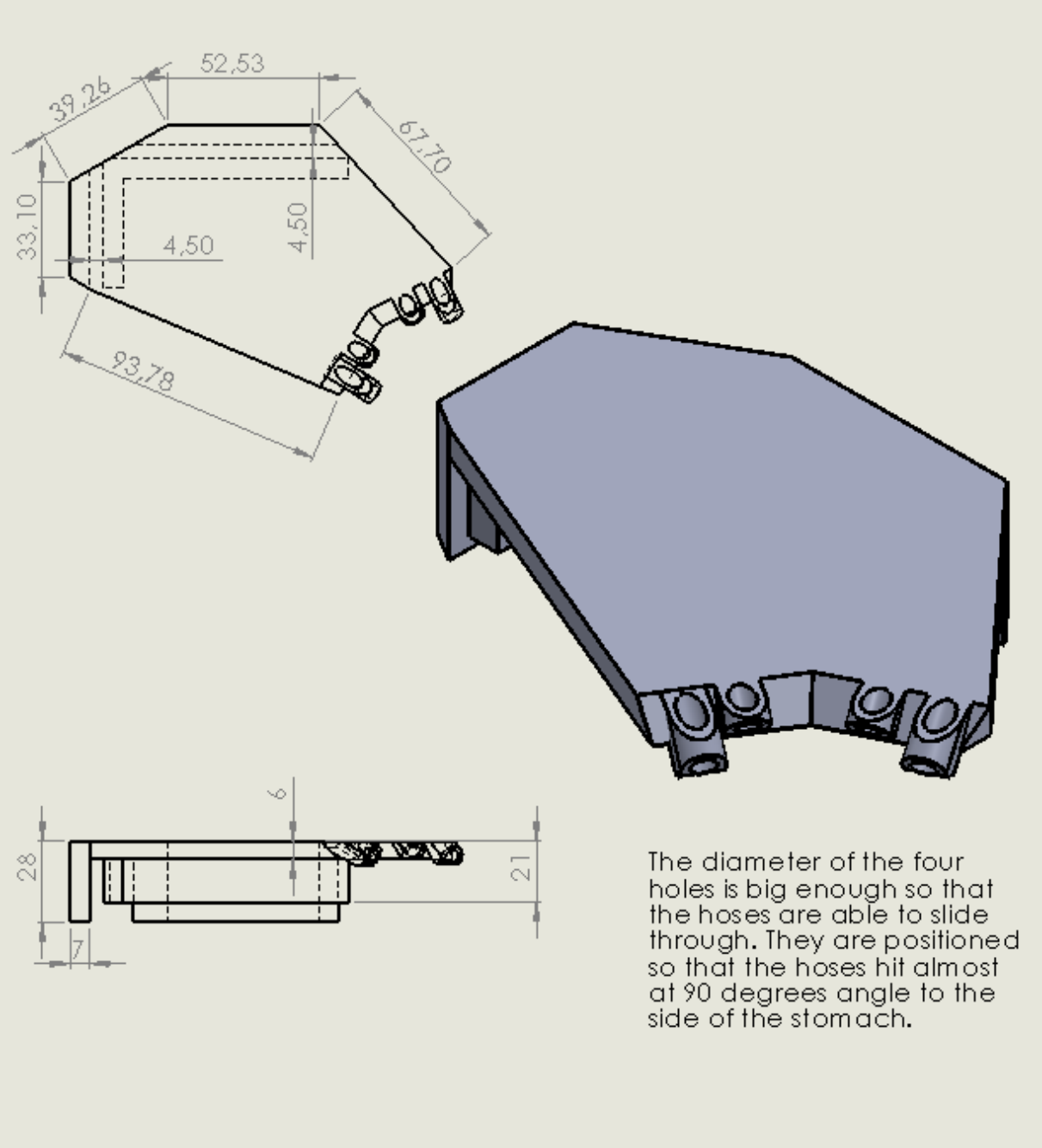

Figure 56: Drawing of the "Hose fixture for water bath" with dimensions.

Appendix O

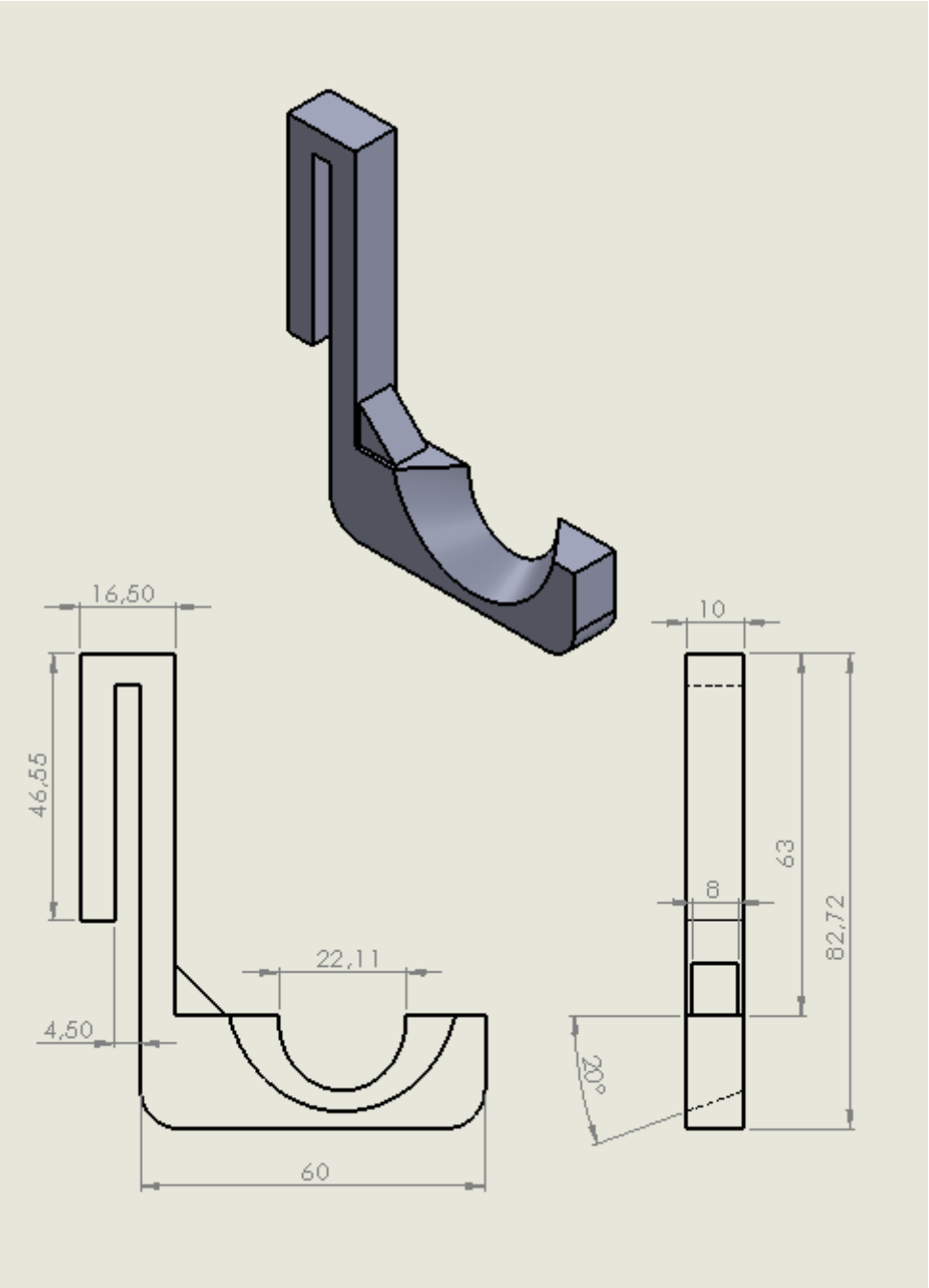

Figure 57: Drawing of the "Buffer glass fixture 1" with dimensions.

Appendix P

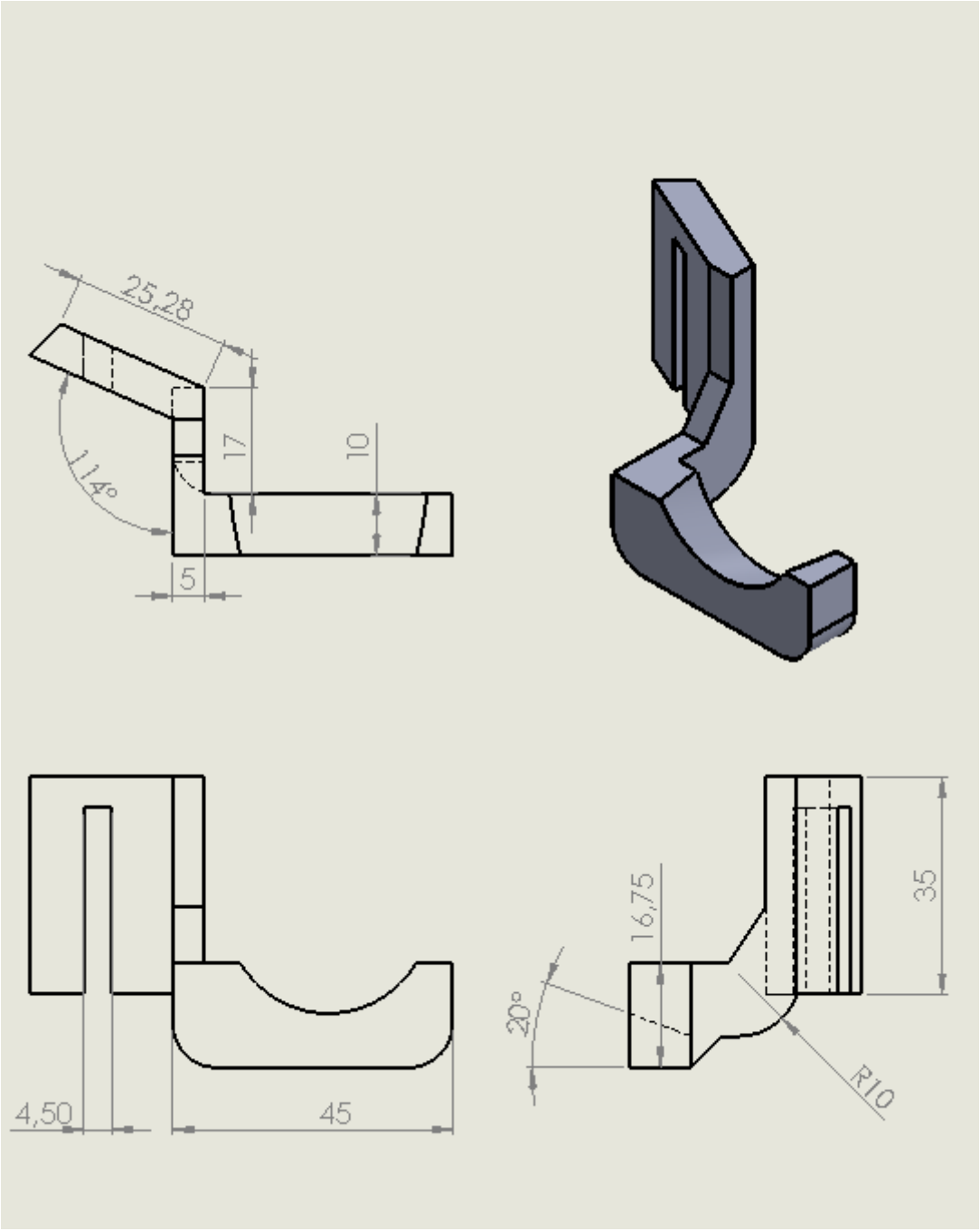

Figure 58: Drawing of the "Buffer glass fixture 2" with dimensions.

Appendix Q

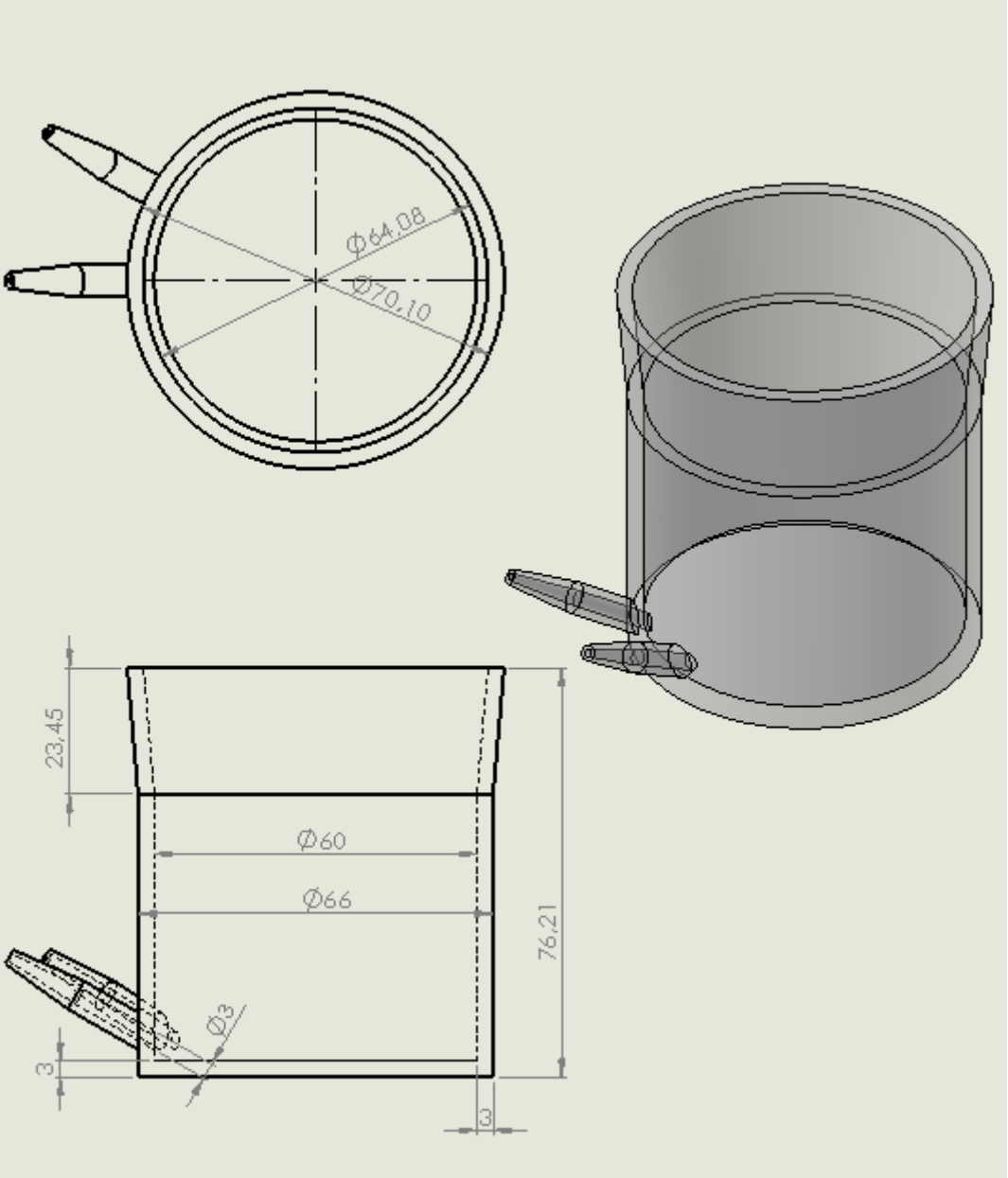

Figure 59: Drawing of the "Buffer tank with lid" with dimensions.

Appendix R

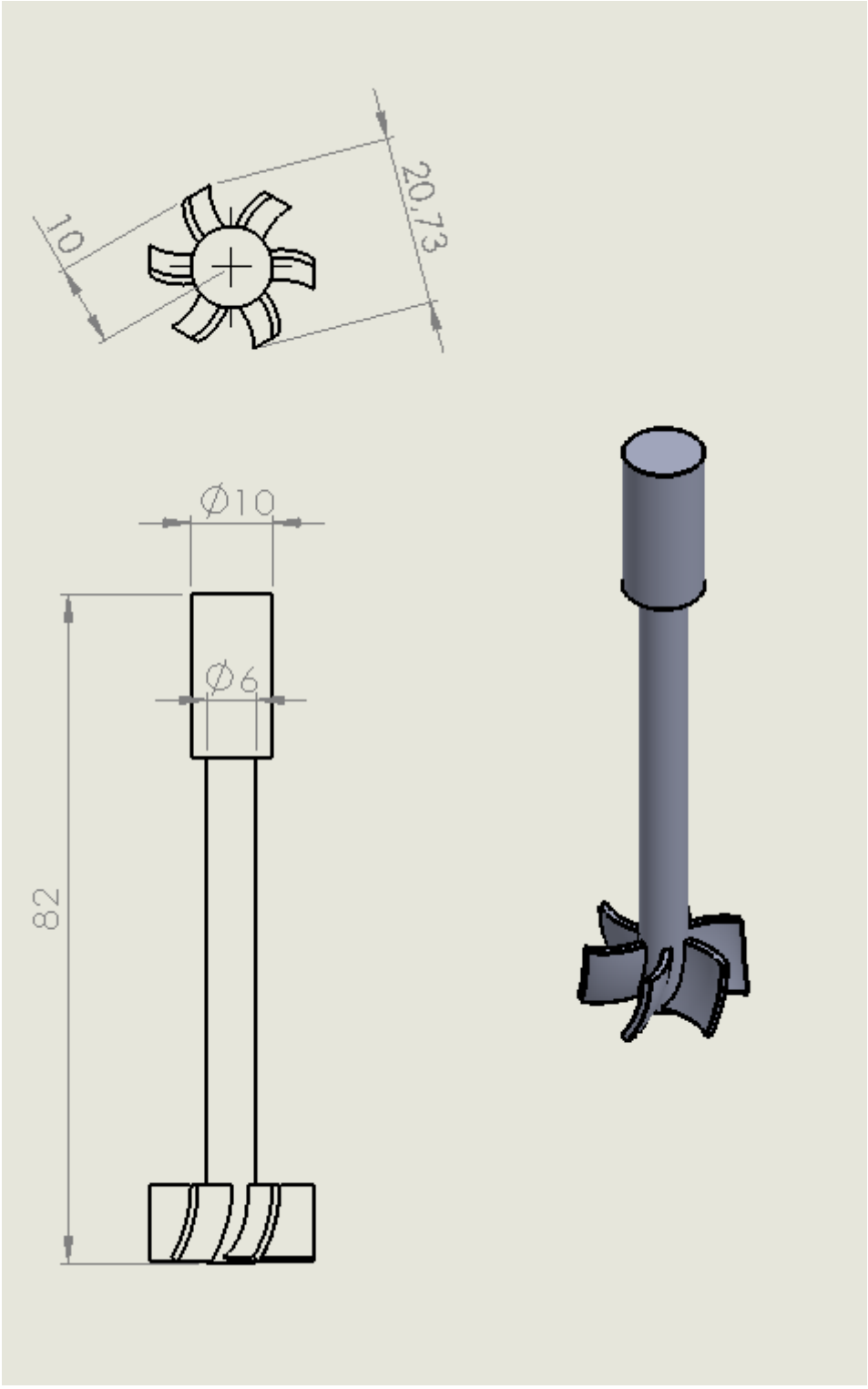

Figure 60: Drawing of the "Rheometer propeller" with dimensions.

Appendix S (Proposal to future design)

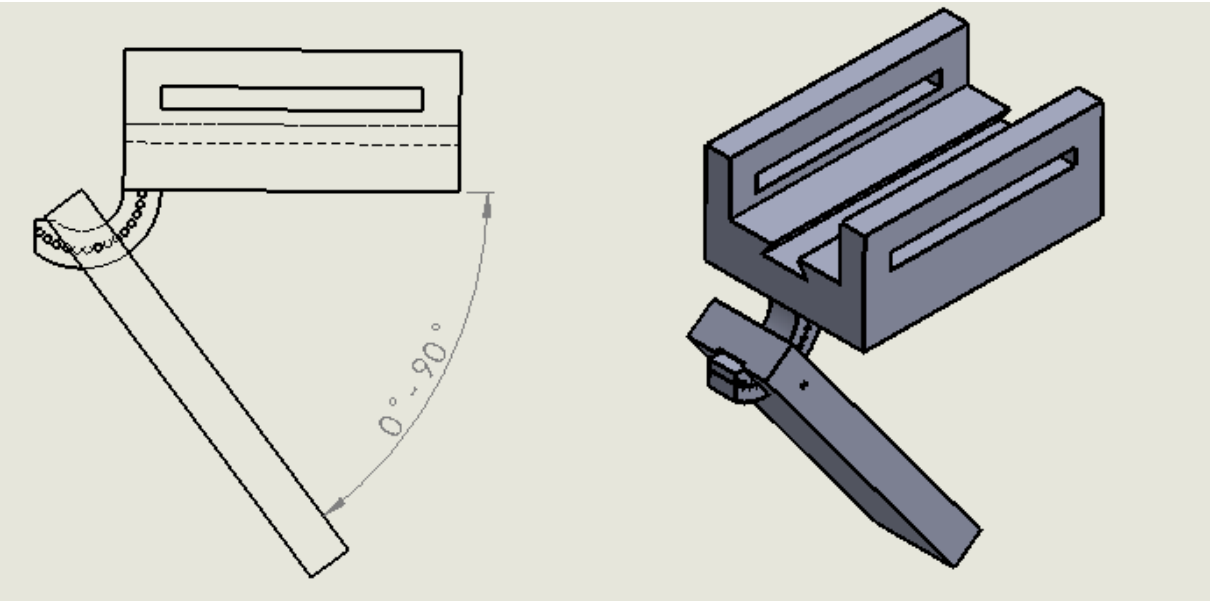

Figure 61: Proposal to future design of the «PH sliding mechanism».

Appendix T (proposal to future design)

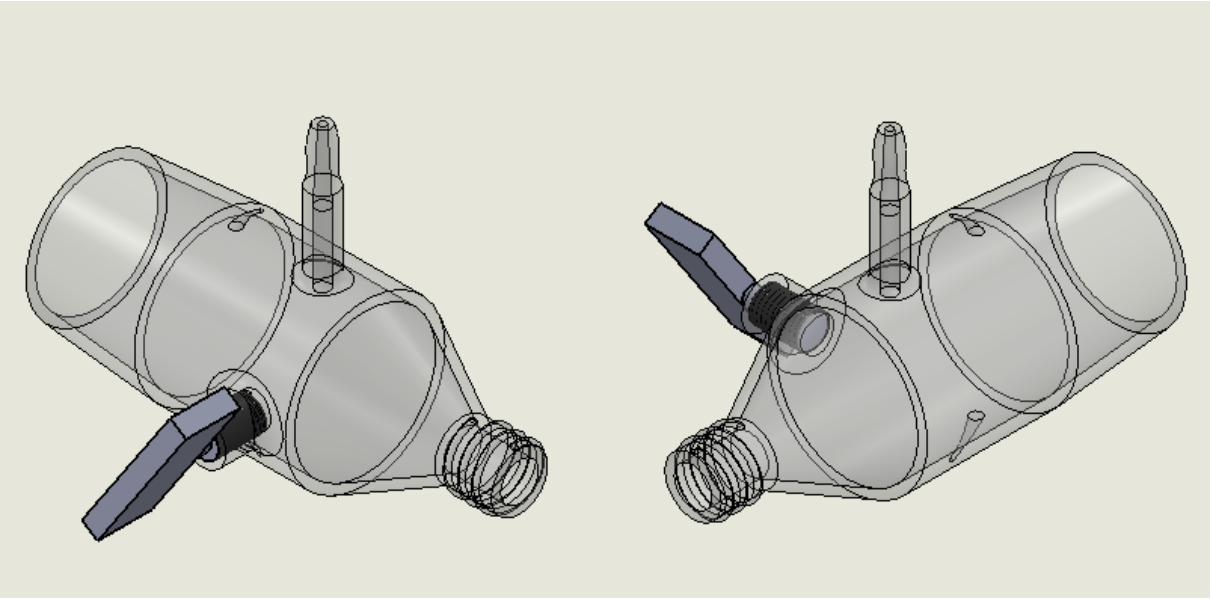

Figure 62: Proposal to future design of the «Buffer glass short end». A screwing device might make it possible to create a vacuum in the buffer circuit.

Appendix U

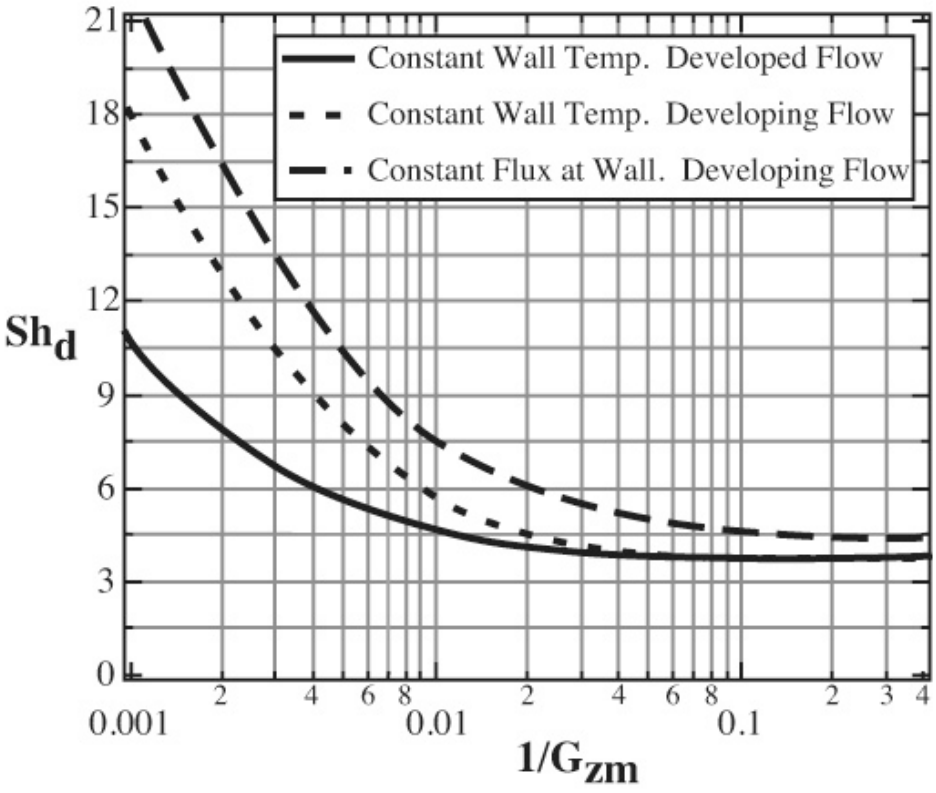

Figure 63: Sherwood number as a function of the Graetz number for developing mass transfer in a tube (Modules).

Norwegian University
of Life Sciences

Postboks 5003
NO-1432 Ås, Norway
+47 67 23 00 00
www.nmbu.no